การสังเคราะห์และวิเคราะห์คุณลักษณะของตัวเร่งปฏิกิริยาซีเกลอร์–นัตตา

ที่มีระบบตัวรองรับต่างกัน

นางสาวศุภนันท์   ปัทมะสังข์

วิทยานิพนธ์นี้เป็นส่วนหนึ่งของการศึกษาตามหลักสูตรปริญญาวิศวกรรมศาสตรดุษฎีบัณฑิต

สาขาวิชาวิศวกรรมเคมี ภาควิชาวิศวกรรมเคมี

คณะวิศวกรรมศาสตร์ จุฬาลงกรณ์มหาวิทยาลัย

ปีการศึกษา 2554

ลิขสิทธิ์ของจุฬาลงกรณ์มหาวิทยาลัย

SYNTHESIS AND CHARACTERIZATION OF ZIEGLER-NATTA CATALYST WITH VARIOUS SUPPORT SYSTEMS

Miss Supanan Patthamasang

A Dissertation Submitted in Partial Fulfillment of the Requirements

for the Degree of Doctor of Engineering Program in Chemical Engineering

Department of Chemical Engineering

Faculty of Engineering

Chulalongkorn University

Academic Year 2011

Thesis Title   SYNTHESIS AND CHARACTERIZATION OF ZIEGLER-NATTA CATALYST WITH VARIOUS SUPPORT SYSTEMS

By   Miss Supanan Patthamasang

Field of Study   Chemical Engineering

Thesis Advisor   Professor Piyasan Praserthdam, Dr.Ing.

Thesis Co-advisor   Professor Minoru Terano, D. Eng.

Accepted by the Faculty of Engineering, Chulalongkorn University in Partial Fulfillment of the Requirements for the Doctoral Degree

………………………………..…….Dean of the Faculty of Engineering

(Associate Professor Boonsom Lerdhirunwong, Dr.Ing.)

THESIS COMMITTEE

………………………………………….Chairman

(Professor Suttichai Assabumrungrat, Ph.D.)

………………………………………….Thesis Advisor

(Professor Piyasan Praserthdam, Dr.Ing.)

………………………………………….Thesis Co-advisor

(Professor Minoru Terano, D.Eng.)

………………………………………….Examinor

(Assistant Professor Anongnat Somwangthanaroj, Ph.D.)

………………………………………….Examinor

(Associate Professor Bunjerd Jongsomjit, Ph.D.)

………………………………………….External Examinor

(Sirachaya Kunjara Na Ayudhya, D.Eng.)

ศุภนันท์ ปัทมะสังข์ : การสังเคราะห์และวิเคราะห์คุณลักษณะของตัวเร่งปฏิกิริยาซี เกลอร์–นัตตาที่มี ระบบตัวรองรับต่างกัน (SYNTHESIS AND CHARACTERIZATION OF ZIEGLER-NATTA CATALYST WITH VARIOUS SUPPORT SYSTEMS) อ.ที่ปรึกษาวิทยานิพนธ์หลัก : ศ.ดร.ปิยะสาร ประเสริฐธรรม , อ.ที่ ปรึกษาวิทยานิพนธ์ร่วม:ศ.ดร. มิโนรุ เทอราโน, 102 หน้า

งานวิจัยนี้ได้ศึกษาตัวเร่งปฏิกิริยาซิกเลอร์-แนตตาที่มีระบบตัวรองรับต่างกัน สำหรับใช้ในเอทิลีนพอลิ เมอไรเซชั่น ซึ่งมีด้วยกันสามระบบ คือ $MgCl_2/TiCl_4$ $MgCl_2/SiO_2/TiCl_4$ และ $Mg(OEt_2)/TiCl_4$ โดยมีจุดประสงค์ เพื่อปรับปรุงสัณฐานของตัวเร่งปฏิกิริยาให้มีความกลมและแข็งแรงขึ้น เพื่อลดการแตกหักของอนุภาคตัวเร่ง ปฏิกิริยา ขณะทำการ สังเคราะห์ตัวเร่งปฏิกิริยา การสังเคราะห์ตัวรองรับ $MgCl_2$ ใช้วิธีการตกผลึก (Recrystallization) $MgCl_2$ ในสารละลายเอทานอลในไฮโดรคาร์บอน ในระบบตัวรองรับผสมจะเพิ่มขั้นตอนการ เคลือบฝัง $MgCl_2 \cdot nEtOH$ ลงบนผิว SiO_2 ในเฮปเทนซึ่งเป็นตัวกลาง จากนั้นตัวรองรับจะทำปฏิกิริยากับ $TiCl_4$ ต่อไป การเตรียมตัวรองรับ $MgCl_2$ ในตัวเร่งปฏิกิริยา $Mg(OEt_2)/TiCl_4$ ใช้วิธีการทำปฏิกิริยาทางเคมีระหว่าง $Mg(OEt_2)$ และ $TiCl_4$ จากผลการศึกษาพบว่าการใช้ SiO_2 เพื่อให้เกิดเป็นตัวรองรับผสม สามารถช่วยให้ตัวเร่ง ปฏิกิริยามีสัณฐานที่กลมและแข็งแรงขึ้น ซึ่งสัณฐานของตัวเร่งปฏิกิริยาขึ้นอยู่กับสัณฐานของ SiO_2 ที่ใช้ และการ ใช้ SiO_2 สามารถช่วยลดผลกระทบจากการใช้เอทานอล ซึ่งเป็นปัจจัยสำคัญที่ส่งผลต่อสัณฐานและความว่องไว ในการเกิดปฏิกิริยาของตัวเร่งปฏิกิริยา $MgCl_2/TiCl_4$ และได้ทำการศึกษาคุณสมบัติของตัวเร่งปฏิกิริยาในด้าน อื่นๆ เช่น การตอบสนองต่อไฮโดรเจนในการทำเอทิลีนพอลิเมอไรเซชั่นและความทนทานต่อการเสื่อมสภาพ ของตัวเร่งปฏิกิริยาด้วย ในตัวเร่งปฏิกิริยา $Mg(OEt_2)/TiCl_4$ พบว่าสัณฐานของ ตัวเร่งปฏิกิริยาที่ได้ มีรูปร่างจำลอง จาก $Mg(OEt_2)$ ที่เป็นสารตั้งต้นและตัวเร่งปฏิกิริยาที่สังเคราะห์ขึ้นมีความว่องไวสูง ตัวเร่งปฏิกิริยาระบบนี้ยังได้ ทำการศึกษาผลของการเติม internal electron donor และสภาวะที่ใช้ในการสังเคราะห์ตัวเร่งปฏิกิริยาที่มีต่อการ เกิดโครงสร้างของ $MgCl_2$ รวมถึงได้ทำการทดลองใช้ตัวเร่งปฏิกิริยาทั้งในเอทิลีนและโพรพิลีนพอลิเมอไรเซชั่น ด้วย

ภาควิชา............วิศวกรรมเคมี......ลายมือชื่อนิสิต...

สาขาวิชา...........วิศวกรรมเคมี......ลายมือชื่อ อ.ที่ปรึกษาวิทยานิพนธ์หลัก ……………..………..……………

ปีการศึกษา.........2554................ลายมือชื่อ อ.ที่ปรึกษาวิทยานิพนธ์ร่วม..

5071867921 : MAJOR   CHEMICAL ENGINEERING

KEYWORDS : ZIEGLER-NATTA / ETHYLENE POLYMERIZATION / MORPHOLOGY / SUPPORT

SUPANAN PATTHAMASANG : SYNTHESIS AND CHARACTERIZATION OF ZIEGLER-NATTA CATALYST WITH VARIOUS SUPPORT SYSTEMS. THESIS ADVISOR: PROF. PIYASAN PRASERTHDAM, Dr.Ing., THESIS COADVISOR PROFESSOR MINORU TERANO, D.Eng., 102 pp.

Heterogeneous Ziegler-Natta catalysts for ethylene polymerization were prepared with various support systems, $MgCl_2$, $MgCl_2/SiO_2$ and $Mg(OEt)_2$. The objectives are to improve the morphology of catalyst and to decrease the fragmentation of catalyst's particle during catalyst preparation. For $MgCl_2/TiCl_4$ and $MgCl_2/SiO_2/TiCl_4$, the $MgCl_2$ support was prepared via recrystallization of anhydrous $MgCl_2$ in ethanol-hydrocarbon solution. The bi-support ($MgCl_2/SiO_2$) was prepared by impregnation of $MgCl_2 \cdot nEtOH$ adduct on SiO_2 surface in heptane media. After that, reaction with $TiCl_4$ was performed to obtain the catalyst. In the case of $Mg(OEt)_2/TiCl_4$, the $MgCl_2$ support was prepared by chemical reaction between $Mg(OEt)_2$ and $TiCl_4$. The result shows that using of SiO_2 in bi-support system could improve morphology of $MgCl_2$-based catalyst with spherical shape. Moreover, SiO_2 could reduce the effect of ethanol, which is the key parameter to control the morphology and activity of $MgCl_2/TiCl_4$ catalyst. Hydrogen response in ethylene polymerization and stability of catalyst were also studied. For $Mg(OEt)_2/TiCl_4$ system, the results show that the morphology of catalyst replicated the morphology of $Mg(OEt)_2$ precursor and highly catalytic activity was achieved. Additional, the effect of internal electron donor and catalyst's preparation conditions and catalyst's performance in ethylene and propylene polymerization were also studied.

Department:…..Chemical Engineering ….. Student's Signature……………….............

Field of Study :Chemical Engineering…….Advisor's Signature………………..……..

Academic Year:…………2011…………....Co-advisor's Signature………………..…

ACKNOWLEDGEMENTS

First and foremost, I would like to express my most sincere thanks to my advisor, Professor Piyasan Praserthdam, for his great guidance and support. I really appreciate the opportunities given to me to work freely in the Ziegler-Natta and Metallocene group. I am most deeply indebted to Associate Professor Bunjerd Jongsomjit for his continuous support and encouragement over the years. I would also like to thank Associate Professor ML. Supakanok Thongyai for the fruitful ideas and valuable suggestions during this work. Special thanks belong to Associate Professor Suttichai Assabumrungrat and Dr. Sirachaya Kunjara Na Ayudhya for kindly serving as my committee members.

I wish to express my warmest thanks to Professor Minoru Terano for a great opportunity and experience to carry out research work at Japan Advanced Institute of Science and Technology. Sincere thank is given to Dr. Toshiaki Taniike for the invaluable guidance concerning the polypropylene polymerization catalyst. I owe special thanks to the whole students of Terano laboratory for the warm welcome, supports and wonderful times we have had during my stay. I would like to express my sincere gratitude to Professor S.E. Wanke for his guidance and knowledge concerning silica-based catalyst.

I am grateful to all former and current students for making the laboratory such an agreeable workplace. I would like to acknowledge my friends for the good spirit shared especially Mr. Patcharaporn Weerachawanasak. Their friendship encouraged me to overcome many difficulties. Thanks also to Ms. Pramrutai Kruachot for her kind help in diverse matters.

I am appreciative thanks to Miss Supaporn Kobulsongserm for all her supports and inspirations. The financial support from PTT Public Co.,Ltd.

Finally, I would like to dedicate this dissertation to my family for their edification, support and endless love. Without them, I would not have been the person I am and certainly this work would never have reached completion.

CONTENTS

CHAPTER   Page

LIST OF TABLES

LIST OF FIGURES

LIST OF ABBREVIATIONS

Abbreviations

A1	Aluminum
Ti	Titanium
BET	Brunauer Emmett Teller
DIBP	Diisobythylphthalate
EB	Ethylbenzoate
ED	External electron donor
EtOH	Ethanol
FTIR	Fourier transform infrared
HDPE	High density polyethylene
ICP	Inductively coupled plasma spectroscopy
ID	Internal electron donor
IPIPDMP	2,2-isopentyl-isopropyl-1,3-dimethoxy propane
LDPE	Low density polyethylene
LLDPE	Linear low density polyethylene
NMR	Nuclear magnetic resonance
PE	Polyethylene
PP	Polypropylene
PSD	Particle size distribution
SEM	Scanning electron microscopy
TEA	Triethylaluminium
TGA	Thermogravimetric analysis
TIBA	Triisobuthylaluminium
XRD	X-ray diffraction
ZN	Ziegler-Natta

CHAPTER I

INTRODUCTION

1.1 Rationale

The discoveries of Ziegler and Natta catalyst (ZN) concerning the ability of the $TiCl_4/AlR_3$ mixture to promote the polymerization of ethylene and of propylene, continuous research in the field, mainly driven by industrial requirements, has led to the development of various families and generations of catalysts having a level of complexity [1].

Today, activation of $MgCl_2$ is generally performed via chemical methods that not only allow the fine tuning of catalyst performances but also provide an unprecedented control over the morphology of the catalyst particles [2-4].

The synthetic method for catalyst preparation can be conducted in many ways such as mechanical routes like ball-milling of $MgCl_2$ with $TiCl_4$ and /or Lewis base. In order to get morphology control, the active $MgCl_2$ is prereacted with some amounts of a Lewis base (eg, an alcohol). $MgCl_2/TiCl_4$ systems can starting from $MgCl_2 \cdot nEtOH$ supports, they can be shaped into perfectly spherical particles having control of size, size distribution, and porosity to fit any polymerization process and/or product requirements or constraints [5-12]

In some cases, the $MgCl_2$ can be deposited on a support, eg, silica, alumina, or other inorganic carriers to get bi-support carrier, before the reaction. The final step is the usual treatment with $TiCl_4$ and, when desired, the internal donor. In this case, however, the degrees of freedom concerning both size and porosity control are more limited than in the case of pure $MgCl_2 \cdot nEtOH$ supports [13-16].

Additional, chemical reaction of $Mg(OEt)_2$ precursor with $TiCl_4$ is the one way to get morphology control catalyst support, the obtained catalyst have high performance with good morphology and lower Cl content. ZN catalysts synthesized from spherical $Mg(OEt)_2$ solid precursors are known to show the highest level of performance, that is, good replication and highly stable activity, and therefore are widely used in

industrial applications worldwide in competition with alcohol adduct-based spherical catalysts [3].

However, up to now only a few studies have been conducted in relation to their kinetics and morphology [17-19]. The morphology of the supported Ziegler-Natta catalysts has an important influence on olefin polymerization. The morphology of polymer particle replicates the catalyst particle morphology. Generally, good replication of catalyst particles takes place with a uniform polymerization rate, which is the result of homogeneous distribution of the active complex among the catalyst particles as well as the absence of concentration and temperature gradients within the reacting particles. If requirements for shape replication are not achieved, growing polymer particles can suffer from morphological deformations and particle breaking could result, causing a complete loss of the original shape.

In general, catalyst fragmentation depends mainly on two factors: hydraulic pressure generated by the formed polymer inside the catalyst pores and the rigidity of the support material. The support must have a mechanical strength great enough to withstand handling and low enough to break down during polymerization.

Therefore, controlling of catalyst particle is very important for good morphology polymer particles. We have interested in controlling the catalyst particle during the synthesis and control the parameters that effect on the strength and shape of catalyst particles.

In this study, three supported Ziegler-Natta catalyst systems were investigated in the order to control catalyst morphology and modify the catalyst performance in the same time. The $MgCl_2$-supported, $SiO_2/MgCl_2$-supported and $MgCl_2$(ethoxide type)–supported ZN catalyst were synthesized with various conditions. The ethanol effect on $MgCl_2$-supported and $SiO_2/MgCl_2$-supported ZN catalysts morphology and catalyst performance were investigated, and hydrogen response in ethylene polymerization was also studied. Additional, the stability of both catalysts were investigated in comparison of the decay rate with holding time. Furthermore, the synthesis of $MgCl_2$(ethoxide type)-supported ZN catalyst was performed in order to study the preparation condition that effect on the catalyst morphology and their polymerization

performance. Moreover, the internal donor effect on the catalyst particle morphology and polymerization performance of ethylene and propylene were also studied.

1.2 Objectives of this work

1. To improve the morphology of heterogeneous Ziegler-Natta catalyst for ethylene polymerization.

2. To study the preparation of support system for Ziegler-Natta catalyst e.g. $MgCl_2$, $SiO_2/MgCl_2$ and $Mg(OEt)_2$.

3. To investigate the parameter controlling catalyst's morphology and decrease fragmentation process.

4. To characterize the heterogeneous Ziegler-Natta catalyst with various support systems.

CHAPTER II

THEORY

2.1 The important of Ziegler-Natta catalysts

A Ziegler-Natta catalyst is a catalyst used in the production of polymers of 1-alkenes (α-olefins). Ziegler-Natta catalysts are typically based on titanium compounds and organometallic aluminium compounds, such as the undefined methylaluminoxane (MAO) or well defined triethylaluminium, $(C_2H_5)_3Al$.

Ziegler-Natta catalysts are used to polymerize terminal 1-alkenes.

$$n\ CH_2=CHR \rightarrow -_n-$$

German Karl Ziegler, for his discovery of these titanium based catalysts, and Italian Giulio Natta, for using them to prepare stereoregular polymers, were awarded the Nobel Prize in Chemistry in 1963.
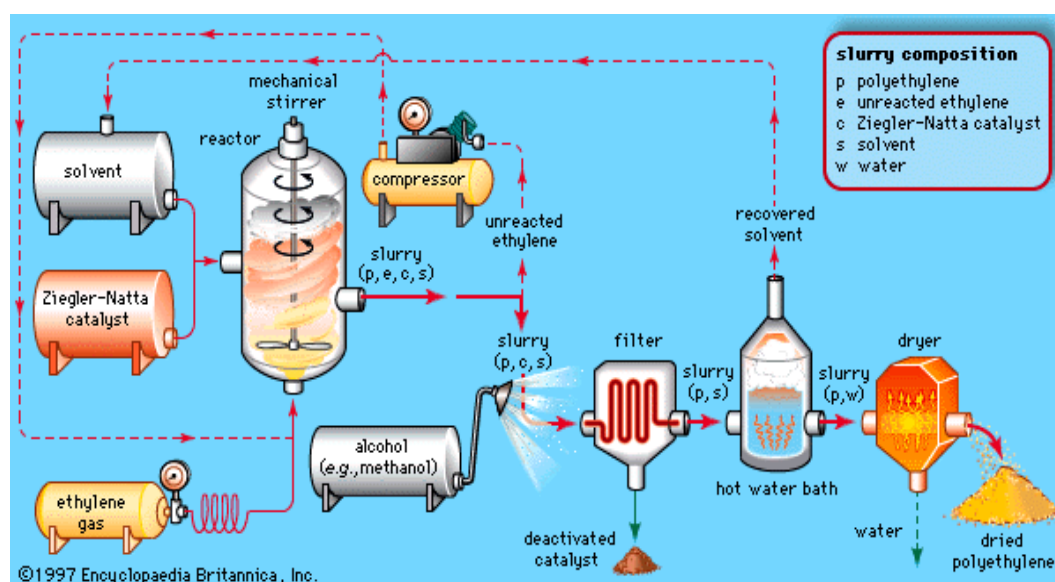
Figure 2.1: The Ziegler-Natta polymerization of ethylene process [20].

Ethylene gas is pumped under pressure into a reaction vessel, where it polymerizes under the influence of a Ziegler-Natta catalyst in the presence of a solvent. A slurry of polyethylene, unreacted ethylene monomer, catalyst, and solvent

exits the reactor. Unreacted ethylene is separated and returned to the reactor, while the catalyst is neutralized by an alcohol wash and filtered out. Excess solvent is recovered from a hot water bath and recycled, and a dryer dehydrates the wet polyethylene to its final powder form.

Table 2.1: Generations of Ziegler-Natta Catalysts for the Polymerization of Propylene[a] [20].

Generation (year)	Catalyst composition	Productivity (kg_{pp}/g_{cat})	I.I[b] %	mmmm %	M_w/M_n
First (1954)	$\delta\text{-TiCl}_3 \cdot 0.33\text{AlCl}_3 + \text{AlEt}_2\text{Cl}$	2–4	90–94		
Second (1970)	$\delta\text{-TiCl}_3 + \text{AlEt}_2\text{Cl}$	10–15	94–97		
(1968)	$\text{MgCl}_2/\text{TiCl}_4 + \text{AlR}_3$	15	40	50–60	
Third (1971)	$\text{MgCl}_2/\text{TiCl}_4/\text{benzoate} + \text{AlR}_3/\text{benzoate}$	15–30	95–97	90–94	8–10
Fourth (1980)	$\text{MgCl}_2/\text{TiCl}_4/\text{phthalate} + \text{AlR}_3/\text{silane}$	40–70	95–99	94–99	6.5–8
Fifth (1988)	$\text{MgCl}_2/\text{TiCl}_4/\text{diether} + \text{AlR}_3$	100–130	95–98	95–97	5–5.5
	$\text{MgCl}_2/\text{TiCl}_4/\text{diether} + \text{AlR}_3/\text{silane}$	70–100	98–99	97–99	4.5–5
"Next" (1999)	$\text{MgCl}_2/\text{TiCl}_4/\text{succinate} + \text{AlR}_3/\text{silane}$	40–70	95–99	95–99	10–15

[a] (Polymerization conditions : liquid propylene, 70 °C, H_2).

[b] Isotactic Index

2.2 The Catalyst (Solid Component)

2.2.1 Preparation of Catalysts for the Synthesis of Polyolefins Consisting of $MgCl_2$ and Titanium Compounds.

Scientific and, particularly, patent literature report several detailed outlines of methods for the preparation of catalysts mainly consisting of $MgCl_2$ and titanium compounds.

The synthetic procedures for catalyst preparation can thus be divided into three main classes: mechanical routes, chemical routes, and mixed mechanical–chemical routes.

1. Mechanical Routes. This approach is directly derived from the methods used for the activation of the early $TiCl_3$-based catalysts: it consists of a step in which the catalyst components ($MgCl_2$, $TiCl_4$ and, optionally, the Lewis base or internal donor) are milled together for several hours [21-28].

A ball mill is usually employed. $MgCl_2$ can also be generated during the milling process by reacting a magnesium compound with a chlorinating agent (eg, $TiCl_4$).

2. Mechanical Plus Chemical Routes. There are two different approaches belonging to this type of catalyst synthesis.Co-milling of $MgCl_2$ or a $MgCl_2$-precursor and, optionally, a Lewis base or internal donor. The resulting solid is then separately treated with anexcess of $TiCl_4$ at a temperature usually higher than 808C, and washed with hydrocarbons to remove all the unreacted $TiCl_4$ [29-40].

The treatment with $TiCl_4$ has a double role: (1) binding itself to the $MgCl_2$ surface and, in particular to the vacant Mg coordination sites, displacing part of the internal donor, if present; and (2) removal from the catalyst surface all the undesired by-products formed during the reaction.

In some cases, $TiCl_4$ can be diluted in aromatic or halogenated compounds that are good solvents for the by-products. Co-milling of all the catalyst components, as described in the pure mechanical approach, followed by one or more washings with halogenated or aromatic solvents. This type of post treatment of the solid increases the activity and the stereospecificity of the final catalyst [41-45].

3. Chemical Routes. In this class of preparation methods, both the formation of the active form of $MgCl_2$ and the incorporation of the other components (titanium derivative and, optionally, internal donor) are carried out by means of a chemical reaction.The most common synthetic procedures can be divided into four families, according to both types of reagents and of reaction(s) involved.

A complex of $MgCl_2$ with a Lewis base (eg, an alcohol) is treated with excess $TiCl_4$ in the presence of an internal donor at 80 ^{o}C or higher temperature. The solid is then carefully washed with hydrocarbon solvents [46-54].

Minor modifications of this approach are either the use of aromatic or halogenated solvents to dilute $TiCl_4$ or a separate treatment with $TiCl_4$ and the Lewis base. The $MgCl_2$–Lewis-base complex can be transformed into the active form of $MgCl_2$ before the treatment with $TiCl_4$ and the internal donor, by removing the Lewis base via either a chemical reaction (eg, with aluminum alkyls or $SiCl_4$) or via thermal decomposition.

$MgCl_2$ is obtained in situ from the reaction of a precursor and $TiCl_4$ in the presence of the internal donor and an aromatic or halogenated solvent. Typical precursors can be $Mg(OR)_2$ and $Mg(OR)Cl$ [eg, obtained from a Grignard compound and $Si(OR)_4$ and the titanium alkoxydes formed are removed during the treatment or in the final washings [55-67].

Active $MgCl_2$ is obtained from the reaction of MgR_2 or $MgRCl$ and a chlorinating agent (eg, $SiCl_4$). In order to get morphology control, the magnesium compound can be dispersed on a support, eg, silica, alumina,or other inorganic carriers, before the reaction. The final step is the usual treatment with $TiCl_4$ and, when desired, the internal donor. In some cases, the active $MgCl_2$ is prereacted with some amounts of a Lewis base (eg, an alcohol) [68-78].

Either $MgCl_2$ or a precursor [eg, $Mg(OR)_2$, $Mg(OCOR)_2$, MgR_2] is dissolved in a solvent (ROH, trialkyl-phosphate, titanium alkoxides, etc). The solution is treated with a chlorinating agent to precipitate the active $MgCl_2$. This can be reacted directly with $TiCl_4$ and the internal donor or treated according to the conditions described above [79-93].

Some parameters are critical for the control and, in particular, for the improvement of the catalyst performances in polymerization. In the case of catalysts obtained from mechanical or mixed (mechanical plus chemical) routes, the main factors affecting the catalyst performances are the time and the efficiency of milling and the ratio between the components. For example, a longer milling time brings about an increase of catalyst activity.

For catalysts obtained from chemical routes, the purity of the reagents, their ratio, the order of mixing, the reaction time, and the treatment temperature are the main factors to be optimized in order to obtain high-performance catalysts. For example, during the treatment with $TiCl_4$ both temperature and reaction time must be carefully controlled to prevent the side reactions leading to the formation on the catalyst of complexes or by-products between $TiCl_4$, the ID, and $MgCl_2$ that are inactive in polymerization.

An important distinction between the former preparation method based on the milling of the catalyst components and the more recent, pure chemical routes, is the difference in the physical status of the solid catalyst precursor.In fact, supports obtained through a mechanical treatment of $MgCl_2$ appear as powders with no morphology control in terms of shape, size, and size distribution. On the contrary, catalysts prepared via pure chemical routes can be obtained as particles with controlled shape (either spherical or granular), size, and size distribution. This is the most attractive procedure to prepare advanced catalysts for the industrial production of polyolefins as they are able, thanks to the replication phenomenon to generate polymer particles having, on a larger scale, the same features of the parent catalyst particles.

To obtain supports and catalysts having finely controlled morphology, different approaches have been developed. The most used are:

- Controlled precipitation of the solid support.

- Spray-drying or -cooling of either dissolved or molten magnesium derivatives.

- Use of silica or other solid carriers having controlled shape to support $MgCl_2$ or $MgCl_2$ precursors.

- Fast cooling of an emulsion, eg, in paraffin oil, of $MgCl_2$-nROH complexes.

The latter procedure not only allows us to obtain almost perfect spherical particles with narrow size distribution, but also to get a very fine control of the size of catalysts particles, at least in the range of 10–100 mm.

In addition, the resulting MgCl$_2$ particles can be further ''manipulated'', eg, to alter their surface area and porosity. It has been demonstrated that, via controlled removal of the alcohol from the support (dealcoholation) it is possible to both improve the morphological stability and tune the porosity of the resulting catalyst particles, at least in the range 0.3–0.6 cm^3/g.

The control of the porosity of the catalyst particles is particularly important for the synthesis of in situ polypropylene alloys.

The above reported general synthetic methods can be applied to catalysts for both polypropylene and polyethylene. The use of electron donors is mandatory for catalysts for isotactic polypropylene, whereas it is optional for catalysts for polyethylene. On the other hand, the best catalysts for the synthesis of LLDPE usually require the presence of donors [94-99].

2.2.2 Crystalline Forms of the Anhydrous MgCl$_2$

The most common crystalline form of anhydrous MgCl$_2$, the a-form, has a rhombohedral structure with a close packed stacking of double chlorine layers with interstitial Mg^{2+} ions in six fold coordination as represented in Figure 2.2). The X-ray diffraction spectrum is characterized by a strong reflex (104) for d = 2.56 A^o , due to the cubic packing of the CI atoms (Figure 2.3a). Figure 2.4 shows a tridimensional drawing of a MgCl$_2$ crystal; the main crystallographic planes which will be more frequently cited later on, (012) (003) (104) (110), as well as the dimensions, are indicated [101].
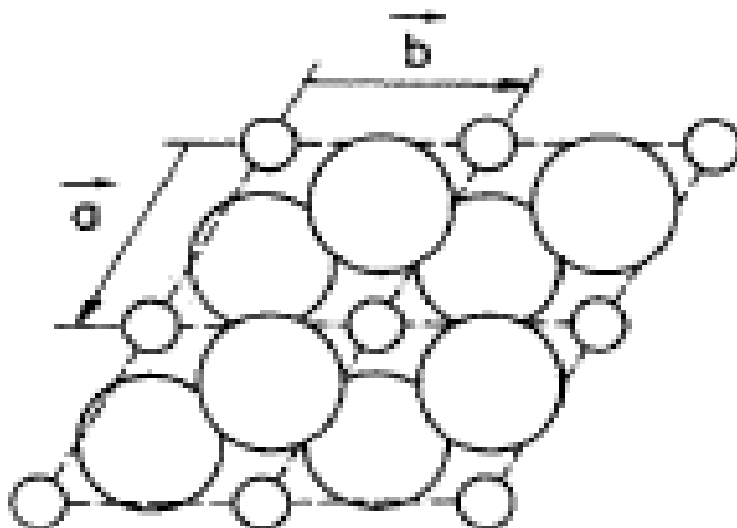
Figure 2.2: Triple layer C1--Mg--CI in ct- MgCl$_2$. Large spheres,C1 atoms [102].
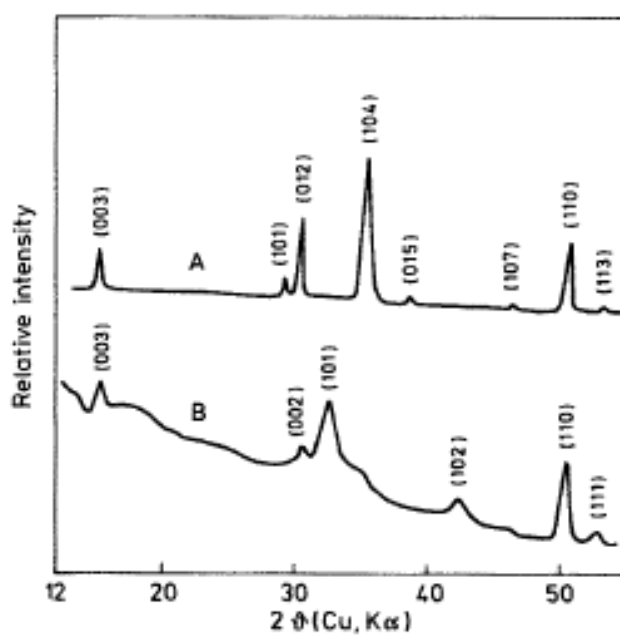
Figure 2.3: X-ray powder spectra of a- MgCl$_2$ (A) and 13- MgCl$_2$ (B) [102].
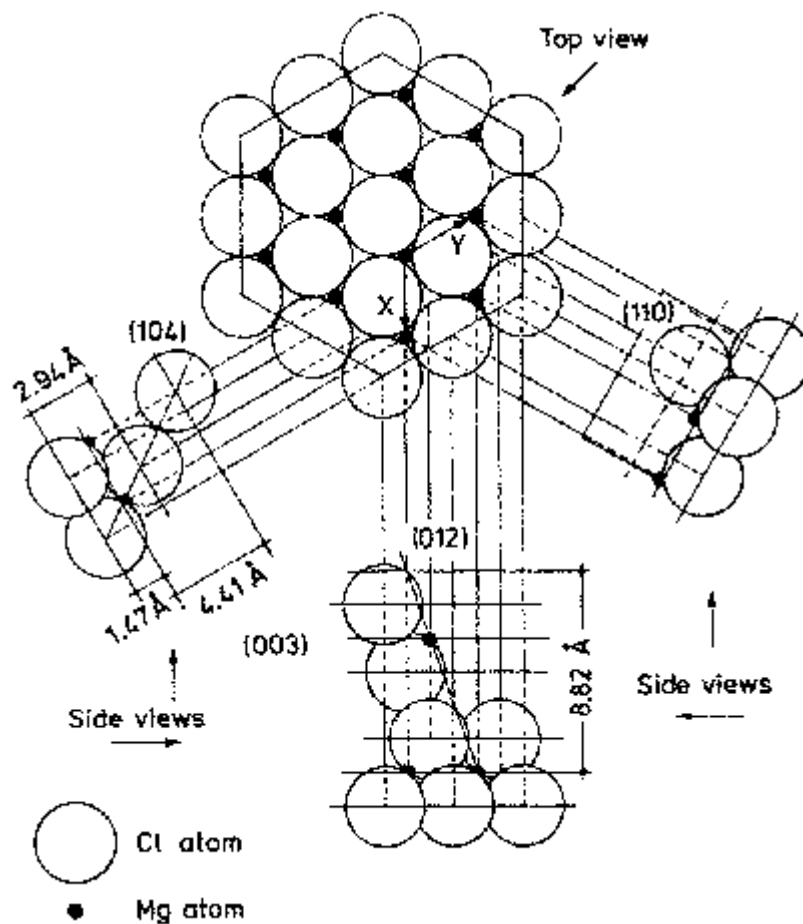
Figure 2.4: Model of the structure of the $\propto$-form of $MgCl_2$ [104].

The less known crystalline β-form of $MgCl_2$ can be obtained by dehydration ofMgCl$_2$• 6H$_2$O with SOCl$_2$ [103].

It is thermodynamically less stable, has hexagonal close packed structure, and is characterized by a strong reflex at d = 2.78 A in the X-ray spectrum (Figure 2.3b). The $\propto$ and β- forms have crystallographic parameters similar to the γ and $\propto$ forms of TiCl$_3$, respectively,(Table 2.2) [104-106].

Table 2.2: Comparison between the crystallographic parameters of $MgCl_2$ and $TiCl_3$ crystalline modifications.

Product	α-MgCl₂	γ-TiCl₃	β-MgCl₂	α-TiCl₃
Structure	Cubic close packed layer structure		Hexagonal close packed layer structure	
Lattice parameters (Å)	$a = b = 3.63$	$a' = b' = 3.54$ $a' = a/\sqrt{3}$	$a = b = 3.64$	$a' = b' = 3.56$ $a' = a/\sqrt{3}$
	$c = 17.79$	$c = 17.58$	$c = 5.93$	$c = 5.87$ $c' = c/3$
Crystalline form	Rhombohedral		Rhombohedral	
Space group	$R\bar{3}m$	$P3_112$ $R\bar{3}m$ for Cl atoms	$P\bar{3}m1$	$P\bar{3}m1$
Specific gravity (g/cm³)	2.33	2.71	2.32	2.71
Cation coordination	Octahedral		Octahedral	
Atomic distances (Å)	Mg—Cl = 2.56	Ti—Cl = 2.51	Mg—Cl = 2.51	Ti—Cl = 2.51

In addition, $MgCl_2$ exhibits active, or 6 forms, which can be obtained, e.g., by mechanical treatment of the ct form, treatment of the ct form with Lewis bases, or by chlorination of Mg-organic derivatives. With respect to the ct form, the8 forms are characterized by the broadening of the (104) reflection, forming a halo shifted with respect the position of the (104) reflection (Figure 2.5).

The X-ray modifications can be explained by the laminar structure of $MgCl_2$ which promotes easier breakages parallel to the chlorine layers, joined together by means of van der Waals' weak forces, and more difficult breakages across these layers, where strong ionic bonds are involved. Only the latter type of breakage (see Figure 2.4) is useful in creating coordinatively unsaturated Mg atoms which can absorb other molecules, e.g. on the faces (110) and (101) where Mg atoms are coordinated with 4 and 5 chlorine atoms, respectively (Figure 2.6). Giannini [107] points out that the gradual disappearance of the reflex (104) and the appearance of a broad halo in the active forms indicate stacking defects in the sequence of the chlorine atom planes along the c-axis. The sequence of stacking no longer corresponds to a cubic close packed structure, but is disordered due to translation and rotation of the

chlorine atom planes. This destroys the crystalline order in the stacking direction while maintaining a close packed arrangement of the chlorine ions.

A border-line case is represented in Figure 2.7 which shows the spectrum of an active $MgCl_2$ obtained by chlorination of a Grignard compound. In this manner it is possible to obtain highly disordered crystalline forms, clearly more disordered than those obtained by even prolonged mechanical treatments. As a further confirmation of the strong similarity between $MgCl_2$ and $TiCl_3$ structures, Table 2.2 shows the crystallographic parameters of the active forms (or δ forms) of $MgCl_2$ and $TiCl_3$[108].
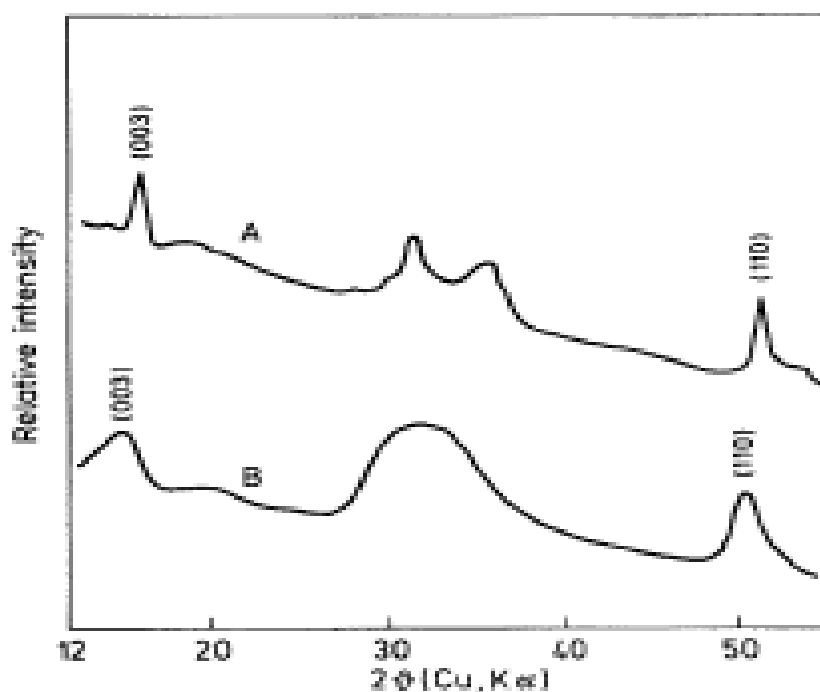
Figure 2.5: X-ray powder spectra of $MgCl_2$ samples with different degree of activation. Milling time: 50 (A) and 100 (B) hours [107].

\
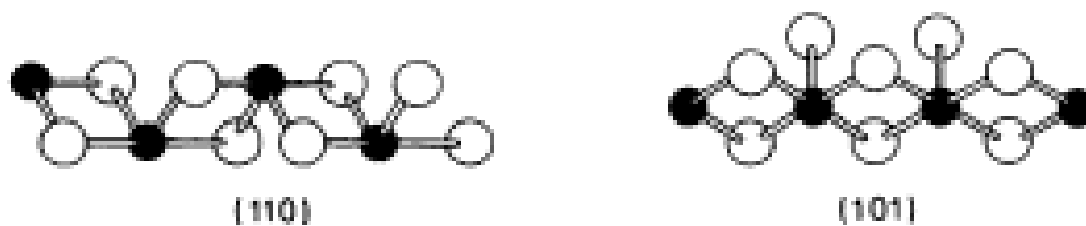
Figure 2.6: Faces (110) and (101) of $MgCl_2$ [107]
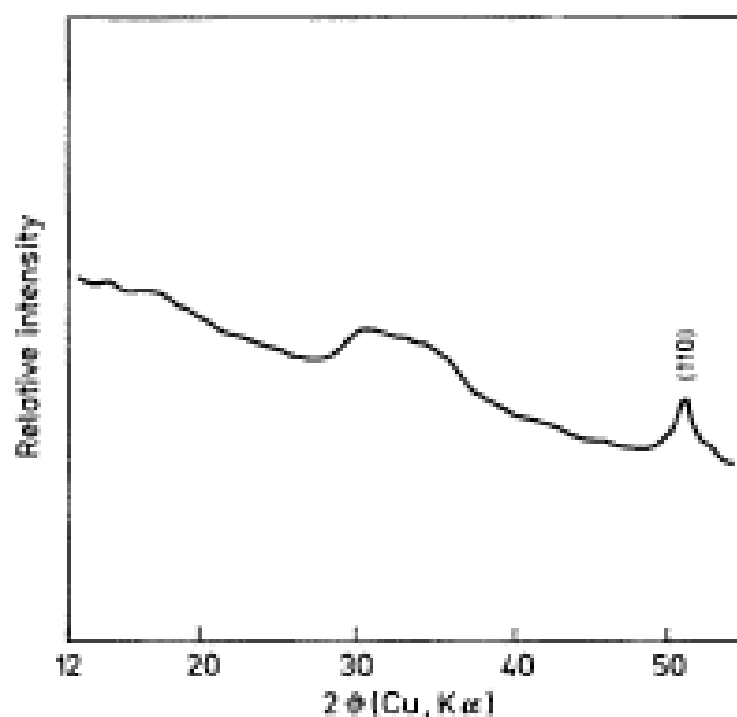
Figure 2.7**:** X-ray powder spectrum of $MgCl_2$ prepared by chlorination of a Grignard compound [107].

2.2.3 Structural Modifications in $MgCl_2$ Subjected to Mechanical Treatments in the Presence of Titanium Compounds

Highly active $MgCl_2$ based catalysts can be obtained by mechanical treatment of mixtures of $MgCl_2$ and Ti-compound. During such treatments the $MgCl_2$ structure

undergoes substantial variations which may affect the catalyst performance considerably.

A Lewis base can also be added to the systems. The presence of the base is essential for the synthesis of isotactic polypropylene. Both cases will be considered separately.

2.2.4 Mechanical Activation of Mixtures of $MgCl_2$ and Ti-Compound

The effect of milling on the $MgCl_2$ structure, as noted by X-ray spectra, is similar to that observed in the case of $MgCl_2$ alone, however, the variations occur within shorter periods of time (Figure 2.8) [109].

Galli [110] showed that the most important effect of the mechanical treatment is the occurrence of a rotational disorder in CI-Mg-C1 triple layers; this was demonstrated through the good fit between observed and calculated diffraction patterns.

The activation rate increases upon increasing the $TiC1_4$ content; at more than 4 wt.%, the effect on the X-ray spectra pattern becomes weaker because of a supposed $TiC1_4$ lubricating effect [111].

The accelerating effect of $TiC1_4$ on the $MgCl_2$ activation could be due to $TiC1_4$ diffusion into the inter layers of the $MgCl_2$ structure thus facilitating the $MgCl_2$ crystal cleavage [110]. The limited extraction by exhaustive washing with hydrocarbons (Figure 2.9) or by treatment under vacuum of the Ti component, after an intensive ball milling, proves the strong bond existing between $TiCl_4$ and $MgCl_2$, probably due to a complexation on (110) or (101) faces as reported by Giannini [107] (Figure 2.10).

Table 2.3: Comparison between the crystallographic parameters of the active forms of $MgCl_2$ and $TiCl_3$ [107].

Product	δ-MgCl$_2$	δ-TiCl$_3$
Structure	Close packed layer structure with stacking defects	
Lattice parameters (Å)	a = b = 3.63 c = 5.93	a = b = 3.54 c = 5.86
Specific gravity (g/cm^3)	2.33	2.71
Cation coordination	Octahedral	
Atomic distances (Å)	Mg–Cl = 2.57	Ti–Cl = 2.51
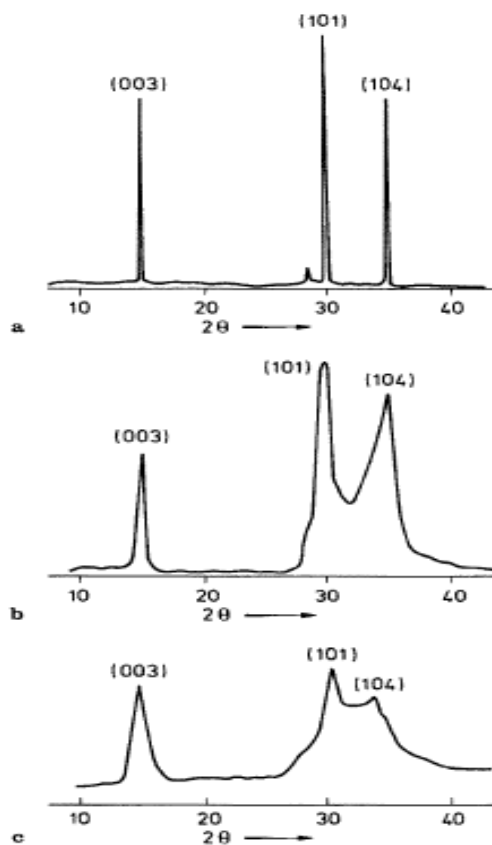
Figure 2.8: X-ray diffraction pattern of milled MgC1$_2$: (A) MgCl$_2$; (B) MgCl$_2$ alone 25 h milling; (C) MgCl$_2$ +0.12 TiCl$_4$, 25 h milling [113].
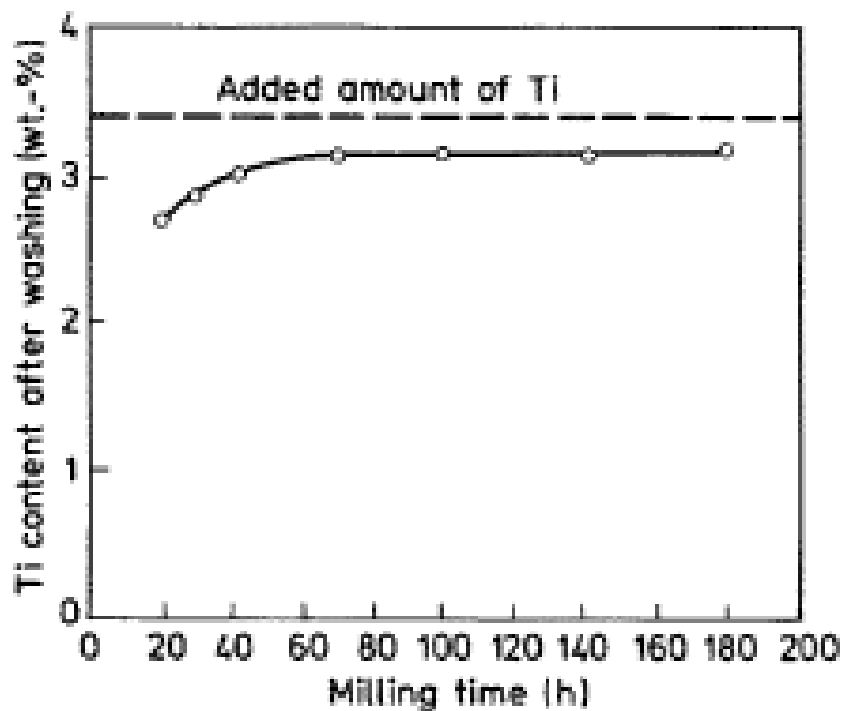
Figure 2.9:. Residual titanium content after washing as a function of the milling in MgCl$_2$ (+TiCl$_4$) samples[114].
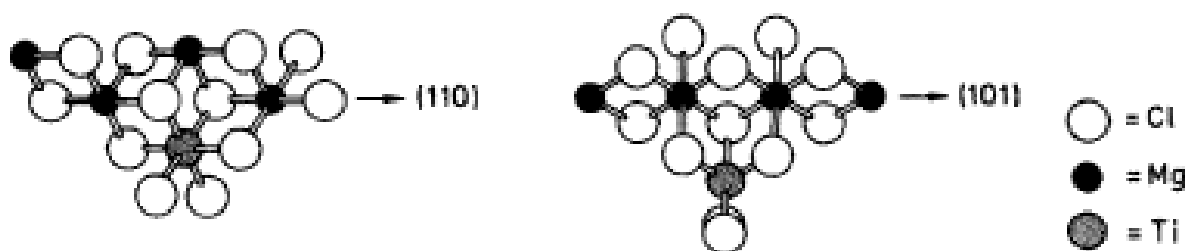
Figure 2.10: Hypotetic complexes of TiCl$_4$ on faces (110) and (101) of MgCl$_2$ [114].

The easy formation and the stability of the complexes may be due to the similarity of Ti^{4+} and Mg 2+ ionic radii (Ti^{4+} = 0.68 A^o, Mg^{2+} = 0.65 A^o) and, consequently, to the possibility of reciprocal substitution.

When fixed on MgCl$_2$ in this manner, Ti atoms have an extremely high catalytic activity for olefm polymerization, clearly superior to unsupported Ti atoms in TiCl$_3$-based conventional catalysts.

CHAPTER III

LITERATURE REVIEWS

3.1 MgCl$_2$-supported Ziegler-Natta Catalyst

MgCl$_2$.nROH effect

Madalena C. Forte and Fernada B. Coutinho [4], used precipitation technique preparing spherical particles of MgCl$_2$n EtOH support and TiCl$_4$, supported Ziegler-Natta catalysts with very good homogeneity in particle size and morphology. The EtOH/MgCl, molar ratio for the support preparation was varied in the range 1.0-10.0, and it was concluded that the best results were between 2.5 and 4.0. At EtOH/Mg ratios lower than 2.5 it was not possible to obtain the adduct in a totally melted form before its precipitation. However, at ratios higher than 4.0 it was not possible to attain good control of the support morphology.

They conclude that, the ethanol content had a strong effect on the MgCl$_2$n EtOH adduct preparation, and its precipitation and dealcoholation are very important factors that must be considered for good morphology to be attained in the spherical catalysts and polymers. Moreover, they reported that an increase in titanium content of final catalyst by decreasing alcohol content. This is due to increase in surface area of support during the dealcoholation that provided new surfaces for reaction of TiCl$_4$.

Choi, J. H., et al. [5], studied the effect of alcohol treatment in MgCl$_2$, preparation for PP. They prepared MgCl$_2$ catalyst support for propylene polymerization by dissolving MgCl$_2$ inethanol and/or i-propanol and recrystallizing it in an n-decane medium with vacuum drying. This support was modified by adding di-n-butyl phthalate as an internal electron donor, and subsequently TiCl$_4$ was impregnated on the modified support. And the effect of alcohol treatment on the catalytic activity and isotactic index (II) was examined. It was found that the propanol-treated catalyst showed a better performance than the ethanol-treated catalyst, owing to different amounts of remaining organic compounds. When the amounts of remaining alcohols were the same, it was also revealed that propanol was effective in enhancing the II. and ethanol was effective in enhancing the catalytic activity.

JalaliDil, E., et al.[6], synthesized the spherical support using melt quenching method. In order to increase support porosity and modifying its pore size distribution, a dealcoholation step was used. SEM images showed that by decreasing alcohol content, support morphology shifted toward a porous structure. Also, two competitive mechanisms were proposed to be engaged in this process: merging of primary particles and cracking of interior surfaces. Comparison of the present results with the previous studies showed that the final support morphology is completely dependent on time–temperature history. Also, this comparison showed that this parameter not only determines porosity and pore size distribution of final support but also controls the strength of support structure. Three support samples with different alcohol contents were used in catalyst preparation step. Results showed that by decreasing alcohol content of support, catalyst activity increased. This increase can be attributed to ready access of monomer to every point of catalyst particle and enhancement of heat transfer from active centers. Besides, by decreasing alcohol content of support, polymer morphology changed from eggshell morphology to a porous particle with an internal network.
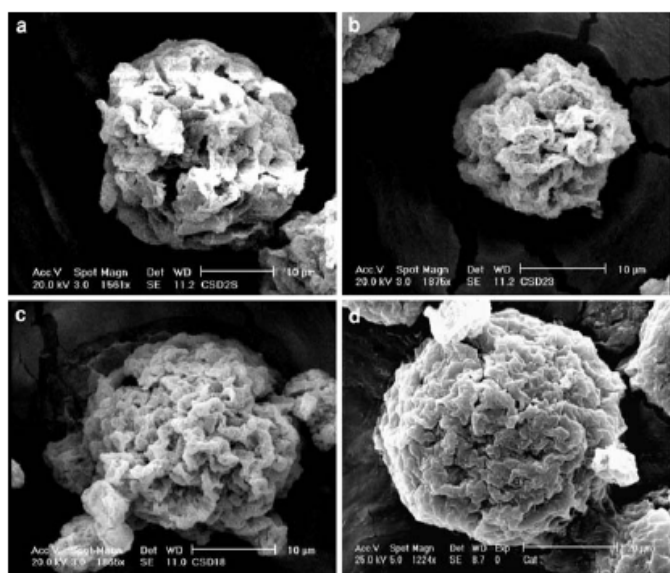
Figure 3.1: SEM image of (a) CSD28, (b) CSD23, (c) CSD18, (d) commercial catalyst [6].
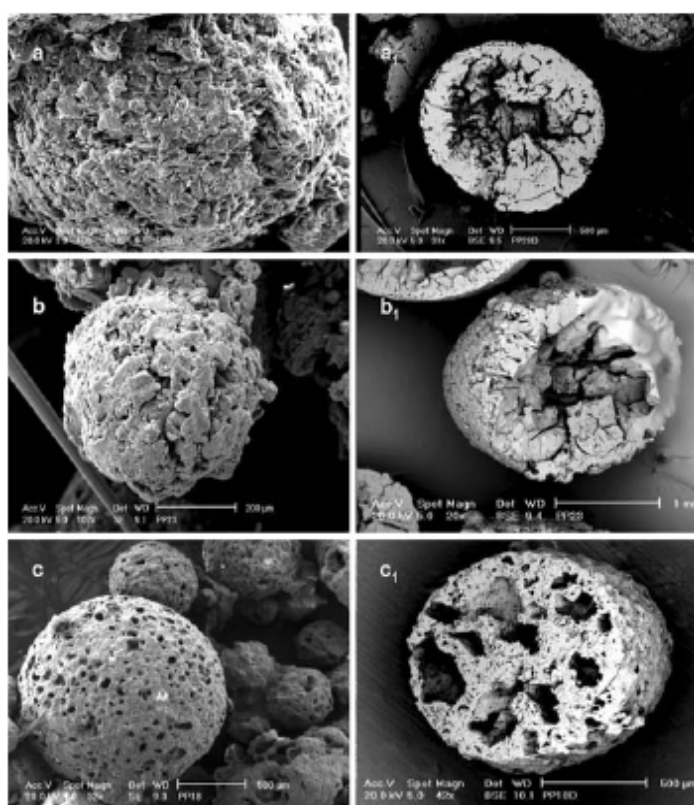
Figure 3.2: SEM image of polypropylene produced by: (a) CSD28, (b) CSD23, (c) CSD18. a1, b1, and c1 (right column) and a, b, and c (left column) show surface morphology and internal morphology of polypropylene particles, respectively [6].

Ye, Z.Y., et al.[7], prepared spherical $MgCl_2$ adducts used as supports for a Ziegler-Natta catalyst for olefin polymerization by precipitation method. The influence of $MgCl_2$/EtOH (mol/mol) and the dispersion speeds on the particle size (PS) and particle size distribution (PSD) were investigated. It was found that the former played a trivial role in controlling the PS and PSD, and the latter was the key factor. In particular, the influence of ethanol on the crystal structure was further examined, with consideration given to the performance of the supported Ziegler-Natta catalyst. It was believed that the reactions between $MgCl_2$ and ethanol had a controlling effect on the destruction of the original anhydrous $MgCl_2$, which was the key point in the preparation of suitable supports for the latest generation Ziegler-Natta catalyst. They also investigated the different factors, e.g. the treatment temperature, the internal donor (ID), the morphology of support and the sequence of adding the reagents, in preparation of spherical Ziegler-Natta catalyst.Their influence on the amount of titanium loading and the morphology of the prepared catalyst were evaluated. It is found that the treatment temperature, times of treatment with $TiCl_4$, ID and particle size of the $MgCl_2$ support play important roles in determining the Ti loading amount [8].

Important Conditions for Supported Catalyst Preparations	
Factor	**Affected Aspect**
Reagent purity	Catalyst performance
Agitation speed	PS and PSD
Time–temperature profile	Performance and composition
Reagent ratios	Particle shape and stereospecificity
Order of reagent addition	Morphology and performance

[8]

Jamjah, R., et al.[9], prepared spherical $MgCl_2 \cdot nEtOH$ by adducting ethanol to $MgCl_2$ using melt quenching method and studied the effect of molar ratio of $[EtOH]/[MgCl_2] = 2.8\text{-}3.05$ on the morphology and particle size of the $MgCl_2 \cdot nEtOH$ adducts. The best adduct of spherical morphology was obtained when 2.9 mol ethanol to 1 mol $MgCl_2$ was used. An emulsion of dissolved $MgCl_2$ in ethanol was prepared in a reactor containing silicon oil. Stirrer speed of the emulsion and its transfer rate to quenching section that work at -10 to -40°C are affected by the particle size of the adduct particle. The adducted ethanol was partially removed with controlled heat primary to catalyst preparation (support). Treatment of the support with excess $TiCl_4$ increased its surface area from 13.1 to 184.4 m^2/g. Heterogeneous Ziegler-Natta catalyst system of $MgCl_2$(spherical)/$TiCl_4$ was prepared using the spherical support. Scanning electron microscopy studies of adduct, support, and catalyst obtained shown spherical particles, however, the polyethylene particles obtained have no regular morphology. The behavior indicates harsh conditions used for catalyst preparation, prepolymerization, and polymerization method used.
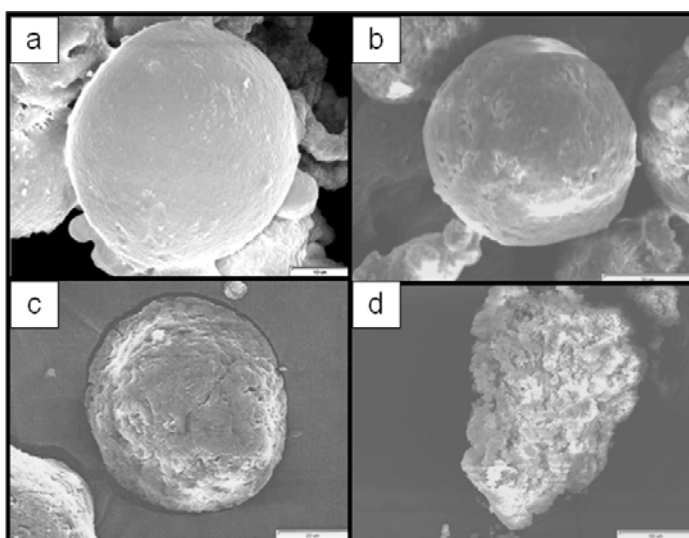
Figure 3.3: SEM micrograph of a) $MgCl_2nEtOH$, magnification 1500x, b) dealcoholated $MgCl_2nEtOH$ using heat magnification 1500, c) $MgCl_2$(spherical)/$TiCl_4$ catalyst: magnification 1200 and d) main polymerized polyethylene obtained: magnification 500x [9].

Wu, L., et al.[10],proposed a new to determine the power-law order of gas-phase ethylene homopolymerization rate with time-varying activities over morphology-controlled repolymerized catalyst at temperatures of 30-70 °C and ethylene concentrations of 120-900 mol/m^3. The prepolymerized catalyst was obtained by ethylene prepolymerization at mild conditions in heptane using a catalyst, in which $TiCl_4$ was supported on spherical $MgCl_2$ prepared by melt quenching of the $MgCl_2$-ethanol complex. Triethylaluminum was used as a cocatalyst for prepolymerization and homopolymerization. During ethylene homo-polymerization, the overall rate changed markedly with time, and two maxima in activity were observed in the absence of mass transfer effects. The order of power-law rate functions with respect to ethylene concentration was not constant and decreased with time on stream from about 1.5 to about 1.0 after about 4 h. These results show the presence of at least two types of catalytic sites having rates with different ethylene concentration dependencies and suggest that the two different types of catalytic sites have different deactivation behavior in this heterogeneous Ziegler-Natta catalyst.
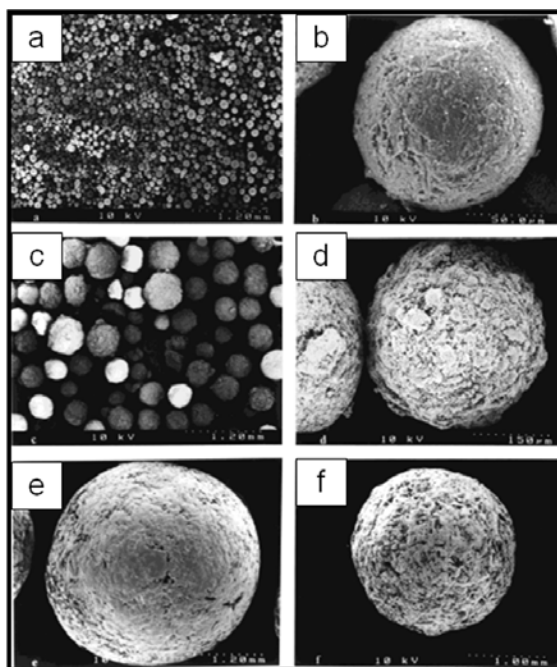
Figure 3.4: SEM micrographs of catalyst particles (a and b), prepolymer particles (c and d), and polymer granules (e and f) [10].

3.2 MgCl₂/SiO₂-supported Ziegler -Natta Catalyst

Zohuri, G., et al.[11], prepared ultra high molecular weight polyethylene using a morphologically improved catalyst system of $SiO_2/MgCl_2$(spherical)/$TiCl_4$. The bisupported catalyst showed a stable polymerization profile within a temperature range of 55ºC to 70ºC.The rate/time profile of the polymerization was a decay type. Polymerization activity of the catalyst was increased with increasing the monomer pressure, while increasing hydrogen concentration decreases the activity of the catalyst. Rate of the polymerization was found to be first order with respect to the monomer concentration. The initial stage of the polymerization, polymerization, including the reaction of the catalyst with the cocatalyst and the high polymerization activity, broke up the catalyst particles into smaller particles of irregular shape and size. The morphology of the polymer particles was almost the same as that of the catalyst, which reacted with the cocatalyst at the early stage of the polymerization. In addition, the morphology of the particles may be affected by polymerization conditions, such as temperature and monomer pressure. However, the parameters of the initial stages may also be critical.
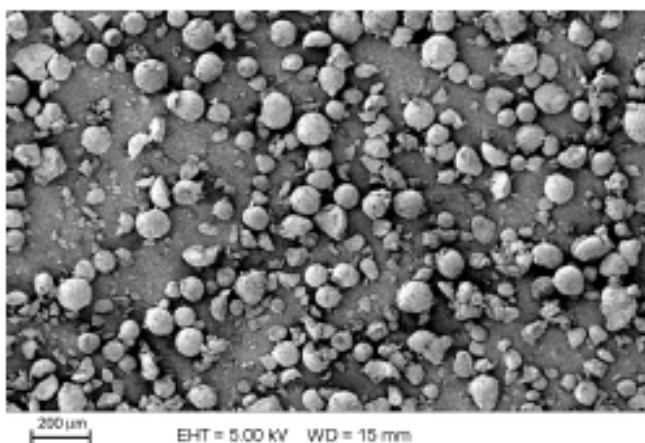
Figure 3.5: SEM micrographs of: (a) $SiO_2/MgCl_2$ (spherical)/$TiCl_4$,magnification 100x [11].
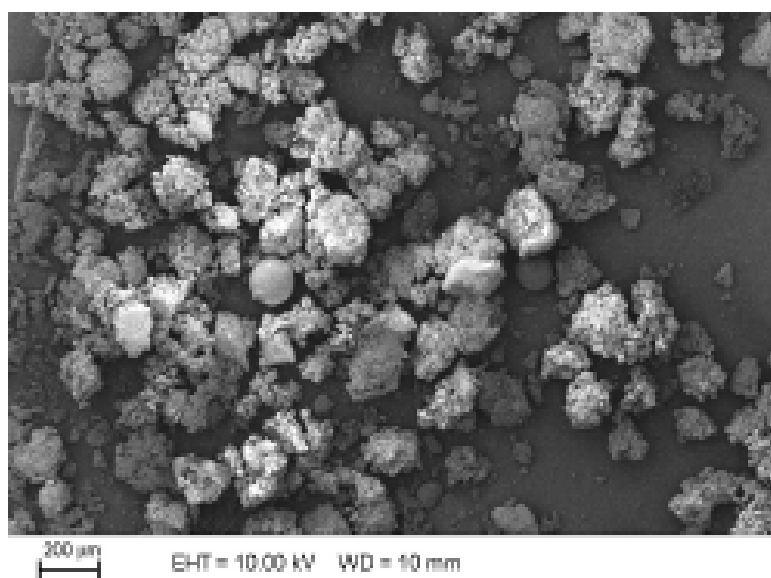
Figure 3.6. SEM micrograph of the polyethylene obtained using $SiO_2/MgCl_2$ (spherical) /$TiCl_4$/TEA catalyst system, polymerization time = 1 min, magnification 100x[11].
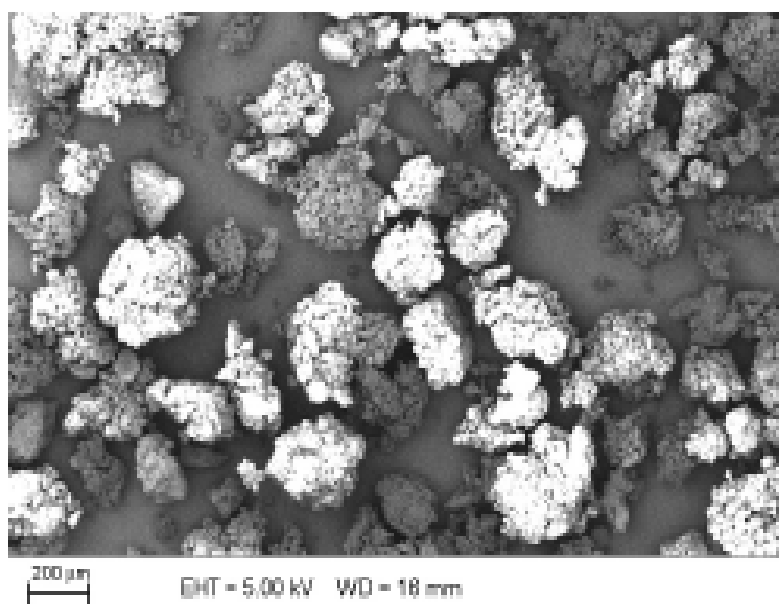
Figure 3.7: SEM micrograph of polyethylene, polymerization at 60ºC, monomer pressure = 2 bars, polymerization time =1 h, magnification 100x[11].

Chung, J.S., et al.[12], prepared ziegler–natta and metallocene hybrid catalysts on a bisupport by the polymerization of colloidal phase of SiO_2 using $MgCl_2$ solution as an initiator. The prepared bisupport was modified by treatment with alkyl aluminum compounds. In terms of the treatment of the prepared bisupport, trimethylaluminum (TMA) was superior to methylaluminoxane (MAO) with respect to the stability of the metallocene catalyst. The prepared hybrid catalysts exhibited characteristics of both Ziegler–Natta and metallocene catalysts. The polyethylene produced on the hybrid catalysts showed a bimodal molecular weight distribution in GPC profile and two different melting points in differential scanning calorimetry (DSC) thermogram.

Young S. K., et al. [13], prepared silica supported $MgCl_2/THF/TiCl_4$ catalyst $(SiO_2/MgCl_2/THF/TiCl_4)$, and then decomposed thermally. The amount of produced gas [tetrahydrofuran (THF) and 1,4-dichlorobutane (DCB)] was measured with gas chromatography (GC) and mass spectrometer. $SiO_2/MgCl_2/THF/TiCl_4$ catalyst started to decompose around 85‡C, and further decomposed at 113, 150 and 213‡C. THF was mainly produced, but very small amount of DCB evolved during temperature programmed decomposition (TPD), while unsupported $MgCl_2THF/TiCl_4$ produced DCB significantly. Polymerization rate of ethylene with $SiO_2/MgCl_2/THF/TiCl_4$ decreased when it was preheated at 85 and 110‡C for 5 and 60 min, respectively, while that of unsupported $MgCl_2/THF/TiCl_4$ increased after same pretreatment condition. It can be suggested that Mg/Ti bimetallic complex anchored on the surface of silica through OH group of it has weak interaction between Mg and Ti species.

Jiang, T., et al. [14], The $MgCl_2/SiO_2$ complex support was prepared by spray drying using alcoholic suspension, which contained $MgCl_2$ and SiO_2. The complex support reacted with $TiCl_4$ and di-n-butyl phthalate, giving a catalyst for propylene polymerization. The catalyst was spherical and porous with high specific surface area. TEA was used as a cocatalyst, and four kinds of alkoxysilane were used as external donors. The bulk polymerization of propylene was studied with the catalyst system. The effect of the reaction conditions and external donor on the polymerization was investigated. The results showed that the catalyst had high activity, high

stereospecificity, and sensitive hydrogen responsibility. Polypropylene has good grain morphology because of duplicating the morphology of the catalyst.

Wang, J., et al. [15], prepared novel $MgCl_2/SiO_2$-supported Ziegler–Natta catalyst using a new one-pot ball milling method. Using this catalyst, polyethylenes with different molecular weight distributions were synthesized. The effects of the [Si]/[Mg] ratio, polymerization temperature and [Al]/[Ti] ratio on the catalytic activity, the kinetic behaviour and the molecular weight and the polydispersity of the resultant polymer were studied. It was found that the polydispersity index of the polymer could be adjusted over a wide range of 5–30 through regulating the [Si]/[Mg] ratio and polymerization temperature, and especially when the [Si]/[Mg] ratio was 1.70, the polydispersity index could reach over 25. This novel bi-supported Ziegler–Natta catalyst is thus useful for preparing polyethylene with required molecular weight distribution using current equipment and technological processes.

Dong, Q., et al [16], investigated the effect of cocatalyst, triethylaluminum (TEA), triisobutylaluminum (TIBA) or TEA/TIBA mixtures of molar ratio 75/25, 50/50 and 25/75,   five different ethylene–propylene copolymer samples were synthesized by a $MgCl_2/SiO_2/TiCl_4$/diester type Ziegler–Natta catalyst in a slurry polymerization process. Both polymerization activity and copolymer structure were found to be markedly changed when the cocatalyst was changed from TEA to TEA/TIBA mixtures of molar ratio 75/25, 50/50, 25/75, or pure TIBA. The synthesized copolymers can be fractionated into two parts: a nearly random copolymer part and a segmented copolymer part. As the content of TEA in cocatalyst increases, yield of the random part of product increases and the yield of the crystalline segmented copolymer part decreases. There is also a decrease in ethylene content of the whole product with increasing TEA amount. Copolymerization behaviors of the TEA/ TIBA mixture activated catalysis systems are not simple superposition of those activated by pure TEA and TIBA. When a 50/50 TEA/TIBA mixture was used as cocatalyst, the copolymerization activity became the highest, and yields of both the random copolymer part and the segmented copolymer part are close to the highest level. On the other hand, both parts of the copolymer produced with a 50/50 TEA/TIBA mixture are relatively more blocky than the products of TEA or TIBA

systems, and the difference in ethylene content between the random part and the segmented part becomes the smallest. The segmented copolymer part can be further fractionated into fractions of different ethylene content and sequence distribution. Changing TEA content in the cocatalyst exerted strong influences also on the fraction distribution of the segmented part of copolymer.
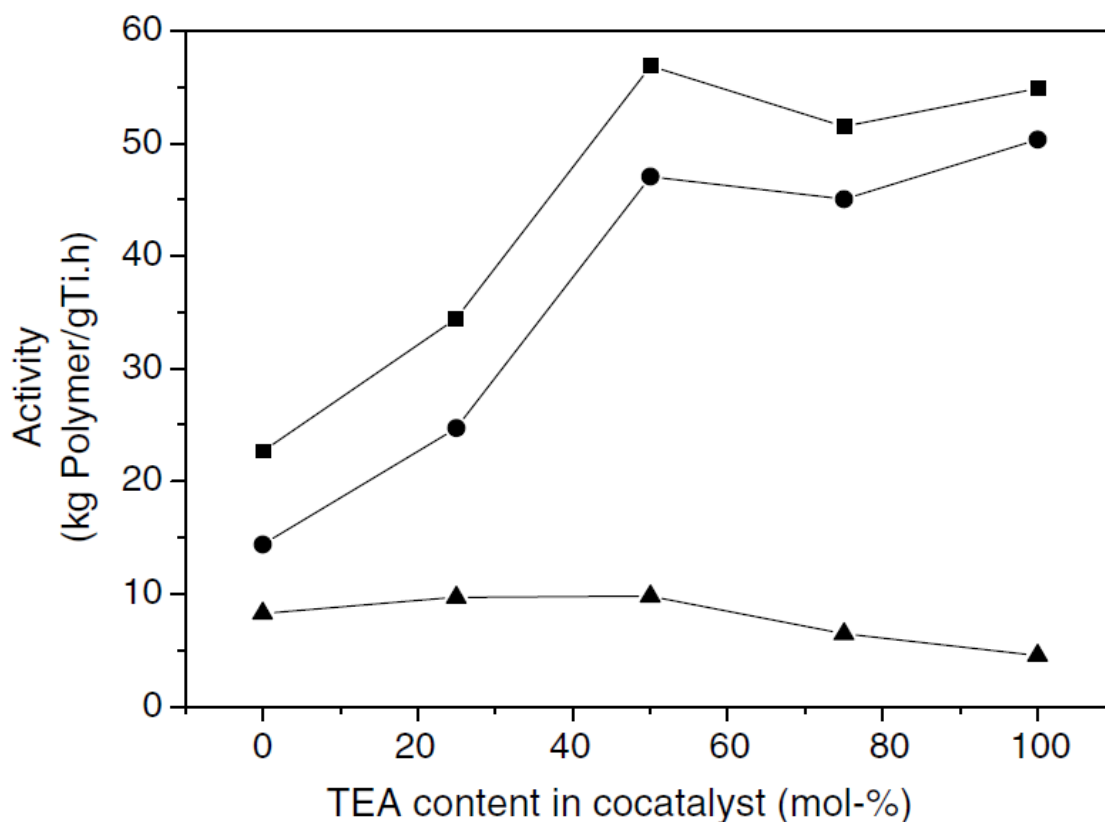
Figure 3.8: Effect of cocatalyst composition on the whole ethylene/propylene copolymerization activity (■) and separate efficiency of the n-octane insoluble copolymer (▲) and soluble copolymer (●) [16].

3.3 Mg(OEt)₂-Based Ziegler-Natta Catalyst

Tanase, S., et al. [17], synthesized $Mg(OEt)_2$ carrier materials by addition of metal dihalide compounds in the synthesis reaction of magnesium diethoxide using metallic magnesium,ethanol and iodine. Poly(propylene) polymerizations were then investigated with the $MgCl_2$-supported $TiCl_4$ catalysts using these carrier materials. As results, magnesium diethoxide with extremely large particle sizes and spherical shapes were obtained and the angles of repose of PP particles obtained by using their catalysts as a flowability index showed high values.

Dashti, A., et al.[3], investigated kinetic and morphological aspects of slurry propylene polymerization using a $MgCl_2$-supported Ziegler–Natta catalyst synthesized from a $Mg(OEt)_2$ precursor and compared with a ball-milled($MgCl_2$) Ziegler–Natta catalyst. The results shown that the two types of catalyst show completely different polymerization profiles: mild activation and long-standing activity with good replication of the catalyst particles for the $Mg(OEt)_2$-based catalyst, and rapid activation and deactivation with severe fragmentation of the catalyst particles for the ball-milled catalyst. The observed differences are discussed in relation to spatial distribution of $TiCl_4$ on the outermost part and inside of the catalyst particles.

The kinetics for Cat-C are of the build-up type with a slow activation rate, followed by a relatively long stationary period for 2 h. On the other hand, Cat-G showed a much higher initial activity followed by a significant decay, regarded as a decay-type profile.Most of the catalyst particles of Cat-C have spherical shapes, indicating good replication of the spherical $Mg(OEt)_2$ particles. It is notable that a few particles (bottom left of Figure 2.12(a)) showed a cracked structure while keeping a spherical shape, which might happen during the reaction of $TiCl_4$ with the $Mg(OEt)_2$ precursor. In Figure 2.12(b), almost all the Cat-G particles exhibit irregular shapes, namely non-spherical and largely different in size and shape, which must be due to the severe physical ball-milling process of the original $MgCl_2$ particles rather than the reaction of $TiCl_4$ with the ball-milled $MgCl_2$.
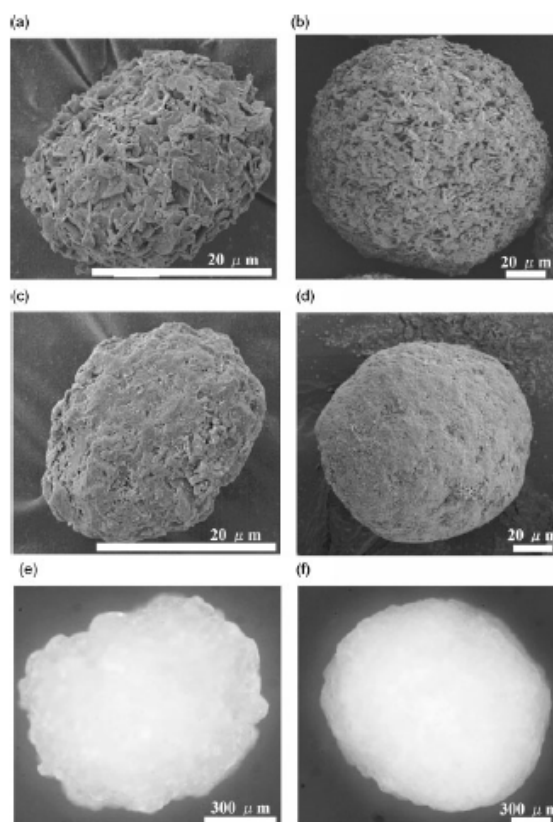
Figure 3.9: Addition effect of MnCl$_2$ for the morphology of carrier material, catalyst and PP particle: a) SEM image of MGE1 carrier without MnCl$_2$; b) SEM image of MGE4 carrier with MnCl2; c) SEM image of Catalyst1 obtained with MGE1 carrier; d) SEM image of Catalyst4 obtained with MGE4 carrier; e) optical microscope image of PP1; and, f) optical microscope image of PP4 [17].

Table 3.1: Details of the ZN catalysts employed [3].

Catalyst	Type	Ti[a] (wt%)	Average particle size[b] (µm)
Cat-C	Mg(OEt)$_2$-based	3.28	28.0
Cat-G	Ball-milled	1.70	21.8

[a] Characterized by titration.
[b] Determined by particle size distribution analysis.

[a] Characterized by titration.

[b] Determined by particle size distribution analysis.
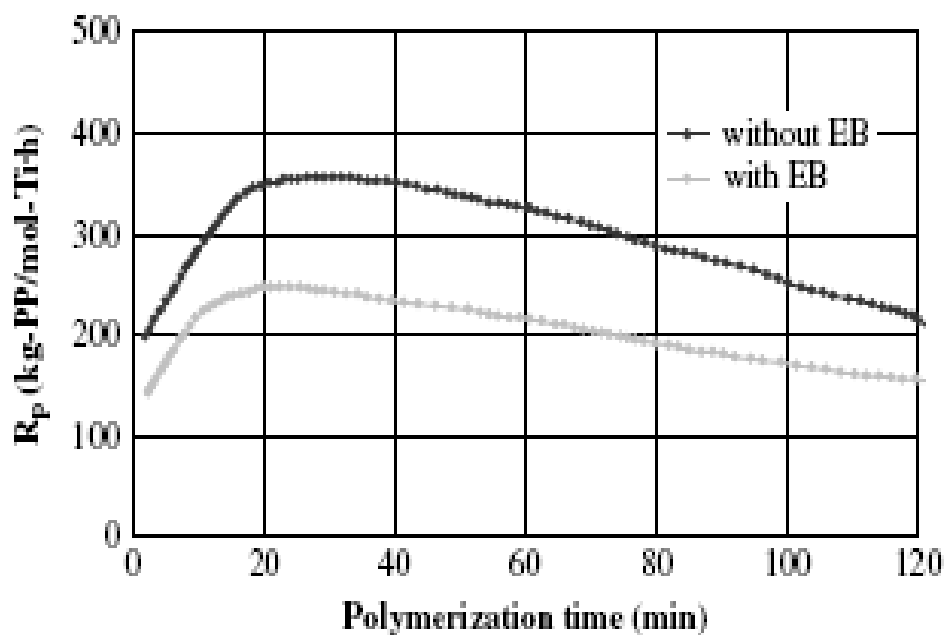
Figure 3.10: Kinetic profiles of propylene polymerization using Cat-C with and without EB as an external donor[3].
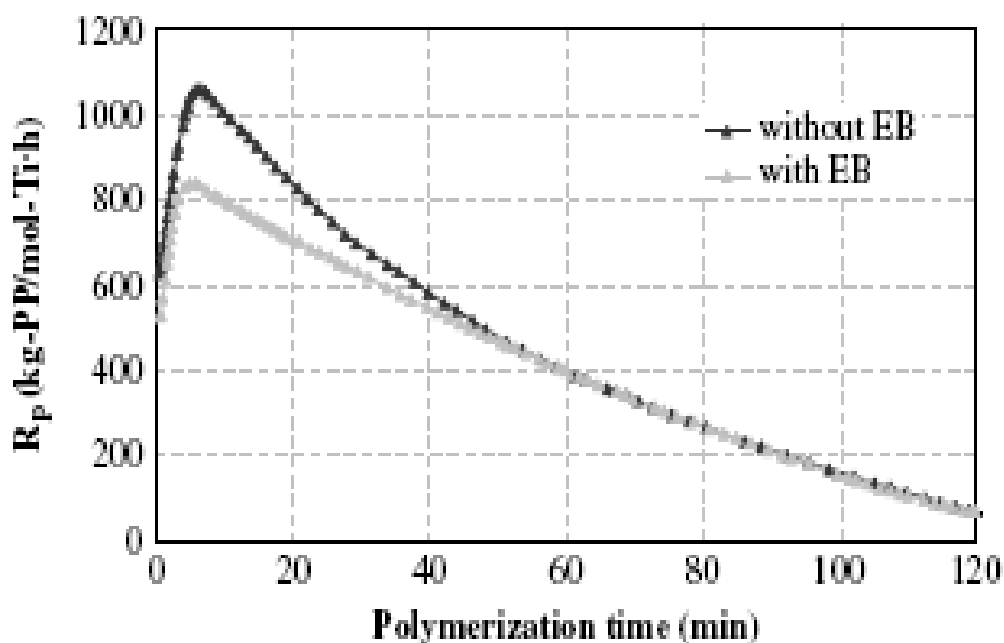
Figure 3.11: Kinetic profiles of propylene polymerization using Cat-G with and without EB as an external donor [3].
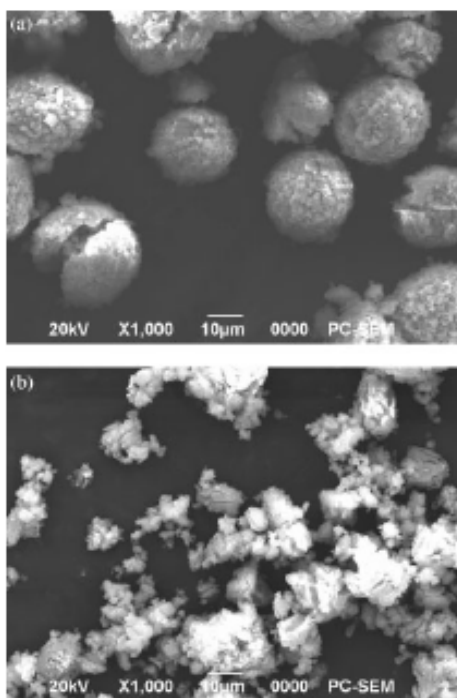
Figure 3.12**:** SEM images of the original catalyst particles: (a) Cat-C; (b) Cat-G [3].
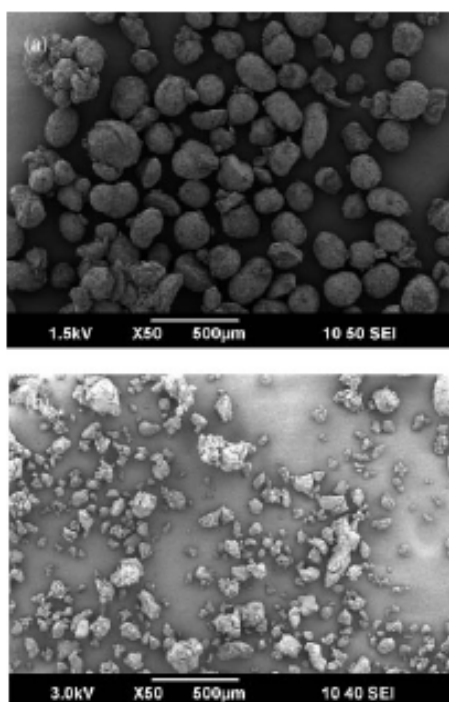
Figure 3.13**:** SEM images of PP particles (a) using Cat-C after 90 min of polymerization in the presence of EB as an external donor and (b) using Cat-G after 60minwith EB [3].

The polymer particles have spherical shapes, replicating the shape of the Cat-C in Figure 3.13(a). A few particles have non-spherical shapes, such as agglomerated or broken ones. A plausible origin of this might be the fracture of the original catalyst particles that was occasionally found in the SEM image of Figure 3.12(a) (bottom left corner). At the early stage of the polymerization, the rapid growth of polymer inside catalyst pores generally forms a tension.This tensile force might overcome the strength of the fractured parts in order to separate them into some irregular particles. The SEM image for the polymer particles produced using Cat-G shown in Figure 3.13(b) reveals poor particle morphology including irregular shapes and fine particles, which look similar to the morphology of the original catalyst.

Abboud, M., et.al [1], studied morphological and kinetic characteristics of novel Ziegler–Natta catalysts . Catalysts were prepared by Borealis Polymers Oy using a new synthesis technique (emulsion technology) consists of *in situ* formation of a liquid/liquid two-phase system in which one phase is a solution of the catalyst components or its precursor ($TiCl_4$, magnesium alkoxide, internal donor) in an inert solvent. The second stage is the emulsification, which is performed using a special kind of surfactant for stabilizing the catalyst droplets. The final stage of the route is solidification of the catalyst droplets. This is performed simply by changing the reaction conditions of the emulsion system. This catalyst called Cat E, nonsupported catalyst because it did not contain an external support. Also prepared was another catalyst that was supported on silica and was based on the same catalyst chemistry. The silica used for catalyst support came from Grace Davison (55SJ, SYLOPOL).This catalyst called Cat B, supported catalyst.
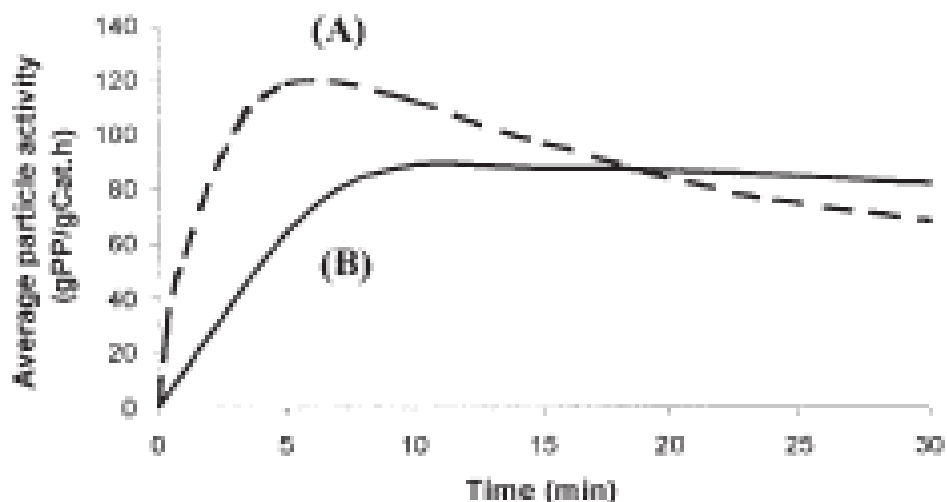
Figure 3.14: Activity profile determined by video microscopy of (a) nonsupported Ziegler–Natta catalyst (Cat E) and (b) silica-supported Ziegler–Natta catalyst (Cat B). Polymerization was performed in the gas phase at a propylene pressure of 5 bar and a temperature of 45°C [1].

They found that a correlation between the activation period during the initial stage of polymerization and catalyst fragmentation. Fragmentation was faster and more uniform with the catalyst without external support than with the silica-supported catalyst. SEM provided information on morphology evolution and shape replication of the catalyst particles. With the catalyst without external support, good shape replication was observed, and compact and spherical particles were formed. With the silica-supported catalyst, shape replication was poor, and non-spherical porous polymer particle were formed. Modeling of the kinetics of propylene polymerization was done using a simple three step reaction scheme neglecting mass and heat transport effects.
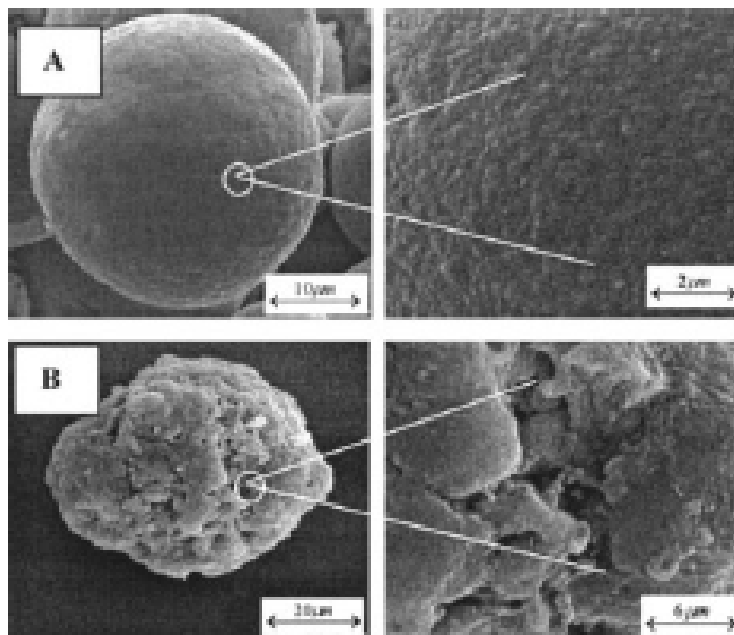
Figure 3.15: SEM images of catalyst particles of the (a) nonsupported (Cat E) and (b) silica-supported (Cat B) Ziegler–Natta catalysts (not activated) [1].
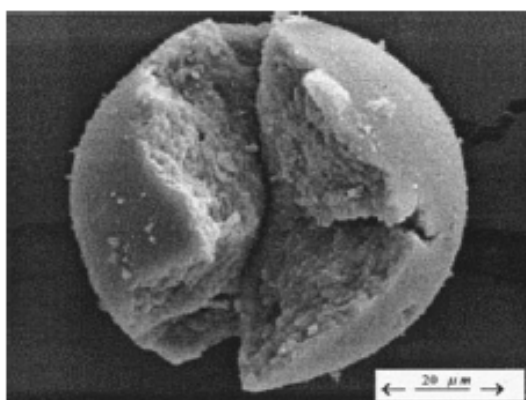
Figure 3.16: A catalyst particle shortly after polymerization (20 s) showing an open structure [polymerization with the nonsupported Ziegler–Natta catalyst (Cat E) performed at a propylene pressure of 5 bar and a temperature of 80 $^{\circ}$C] [1].
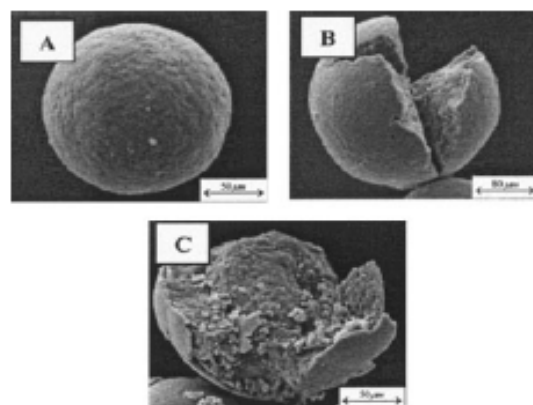
Figure 3.17: SEM images of polypropylene particles produced by the nonsupported Ziegler–Natta catalyst (Cat E) [1].
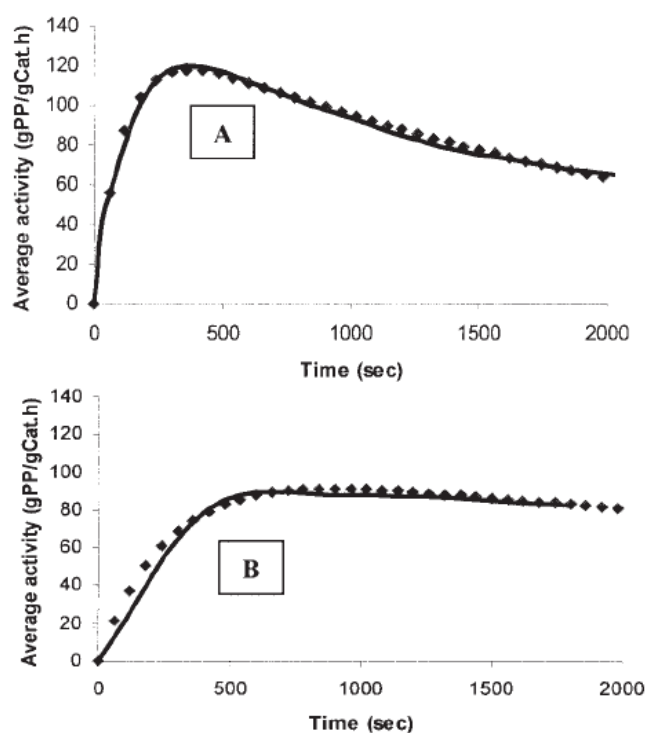
Figure 3.18: Average particle activity of (a) nonsupported (Cat E) and (b) silica-supported (Cat B) Ziegler–Natta catalysts versus time. Polymerization was performed for 1 h in the gas phase at a propylene pressure of 5 bar and a temperature of 45°C (dots : experiment; line : model).

Table 3.2: Fitted Kinetic Parameters at 5 bar and 45°C for Both Catalyst Systems[1].

Catalyst	Rate constants		
	k_i (1/mol s)	k_p (1/mol s)	k_d (1/s)
Cat E	3.5×10^{-2}	550	4.0×10^{-4}
Cat B	2.0×10^{-2}	550	1.4×10^{-4}

Additional, they concluded that a nonporous catalyst may have a high level of activity. Until now, it was believed that a highly porous catalyst was needed in order to achieve high activity. The synthesis of a catalyst system with a narrow activity distribution of catalyst particles requires a support with the characteristics of homogeneous fragmentation and uniform distribution of the active catalyst complex. Mass transport effects seemed to play a minor role during polymerization with the novel catalyst system because the activity of catalyst particles was observed to be independent of their size under the reaction conditions studied.

They also produced two catalyst using Borealis Polymers OY (Finland), and the synthesis methods are compared. The first method (Method One) is based on an emulsion system and consists of an in situ single step preparation. The second method (Method Two) consists mainly of two steps: formation of the catalyst carrier particles, and their subsequent impregnation with the active material. The results showed that Method One produced catalysts of compact, spherical particles with good intra-particle homogeneity and a narrow particle size distribution. On the other hand, Method Two produced catalyst particles whose properties depended directly on that of the catalyst carrier: they were spherical but very porous, with a broad particle size distribution. Polymer particles produced with the two catalyst systems are perfect replicas of the catalyst particles. Fines formed either during catalyst preparation or during polymerization were observed only with the catalyst prepared using Method Two. The particles of the catalysts produced using Methods One and Two had similar activities, independent of the initial particle size. Fragmentation of catalyst particles was very fast for both catalyst systems and was only observed to be 100% completed using the catalyst produced with Method One. Studies of the thermal properties showed that the catalyst prepared using Method One produced poly(propylene) of higher crystallinity and with a narrower melting peak [18].
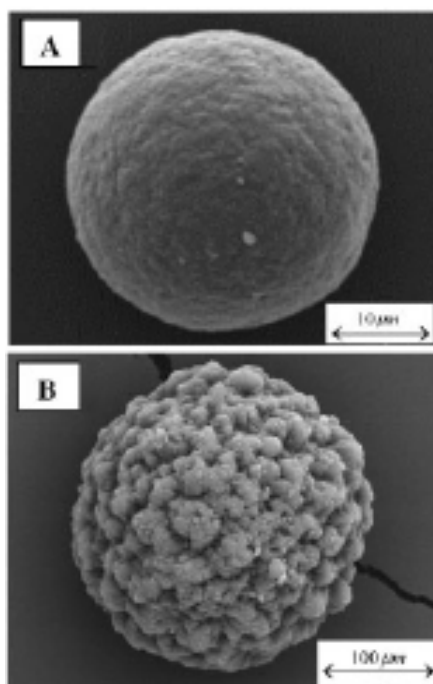
Figure 3.19: SEM images of polymer particles produced by (A) Method One (MGE as precursor) and (B) Method Two (MgCl$_2$ adduct) [18].

Table 3.3: Specifications of the Ziegler-Natta catalysts used for the propylene polymerization [18].

Method	Catalyst	Ti	Mg	Support	Surface area[a]	Average particle size[b]
		wt.-%	wt.-%		$m^2 \cdot g^{-1}$	μm
Method One	Catalyst 1	3.0	10.2	Self-supported	1–2	23
Method Two	Catalyst 2	2.0	21	MgCl$_2$-supported	>300	70

[a] The surface area measured by the BET method using a Micromeritics ASAP 2400.
[b] Measurements were performed using a Coulter LS 200.

[a] The surface area measured by the BET method using a Micromeritics ASAP 2400.

[b] Measurements were performed using a Coulter LS 200.
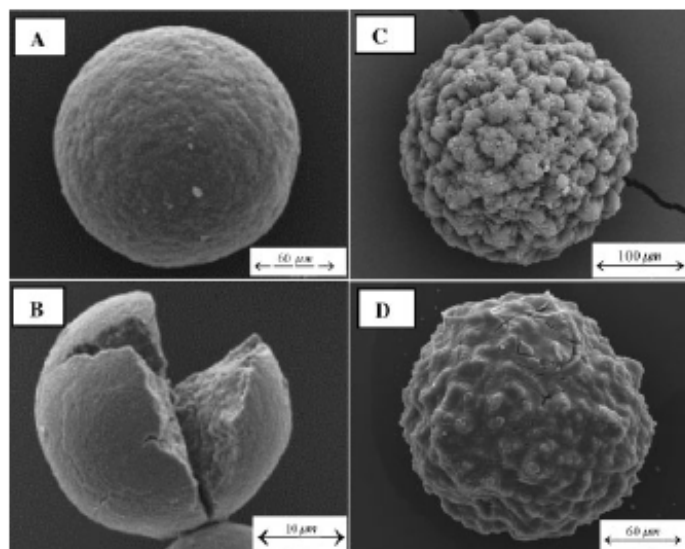
Figure 3.20: SEM images of polymer particles produced with Catalyst 1: (A) mild reaction conditions (polymer/catalyst = 20, $t_{reaction}$ = 60 min), (B) severe reaction conditions (polymer/catalyst = 4, $t_{reaction}$ = 1 min) and with Catalyst 2: (C) mild reaction conditions (polymer/catalyst = 20, $t_{reaction}$ = 60 min), (D) severe reaction conditions (polymer/ catalyst = 4, $t_{reaction}$ = 1 min) [18].
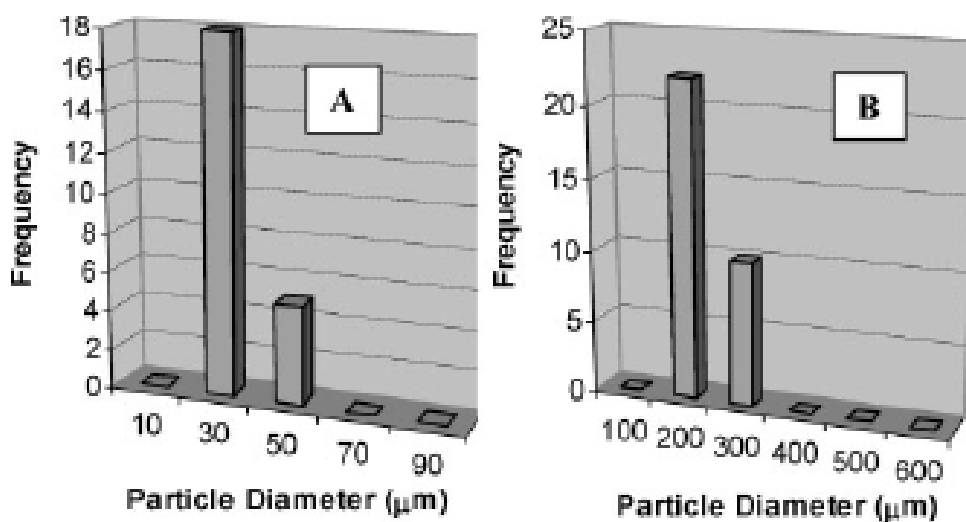
Figure 3.21: Size distribution (particle diameter) determined by video microscopy of (A) catalyst particles of Catalyst 1 and (B) polymer particles produced with this catalyst by gas phase polymerization after 1 hour at 5 bar and 45 ^{o}C [18].

Joseph, J., et al. [19] suggested that magnesium ethoxide formation occurs at the interphase surface of metal and ethanol. The resultant magnesium ethoxide grows on the surface of magnesium particles. Parameters like characteristics of magnesium particles, reaction rate, and shearing in the reaction mass are critical in determining the particle size and shape characteristics of magnesium ethoxide. Rate of the reaction during the synthesis of magnesium ethoxide was found to vary inversely with the mean diameter of magnesium granules. The particle morphology of magnesium ethoxide shows a relation with the size of magnesium particles used in the reaction. Use of small magnesium particles resulted in very high reaction rate, giving rise to increased fines and fragmented particles. The reaction is well controlled when bigger magnesium particles are used, resulting in excellent morphology of resultant magnesium ethoxide. Magnesium ethoxide produced using controlled reaction kinetics has crystallite size of <50nm for different peak positions. Activation energy was found to decrease as the mean particle size of magnesium decreases; consequently the rate of reaction is highest for the reaction where lowest size magnesium granules are used.
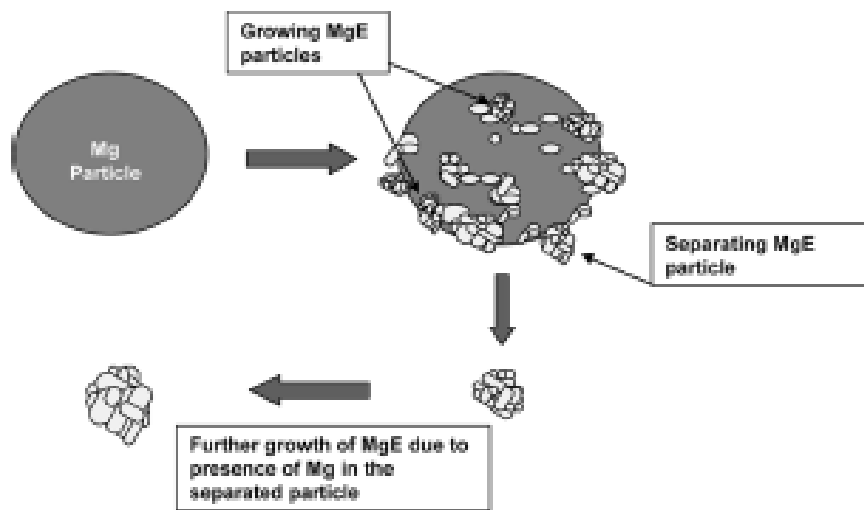
Figure 3.22: Magnesium ethoxide particle formation on the surface of magnesium particle[19].
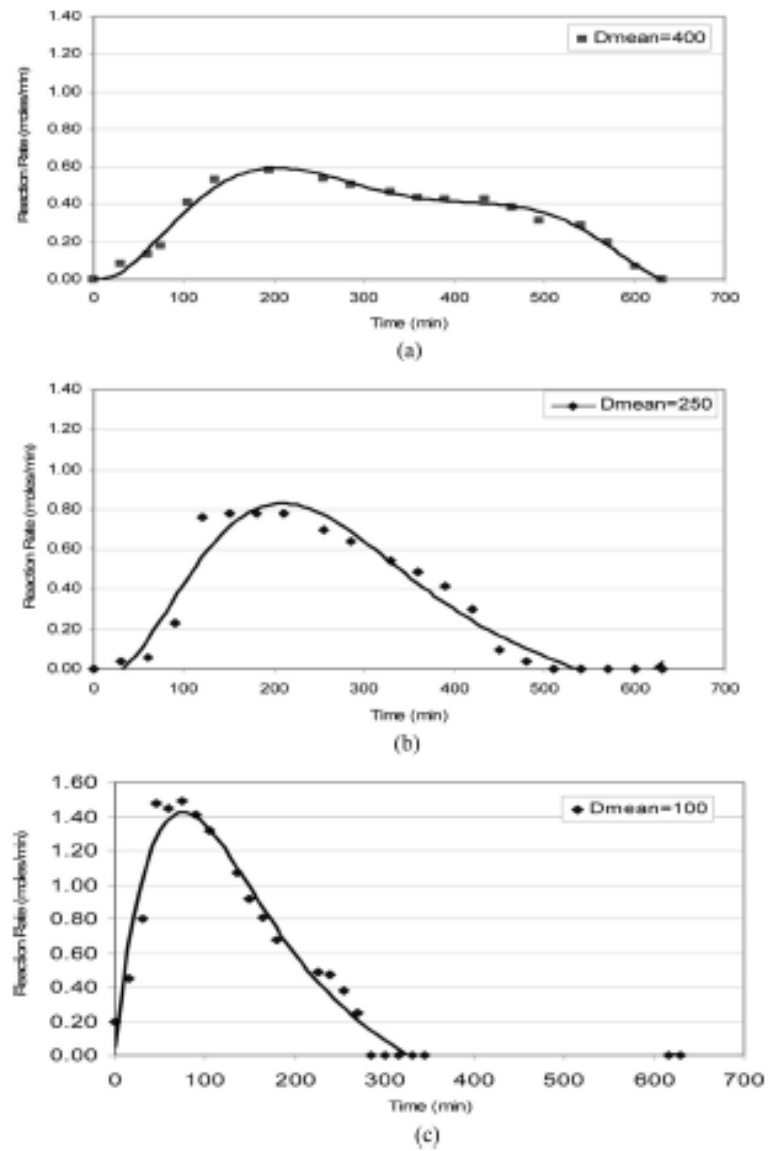
Figure 3.23: Rate of reaction (moles/L˙ min) for magnesium particles having mean diameters of (a) 400 µm, (b) 250 µm, and (c) 100 µm [19].
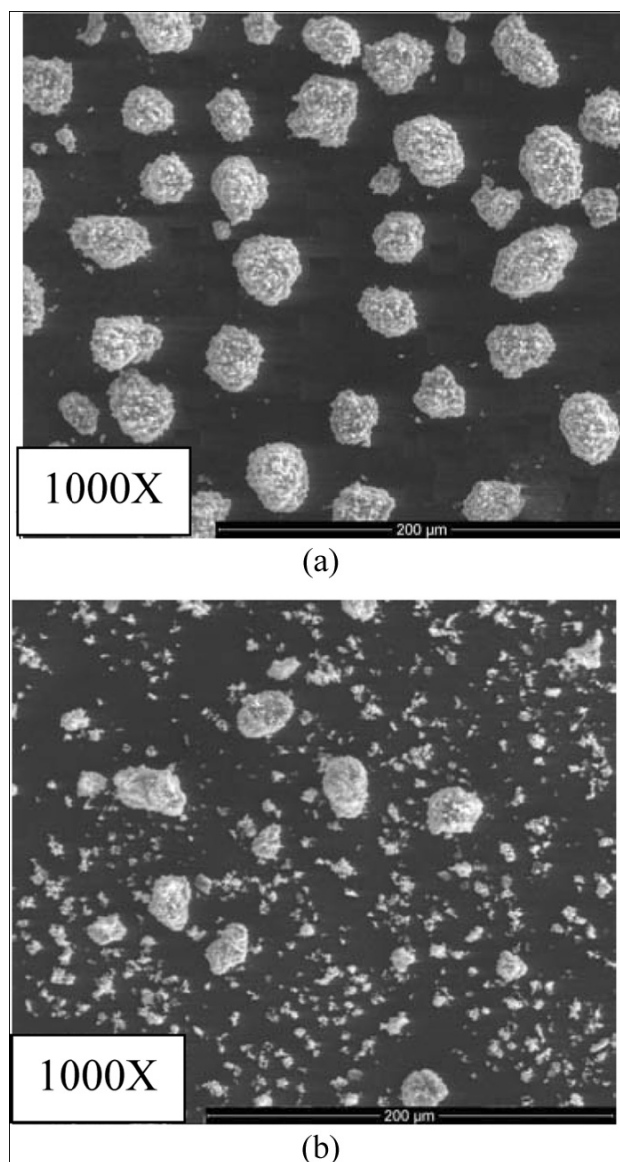
Figure 3.24: SEM image of magnesium ethoxide prepared through (a) controlled reaction kinetics and (b) uncontrolled reaction kinetics[19].

Their results indicate that the controlled reaction kinetics is essential in producing morphological magnesium ethoxide. The uncontrolled reaction resulted in fines generation, which is undesirable for ZN catalyst systems. Optimized conditions such as agitator type, agitator rpm, and controlled reaction rate are required for achieving the desired particle characteristics of magnesium ethoxide from magnesium particles.

CHAPTER IV

EXPERIMENTAL

4.1 Chemicals

4.1.1 Chemical 1

The chemicals used in these experiments, carried out at the Center of Excellence on Catalysis and Catalytic Reaction Engineering, were specified as follows:

1. Polymerization-grade propylene (C_3H_6) was used as received from PTT Chemical Plc. (Thailand)

2. Ultra high purity argon (99.999%) was purchased from Thai Industrial Gas Co., Ltd. (TIG) and was further purified by passing through the column packed with molecular sieve 3Å,

3. Anhydrous magnesium chloride ($MgCl_2$, >98%) was purchased from Sigma-Aldrich Inc.

4. Silica (SYLOPOL 2229) was received from Grace Davison.

5. Titanium tetrachloride ($TiCl_4$, > 99%) was purchased from MERK.

6. Triethylaluminum ($Al(C_2H_5)_3$) in hexane solution, was donated from PTT Chemical Plc., (Thailand)

7. Ethanol was purchased from MERK.

8. n-Heptane (C_7H_{14}, 99.84%) was purchased from SR lab.

9. Toluene ($C_6H_5CH_3$, >98%) was purchased from SR lab.

10. Benzophenone (purum 99.0%) was obtained from Fluka Chemie A.G. Switzerland.

10. Sodium (lump in kerosene, 99.0%) was supplied from Aldrich chemical Company, Inc.

11. Commercial-grade methanol was purchased from SR lab.

12. Hydrochloric acid (Fuming 36.7%) was supplied from Sigma-Aldrich Inc.

4.1.2 Chemical 2

The chemicals employed during the experimental research at Terano Laboratory, Japan. Only critical materials are summarized in the following lists:

1. Propylene of research grade, donated by Chisso Corp., was used without further purification.

2. Anhydrous grade of methanol and ethanol were purchased from Wako Pure Chemical Industries Ltd., were used after degassed, dehydrated with molecular sieves 4Å and stored under argon atmosphere.

3. Ethylbenzoate (EB) and 2,2-isopentyl-isopropyl-1,3-dimethoxy propane (IPIPDMP) were purchased from Wako Pure Chemical Industries Ltd. The internal donors were used after dehydration with molecular sieves 13X under a nitrogen atmosphere.

4. Anhydrous magnesiumethoxide ($Mg(OEt)_2$) donated by Toho Titanium Co. Ltd. and used without further purification.

5. Titaniumtetrachloride ($TiCl_4$) purchased from Wako Pure Chemical Industries Ltd. and used as received.

6. Triethylaluminium (TEA) was donated by Tosoh Akzo Corp.

7. High purity nitrogen, purchased from Uno Sanso Co., was used without further purification.

8. n-Heptane and toluene, purchased from Wako Pure Chemical Industries Ltd., as solvents were purified by passing through molecular sieves 13X

4.2 Catalyst preparation

4.2.1 Preparation of the MgCl$_2$-supportedd Ziegler-Natta catalyst.

The 3-necked round bottom flask equipped with mechanical stirrer, Ar inlet and outlet line and cooling system. Anhydrous MgCl$_2$ (3.0 g) was suspended in heptane (20 ml), then ethanol was added to the slurry with desired amount under a stream of Ar. The mixture was heated to 80 ^{o}C and stirred until MgCl$_2$ was completely dissolved. Then the slurry was cooled down to -20 ^{o}C and TiCl$_4$ was added drop wise with speed of 25 ml/h. The temperature was slowly increased to 80 ^{o}C and cooked for 1 h. The solid was washed with heptane (50 ml) 3 times. TiCl$_4$ (18 ml) and heptane (18 ml) was added to the mixture to activated intermediate at 95 ^{o}C for 1 h. The supernatant was removed, and the solid catalyst was washed with heptane several times. The resultant bi-supported catalysts were dried in a vacuum at room temperature.

4.2.2 Preparation of the bi-supported MgCl$_2$/SiO$_2$-supportedZiegler-Natta catalyst.

The 3-necked round bottom flask equipped with mechanical stirrer, Ar inlet and outlet line and cooling system. Anhydrous MgCl$_2$ (3.0 g) was suspended in heptane (20 ml), then ethanol was added to the slurry with desired amount under a stream of Ar. The mixture was heated to 80 ^{o}C and stirred until MgCl$_2$ was completely dissolved. Then, SiO$_2$ (6.0 g) in heptane (40 ml) was transferred to reactor using teflon tube while stirred and the mixture was stirred for 1 h at 80 ^{o}C. The mixture was cooled down to room temperature with continuous stirring. Bi-support solid was washed with toluene (50 ml) 2 times and heptane (50 ml) 2 times to remove the remaining alcohol. Heptane (60 ml) was added into reactor, then, the slurry was cooled down to -20 ^{o}C and TiCl$_4$ was added drop wise with speed of 25 ml/h. The temperature was slowly increased to 80 ^{o}C and cooked for 1 h. The solid was washed with heptane (50 ml) 3 times. TiCl$_4$ (18 ml) and heptane (18 ml) was added to the mixture to activated intermediate at 95 ^{o}C for 1 h. The supernatant was removed, and the solid catalyst was washed with heptane several times. The resultant bi-supported catalysts were dried in a vacuum at room temperature.

4.2.3 Preparation of the $MgCl_2$(ethoxide type)/$TiCl_4$ catalysts.

The 500 ml of 3-necked round bottom flask equipped with motor stirrer, N_2 inlet and outlet line and cooling system. 10 g of $Mg(OEt)_2$ powder was suspended in toluene (60 ml) at room temperature, then the suspension was cooled down to -20°C. 20 ml of $TiCl_4$ was added drop wise to the suspension at low temperature over 1 h. The mixture was then heated to desired temperature and kept under stirring for 2 h. The excess $TiCl_4$ and by product were washed with toluene several times at desired temperature. The 50 ml of toluene and 20 ml of $TiCl_4$ were added to the intermediate at the same condition as previous. Supernatant was removed and catalyst solid was washed with heptane several times.

It was noted here that the first treatment of $Mg(OEt)_2$ with $TiCl_4$ and the second treatment of obtained $MgCl_2$ with $TiCl_4$ were conducted using the same treatment temperature and treatment time for both step.

4.2.4 Preparation of the $MgCl_2$(ethoxide type)/ID/$TiCl_4$ catalysts.

The catalysts were prepared similarly to the above procedure except for after adding $TiCl_4$ to $Mg(OEt)_2$ then the mixture was heated to desire temperature and internal electron donor (EB or IPIDMP) was added to the reaction mixture and kept under stirring at desired conditions. It was noted here that the first treatment of $Mg(OEt)_2$ with $TiCl_4$ in the presence of ID and the second treatment of obtained $MgCl_2$ with $TiCl_4$ were conducted using the same treatment temperature and treatment time for both step.

4.3 Polymerizations

4.3.1 Screening catalyst using 100 ml stainless steel, autoclave reactor

Ethylene polymerization was conduct using 0.01 g of catalyst powder, Al/Ti = 100, for ethylene monomer consumption 6 psi, under 80°C and 50 psi total pressure. A 100 ml stainless steel autoclave was used, with magnetic agitation, in 30 ml of n-hexane.

The reaction was stopped by venting the monomer and quenching with HCl/methanol. The obtained polymer was washed several times with methanol, filtered and dried under vacuum at 60°C

4.3.2 High pressure slurry propylene polymerization

A 1 L stainless steel autoclave was purified with N_2 several times. Heptane was transferred to the reactor with desired amount (total solution = 300 ml), 3 mmol of TIBA as cocatalyst and catalyst corresponding to Al/Ti= 30 and 300 for ethylene and propylene polymerization, respectively, were injected under inert gas flow. Monomer was introduced to reactor for 5 MPa and polymerization was performed at 50 ^{o}C for 1 h. For stop the polymerization, EtOH/HCl was added to reactor. The resultant polyethylene and polypropylene were filtered and dried under vacuum at 60 ^{o}C for 6 h.

4.4 Characterizations

4.4.1 Scanning electron microscopy (SEM)

4.4.1.1 SEM 1

Morphological study of $MgCl_2$-SiO_2-supported catalyst was investigated using scanning electron microscopy (SEM, JEOL mode JSM-6400).

4.1.2 SEM 2

Macroscopic catalyst morphology was observed by a scanning electron microscopy (SEM, Hitachi, S-4500). The samples were attached on a sample stage covered by a carbon tape under N_2 atmosphere, and then sputtered by Pt/Pd ionsputter

(Hitachi, E-1030) rapidly to minimize exposure of the samples to air. SEM observation was performed with an accelerating voltage of 20 kV. Cross-section of $Mg(OEt)_2$ precursor and catalyst particles were prepared by random cutting by a razor under N_2 atmosphere.

4.4.2 Nuclear magnetic resonance (NMR)

The stereroregularity (mmmm) of synthesized PP was determined by ^{13}C NMR spectroscopy (BRUKER AVANCE II 400 spectrometer) operating at 100 MHz and 110°C with an acquisition number of 7000. Sample solutions were prepared by dissolving of polymer in 1,2,4-trichlorobenzene and deuterated chloroform-d6 (CDCl3-d_6) was used for an internal lock signal.

4.4.3 BET surface area

Measurement of BET surface area, pore volume and pore size diameter of catalysts were determined by N_2 physisorption and Kelvin condensation using a Micromeritics ASAP 2000 automated system.

4.4.4 Thermogravimetric analysis (TGA)

TGA was performed using a TA Instruments SDT Q 600 analyzer with temperature ramping from 40 to 500 °C at 10 °C/min. The carrier gas was N_2 (UHP).

4.4.5 Inductively coupled plasma spectroscopy (ICP)

The Ti content in catalysts was determined by inductively coupled plasma spectroscopy (ICP) using the Perkin-Elmer Plasma 1000 system.

4.4.6 X-ray diffraction(XRD)

The crystallite structure was evaluated by the wide-angle X-ray diffraction (WAXD, Rigaku, Rint 2500) using $CuK_\propto$ radiation at 40 kV and 20 mA. The X-ray diffractograms were recorded using a step scanning program in 2θ range from 5- 55° at a recording rate of 0.75 deg/ min with 3 integration times. Samples were fill in a sample holder and smoothing with glass and covered with poly(cthylene terephthalate) (Mylar) film of 2.5 µm thickness. The samples were handled under N_2 atmosphere using glove bag to avoid air exposure.

4.4.7 Fourier transform infrared (FTIR)

FTIR analysis was performed using a Bruker EQUINOX 55 instrument, with 4 cm^{-1} resolution and 400 scans. The sample was prepared in glove box under Ar atmosphere. The catalyst powder was sandwiched between two plates of a NaCl and sealed the side with tape to protect the catalyst from moisture and air.

4.4.8 Titanium titration

Titanium content was determined using titration method. The catalyst (1g), distillated water (50 ml), HCl (50 ml), H_2SO_4 (30 ml) and Al pellet (5 pellets) were transferred into erlenmeyer flask, the mixture was stirred until clear solution appear. The solution was continuously stirred until cool down to room temperature. Potassium thiocyanate (SCN) as the indicator was introduced to clear solution then titration was performed with ferric sulphate solution.

$$Ti^{3+} + Fe^{3+} = Ti^{4+} + Fe^{2+}$$

$$Fe^{3+} + SCN^- = Fe(SCN)^{2+} \text{ (red)}$$
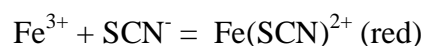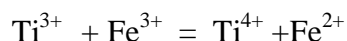
CHAPTER V

RESULTS AND DICUSSION

5.1 MgCl$_2$-supported and SiO$_2$/MgCl$_2$-supported Ziegler-Natta catalyst for ethylene polymerization

5.1.1 Effect of [EtOH]/[MgCl$_2$] on morphology of catalysts

Scanning electron microscopy (SEM) measurements revealed that the spherical morphology of SiO$_2$ is retained by the catalyst. In this study, MgCl$_2$-ethanol solutions with [EtOH]/[MgCl$_2$] ratios of 6, 7,8, 9 and 10 were used to prepare catalysts. The minimum amount of ethanol to completely dissolve the MgCl$_2$ and for impregnation of the SiO$_2$ was 6 under the experimental conditions used. The viscosity of the adduct solution increases with decreasing amounts of ethanol, hence being more difficult with impregnation at [EtOH]/[MgCl$_2$] ratios <6.

The external morphology of the SiO$_2$ and the MgCl$_2$-SiO$_2$-supported catalysts was seen by SEM (Figure 5.1). The SEM micrographs of the bi-supported catalysts shown in Figure 5.1, indicating that the catalyst particles retain the shape of the SiO$_2$ precursor particles. However, the SEM images also revealed that some breakage of particles occurred. The surfaces of bi-supported catalysts were rough, with some agglomeration of MgCl$_2$, as shown in the SEM images. Figures 5.1(c-d) show images of SM6 catalyst prepared with [EtOH]/[MgCl$_2$] = 6. It was found that the MgCl$_2$ was crystallized on the surface of bi-supported catalyst. The concentration of MgCl$_2$ in ethanol is one of important factors in the impregnation process. As known, if the adduct solution prepared has a high concentration of MgCl$_2$, it will exhibit high viscosity that will make it unable to disperse into the pores of SiO$_2$ and resulting in agglomeration on the external surface.

However, upon drying precipitation of MgCl$_2$ on the external surface of the SiO$_2$ was observed as an external rough surface for SM6. On the other hand, at higher [EtOH]/[MgCl$_2$] values of 7 and 8, the catalyst surface became smooth and very little agglomeration of MgCl$_2$ on the catalyst surface was observed, as shown in Figures 5.1 (e-f) and (g-h),while at [EtOH]/[MgCl$_2$] values of 9 and 10, cracking on the bi-supported catalyst surfaces was observed, as shown in Figures 5.1(i-j) and (k-l). This

may be due to brittle films of impregnated MgCl$_2$ caused by the high ethanol content. Therefore, the effect of [EtOH]/[MgCl$_2$] on morphology structure of MgCl$_2$ deposited on the SiO$_2$ surface is similar to that on the MgCl$_2$-supported catalyst in terms of producing loose and breakable MgCl$_2$ structures with high ethanol content [115]. Therefore, MgCl$_2$-SiO$_2$-supported catalyst requires an optimal [EtOH]/[MgCl$_2$] ratio due to the viscosity limitation that can affect the impregnation and dispersion of MgCl$_2$ on the SiO$_2$ surface. MgCl$_2$ can agglomerate on the SiO$_2$ surface with low [EtOH]/[MgCl$_2$] and it is not suitable for loading TiCl$_4$ on the MgCl$_2$-SiO$_2$-support. The optimized [EtOH]/[MgCl$_2$] value for preparing bi-supported catalysts having high activity and good spherical morphology with little agglomeration of MgCl$_2$ is 7 under these experimental conditions.
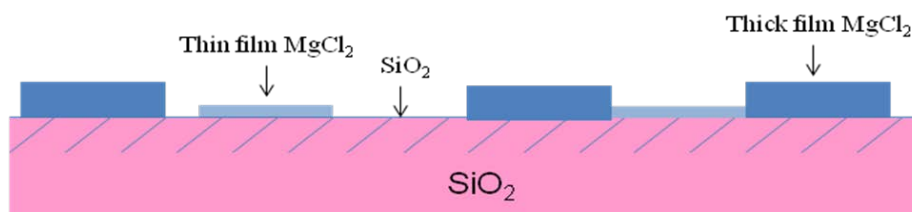
Scheme 5.1: Impregnation of MgCl$_2$ on silica surface of SiO$_2$/MgCl$_2$-supported Ziegler-Natta catalyst.
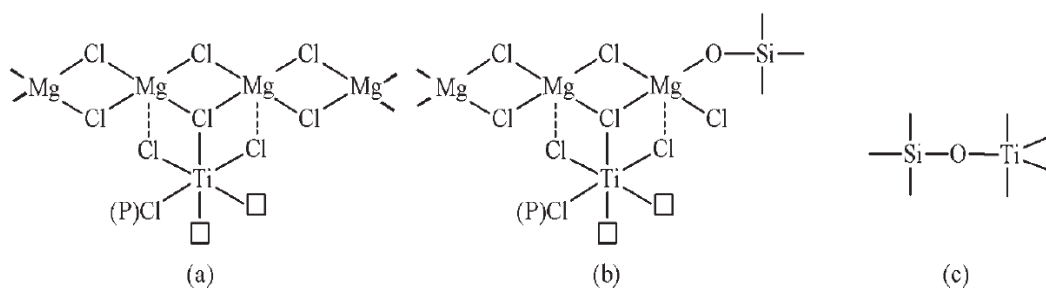
Scheme 5.2: Plausible structures of active centers in the supported ZN catalysts redrawn from ref. [131].
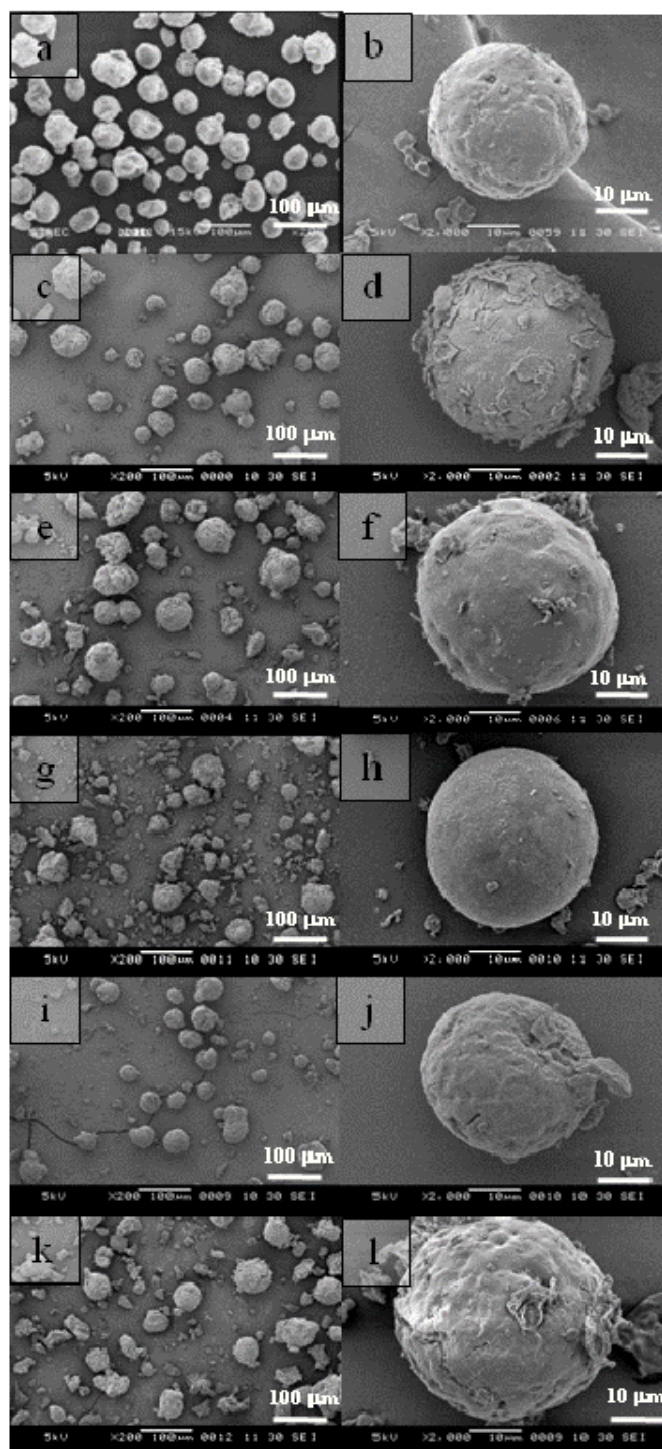
Figure 5.1: SEM images of (a) and (b) SiO_2 and $MgCl_2$-SiO_2-supported catalysts prepared with various of [EtOH]/[$MgCl_2$] ratios; (c) and (d) SM6, (e) and (f) SM7, (g) and (h) SM8, (i) and (j) SM9, (k) and (l) SM10.

5.1.2 Polymerization activity

5.1.2.1 Decreasing of activity with ethanol

$MgCl_2$-supported catalysts (M) and $MgCl_2$-SiO_2-supported catalysts (SM) were synthesized with various $MgCl_2 \cdot nEtOH$ adducts having n values ranging from 6 to 10. The supports were then treated with $TiCl_4$ to obtain the corresponding mono-supported and bi-supported catalysts. The preparation conditions of both catalyst systems are shown in Table 5.1. The results show that Ti content of $MgCl_2$-supported catalysts was relatively higher than for $MgCl_2$-SiO_2-supported catalysts in the range of 7.00–7.60 and 6.70–7.32 wt%.

Ethylene polymerization was performed using both catalyst systems. Figure 5.2 shows that the relative activities of the mono-supported (M) catalysts were markedly decreased with increased [EtOH]/[$MgCl_2$] ratios of 6 to 10, whereas the activities were only slightly decreased for the bi-supported (SM) catalysts for the identical [EtOH]/[$MgCl_2$] ratios. It should be mentioned that the $MgCl_2$-SiO_2-supported catalysts usually have lower activity than $MgCl_2$-supported catalysts because of the high number of silanol groups on the SiO_2 surface [115-116].

However, based on this study at [EtOH]/[$MgCl_2$] ratios of 9 and 10, the bi-supported catalysts showed higher activity than the mono-supported catalyst, as seen in Figure 5.2 for SM9 and SM10 compared to M9 and M10. In the case of $MgCl_2$-supported catalysts, [EtOH]/[$MgCl_2$] ratio is an important parameter and this catalyst system prefers lower [EtOH]/[$MgCl_2$] during support preparation to give better catalytic activity and performance [117-118]. An excess amount of EtOH in the support could react with $TiCl_4$, and produce inactive species like Ti alkoxide [119]. In contrast, the bi-supported catalysts showed the interesting result that the activity was relatively independent of the [EtOH]/[$MgCl_2$] ratio. This indicates that the SiO_2 probably prevents the Ti active species from reacting further with ethanol.

Table 5.1: MgCl$_2$-supported and MgCl$_2$-SiO$_2$-supported catalysts preparation conditions.

		MgCl$_2$-supported catalyst			
Sample	EtOH (mL)	[EtOH]/[MgCl$_2$]	TiCl$_4$ (mL) [a]	SiO$_2$ (g)	Ti (wt%)
M6	11.0	6	18.3	0	7.00
M7	12.9	7	21.4	0	7.34
M8	14.7	8	24.4	0	7.54
M9	16.6	9	27.5	0	7.43
M10	18.0	10	30.0	0	7.60
		MgCl$_2$-SiO$_2$-supported catalyst			
Sample	EtOH (mL)	[EtOH]/[MgCl$_2$]	TiCl$_4$ (mL) [a]	SiO$_2$ (g)	Ti (wt%)
SM6	11.0	6	18.3	6	6.93
SM7	12.9	7	21.4	6	6.80
SM8	14.7	8	24.4	6	6.77
SM9	16.6	9	27.5	6	6.70
SM10	18.0	10	30.0	6	7.32

Note: [a] The desired amount of TiCl$_4$ using for removing of EtOH from MgCl$_2$ adduct calculated by [EtOH]/[TiCl$_4$] = 1.13.

Table 5.2: Catalytic activity and relative activity of MgCl$_2$-supported and MgCl$_2$-SiO$_2$-supported catalysts with various [EtOH]/[MgCl$_2$] ratios.

MgCl$_2$-supported catalyst			SiO$_2$/MgCl$_2$-supported catalyst		
Catalyst	Activity (kgPE/gTi/h)	Relative activity [a]	Catalyst	Activity (kgPE/gTi/h)	Relative activity [a]
M6	21.03	1.00	SM6	15.17	1.00
M8	17.69	0.84	SM8	15.11	1.00
M10	14.78	0.70	SM10	15.04	0.99
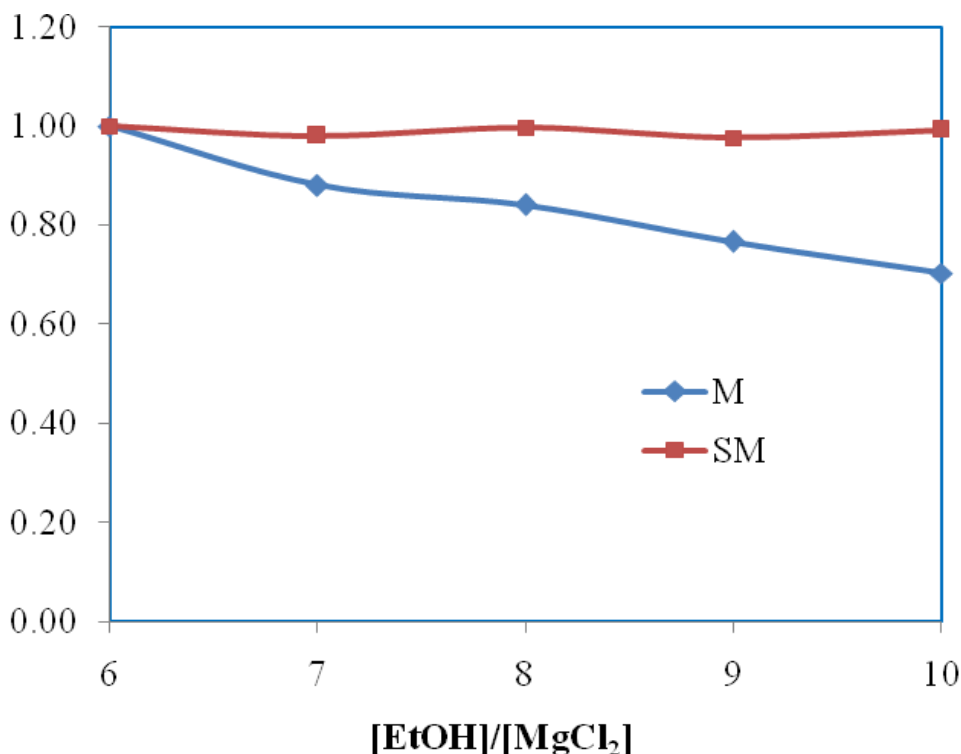
Figure 5.2: Effect of [Ethanol]/[MgCl$_2$] on relative activity of MgCl$_2$-SiO$_2$-supported catalyst (SM) and MgCl$_2$-supported catalyst (M). Ethylene polymerization condition: temperature = 80 °C; catalyst loading = 10 mg; [A1]/[Ti] = 100; ethylene consumption = 18 mmol.

5.1.2.2 Hydrogen effect on ethylene polymerization

Table 5.3 lists the values of catalytic activities, M and SM catalysts obtained with and without hydrogen. For the ethylene polymerization in the absence of hydrogen, M catalysts show higher activity than SM catalysts that M6, M8 and M10 were 21.03, 17.69 and 14.78 kgPE/gTi/h, respectively, and SM6, SM8 and SM10 were 15.17, 15.11 and 15.04 kgPE/gTi/h, respectively. Typically, MgCl$_2$-supported ZN catalyst is highly active olefin polymerization while SiO$_2$-supported ZN catalyst is low polymerization activity. So, SiO$_2$/MgCl$_2$-supported ZN catalysts have moderate activity that is combination of MgCl$_2$ and SiO$_2$ supports. The activity decreasing by hydrogen was remarkable during polymerizations with MgCl$_2$-supported ZN catalysts, that M6, M8 and M10 were 15.29, 12.89 and 9.64 kgPE/gTi/h, respectively, and SM6, SM8 and SM10 were 14.82, 15.06 and 14.43 kgPE/gTi/h, respectively. The

results indicated that MgCl$_2$-supported ZN catalyst had more pronouced on the hydrogen addition in ethylene polymerization and the activities were decreased with increasing of [EtOH]/[MgCl$_2$]. While SiO$_2$/MgCl$_2$-supported ZN catalyst has relatively constant in activity regardless to introduction of hydrogen in ethylene polymerization and increasing of [EtOH]/[MgCl$_2$].

Table 5.3: The catalytic activities of MgCl$_2$-supported and SiO$_2$/MgCl$_2$-supported catalysts in ethylene polymerization in the absence and presence of hydrogen.

Run no.	Catalyst system	Hydrogen	Activity (kgPE/gTi/h)	Activity$_H$/Activity$_0$ [a]
1	M6	present	15.29	
				0.727
2	M6	absent	21.03	
3	M8	present	12.89	
				0.729
4	M8	absent	17.69	
5	M10	present	9.64	
				0.653
6	M10	absent	14.78	
7	SM6	present	14.82	
				0.977
8	SM6	absent	15.17	
9	SM8	present	15.06	
				0.997
10	SM8	absent	15.11	
11	SM10	present	14.43	
				0.959
12	SM10	absent	15.04	

Note: [a] Ratios of activity obtained by the polymerization with hydrogen to that without hydrogen.

In order to give a better understanding, the ratios of the activities with hydrogen to those without hydrogen are normalized and shown in Table 5.4. For the ethylene polymerization with $MgCl_2$-supported ZN catalysts, the ratios of activities with hydrogen to those without hydrogen are 0.727, 0.729 and 0.653 for M6, M8 and M10, respectively. While, the ethylene polymerizations with $SiO_2/MgCl_2$-supported ZN catalysts, the ratios are 0.977, 0.997 and 0.959 for SM6, SM8 and SM10, respectively. This result indicated that hydrogen affected on the catalyst systems with different degree, regard to $[EtOH]/[MgCl_2]$ in $MgCl_2$-supported ZN catalyst system, but regardless of the $[EtOH]/[MgCl_2]$ in the case of $SiO_2/MgCl_2$-supported ZN catalyst. The influence of hydrogen on the catalyst system was to inhibit the activation of $MgCl_2$-supported ZN catalyst not for $SiO_2/MgCl_2$-supported ZN catalyst.

From our previous study [125], the effect of $[EtOH]/[MgCl_2]$ was found in the$MgCl_2$-supported ZN catalysts, but it was absence in $SiO_2/MgCl_2$-supported ZN catalysts. It is well-known that $MgCl_2$-supported ZN catalyst activity decreases with increasing of $[EtOH]/[MgCl_2]$ value [124], but the $SiO_2/MgCl_2$-supported ZN catalyst has a property to resist this effect of ethanol. Typically, the $MgCl_2$-supported ZN catalyst exhibits a decrease in ethylene polymerization activity in the presence of hydrogen because of the formation of β-agostic coordination from hydrogen atom in the ethyl group formed after hydrogen termination and the first monomer insertion [126-129]. Hydrogen expelling C2″, is caused by a delay in the activation reactions of the tetravalent Ti. Even the presence of hydrogen in ethylene polymerization caused the rate depression but the kinetic behavior does not change. Hydrogen does not affect the activation and deactivation rates of the polymerization active centers [130-133].

In present study, we impregnated $MgCl_2$ onto SiO_2 surface via adduct solution form of $MgCl_2·nEtOH$. It is possible that $MgCl_2$ could have two possible form of impregnated $MgCl_2$ on SiO_2 surface as shown in Scheme 5.1. Thin film and thick film of $MgCl_2$ on SiO_2 surface, there are two kinds of catalyst structure (i) Cl-Mg-Cl and (ii) Cl-Mg-O-Si at interface of SiO_2. Hence, the catalyst structure should be as shown in Scheme 5.2 (a) and (b) [131], respectively.

From Scheme 5.2 (b), the $SiO_2/MgCl_2$ bonded via Si-O-Mg should be the reason of different hydrogen effect by support stucture that different from $MgCl_2$-supported ZN catalyst. The Ti-Cl-Mg bond as shown in Scheme 5.2 (a) well-known to be Ti active species of $MgCl_2$-supported ZN catalyst.

Normally, hydrogen remarkable affected on ethylene polymerization using the $MgCl_2$-supported ZN catalyst by replacing C_2" in polymerization process [130] and stabilization of Ti-C_2H_5 bonds by β–hydrogen with the formation of Ti-H bonds in standard mechanism [132]. However, the different effect on $SiO_2/MgCl_2$–supported ZN catalyst was found perhaps due to the structures of $MgCl_2$ in $SiO_2/MgCl_2$-supported ZN catalyst, whicfh is different from those of $MgCl_2$. Some of the Mg component probably react chemically with the surface hydroxyls of SiO_2 [133]. Therefore, the surface structures of the $SiO_2/MgCl_2$-supported ZN catalyst may be more complicated than those of the $MgCl_2$-supported ZN catalyst.

We proposed that SM catalyst does not affect by hydrogen because of SiO_2 in their structure may block hydrogen from expelling C_2". Therefore, in the SM catalyst, the Ti active species are still in Ti-$MgCl_2$ bonds resulting in relatively constant in catalytic activation.

5.1.3 Determination of surface area

Surface areas of mono- and bi-supported catalysts were determined by the BET method. The results are listed in Table 5.4. The bi-supported catalysts exhibited much higher surface areas than the mono-supported catalysts prepared under similar [EtOH]/[$MgCl_2$] ratios due to the high surface area of SiO_2 in the bi-supported catalyst. The bi-supported catalysts containing different [EtOH]/[$MgCl_2$] values of $MgCl_2$ adduct exhibit similar surface area of 414–471 m^2/g, pore size of 44.6–52.5 Å and pore volume of 0.46–0.60 cm^{-3}/g. Therefore, the relatively constant bi-supported catalyst structure is the reason for the relatively constant catalytic activity. The BET measurements of mono-supported catalyst showed that the surface area, pore size and pore volume of the catalysts depended on the [EtOH]/[$MgCl_2$] ratios. The results show that M6 prepared with a lower [EtOH]/[$MgCl_2$] value exhibited much larger

pores than those of M8 and M10, respectively. The larger pores size may be responsible for the higher catalytic activity M6 >M8> M10.

Table 5.4: BET surface area measurement of $MgCl_2$-supported catalysts and $MgCl_2$-SiO_2-supported catalysts.

Sample	Ti (wt%)	BET surface area (m^2/g)	Pore size $(Å)$	Pore volume (cm^3/g)
SiO_2 (SYLOPOL 2229)	-	489	97.22	1.60
M6	7.00	187	88.00	0.53
M8	7.54	350	50.40	0.47
M10	7.60	366	39.30	0.36
SM6	6.93	419	49.60	0.51
SM8	6.97	450	50.40	0.57
SM10	7.32	414	44.60	0.46

5.1.4 Thermal property analysis

Figure 5.3 shows TGA profiles of $MgCl_2$-supported catalysts and $MgCl_2$-SiO_2-supported catalyst. It indicates that bi-supported catalysts exhibited the similar TGA profiles as SiO_2, with a relative decrease the weight loss with temperature after 200 °C. The bi-supported catalysts retained over 80% of their mass when heated to 500 °C (mass loss $\leq$ 20%) while the mono-supported catalyst lost about 50% of their mass for the same thermal treatment. TGA profiles show that the mono-supported catalysts have significant mass losses in the range of 70 to 190 °C (30 to 40%) indicating

ethanol vaporized region. EtOH and moisture escaped from surface and catalyst particles in this temperature range. The mono-supported catalysts have a maximum weight loss from 150–190 °C in M6 catalyst and 70–130 °C in M10 catalyst, indicating that at a higher [EtOH]/[MgCl$_2$] value as 10, ethanol groups were removed easily from the catalysts because of the loose structure of M10 produced with a high content of ethanol [120]. This may be the reason why the decrease of weight loss of M10 was sharper and started earlier than those of M6. On the other hand, the bi-supported catalysts show only a slight decrease of weight loss profile. The results also show that at 200 °C, the bi-supported catalysts have an average weight of 90% corresponding to a weight loss of 10%, whereas the mono-supported catalysts exhibited average weights of 68%, corresponding to a weight loss of 33%.
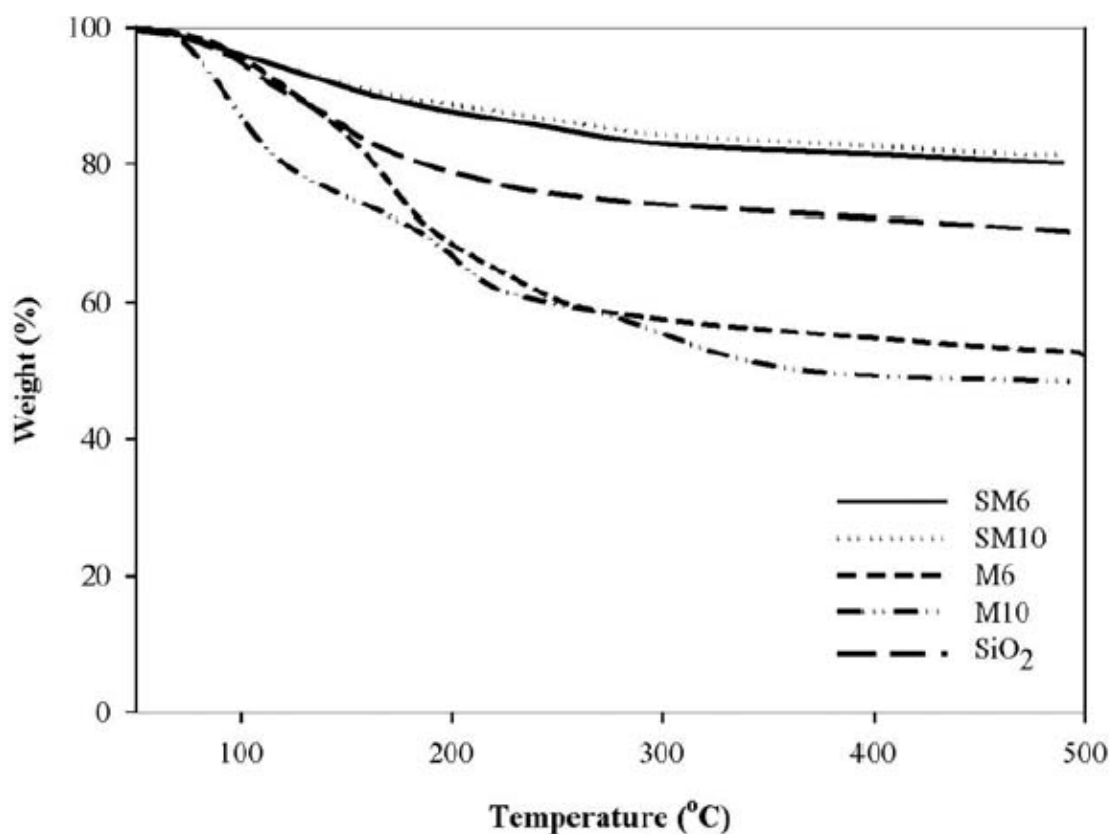
Figure 5.3: TGA profiles of MgCl$_2$-supported catalysts (M) and MgCl$_2$-SiO$_2$-supported catalysts (SM).

Therefore, the ethanol residual in MgCl$_2$-supported catalyst was more than in the SiO$_2$/MgCl$_2$-supported catalyst. Typically, recrystallization of MgCl$_2$ from MgCl$_2$-nEtOH adduct solution was performed by chlorinating reaction with chlorinating agent as TiCl$_4$ [134-136] which remove ethanol from MgCl$_2$ adduct to obtain activated MgCl$_2$. This TGA results implied that the removing of ethanol from SiO$_2$/MgCl$_2$-supported catalyst structure was easier than MgCl$_2$-supported catalyst. So, the residual ethanol of MgCl$_2$-supported catalyst was found in thermal treatment at low temperature with more amount than SiO$_2$/MgCl$_2$-supported catalyst.

5.1.5 Catalyst structure analysis

Figure 5.4 indicates FTIR spectra of final catalyst of MgCl$_2$ and SiO$_2$/MgCl$_2$ supports. The spectrum of MgCl$_2$-supported ZN catalyst show band at 3741 cm^{-1} assigned to the single hydroxyl group [133] and 3426 cm^{-1} indicating the OH group of ethanol residual in catalyst. In the IR spectrum of SiO$_2$/MgCl$_2$-supported ZN catalyst, the peaks at 538 and 800 cm^{-1} are ascribed to the Si-O-Si bending vibration and at 1023 cm^{-1} to the Si-O stretching vibration. The Mg-Cl bond at 1621 cm^{-1} was observed in mono-supported catalyst spectrum having much more higher intensity than in bi-supported catalyst according to the amount of MgCl$_2$ in each catalyst systems. The band corresponding to the hydroxyl group on the surface of the silica was shifted to 3393 cm^{-1} relatively disappears. This indicates that dealcoholation has been almost completed in the bi-supported ZN catalyst. It was suggested that OH-groups in SiO$_2$/MgCl$_2$-supported ZN catalyst were less than in the MgCl$_2$- supported ZN catalyst with corresponding to the TGA results.
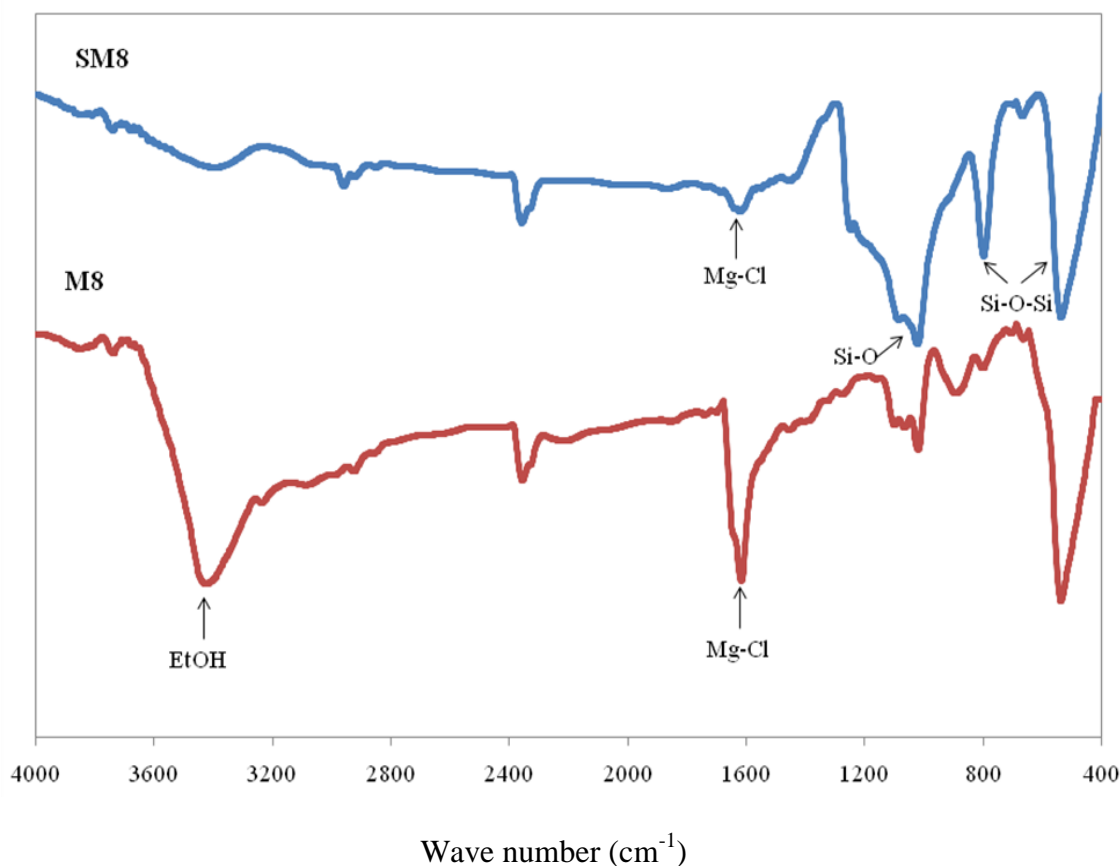
Figure 5.4: FTIR spectra of different Ziegler-Natta catalysts.

5.1.6 Degradation of $MgCl_2$-supported and $SiO_2/MgCl_2$-supported ZN catlaysts

The other $MgCl_2$-supported and $SiO_2/MgCl_2$-supported ZN catlaysts were prepared using [EtOH]/[$MgCl_2$] = 8 for $MgCl_2$ adduct preparation, namely M8 and SM8. The two kinds of catalyst support system were exposed in the glove box under Ar atmosphere with moisture content of 5-20 ppm, oxygen content of 20-30 ppm and dew point of -50 to -60 ^{o}C. The deactivation of catalyst was performed by sampling the catalyst and testing of ethylene polymerization every 24 h.
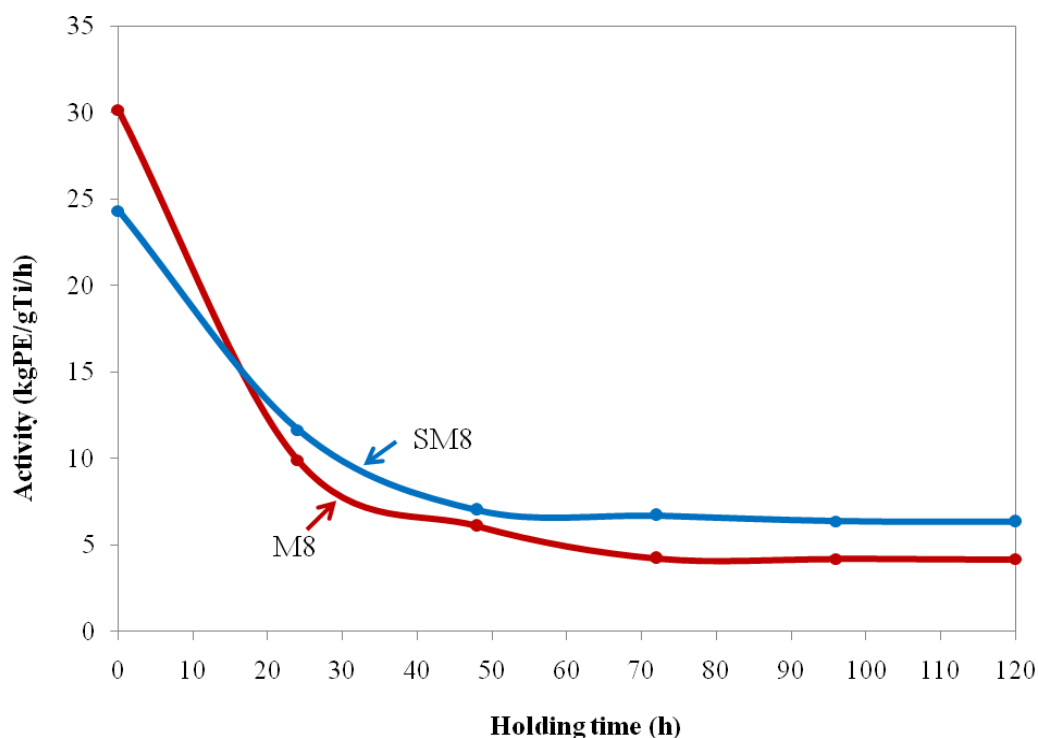
Figure 5.5: Decay rate of different Ziegler-Natta catalysts with holding time after exposed to atmosphere in glove box.

Typically, MgCl$_2$-supported ZN catlaysts was easily destroyed after exposed to the air due to moisture and oxygen are the poison for ZN catalyst. The catalyst structure can be damaged and active species was deactivated further leading to lost of activation performance. Therefore, handling of ZN catalyst needs to conducted under dried inert gas condition to avoid the degradation of catalyst by poison in the atmosphere. Eventhough, keeping of ZN catalyst under inert gas is only decreasing the rate of degradation of catalyst, but degradation still continued with time by reduction reaction.

Figure 5.5 shows decreasing of activity of M8 and SM8. The fresh catalysts of M8 and SM8 show the highest activity of 30.15 and 24.32 kgPE/gTi/h, respectively. After that the activities continuously decreased with holding time until relatively constant for both M8 and SM8. It was found that SM8 exhibited higher activity than M8 when the holding time passed over 24 h. The catalytic activity of SM8 decreased ca. 74% from maximum activity of the fresh catalyst to stable activity. In the case of

M8, the catalytic activity decreased by 86% from maximum activity of fresh catalyst to stable activity. Therefore, the degradation of $SiO_2/MgCl_2$-support ZN catalyst was lower than that of $MgCl_2$-support ZN catalyst. This is perhaps due to the chemical structure and nature of SiO_2 which is included in the support system. This result is inagreement with that from the $SiO_2/MgCl_2$-support ZN catalyst with hydrohen addition. According to previous work, $SiO_2/MgCl_2$-supported ZN catalyst shows resistance property to ethanol which is one of poison for the catalyst.

5.2 Magnesium chloride (ethoxide type)-supported Ziegler-Natta catalyst and olefin polymerizations

The catalysts were prepared with various preparation's conditions by chemical reaction method between $Mg(OEt)_2$ and $TiCl_4$ in the absence and presence of internal electron donors. The first addition of $TiCl_4$ was conducted to convert $Mg(OEt)_2$ to $MgCl_2$ via chlorinating reaction at desired condition and the second addition of $TiCl_4$ was conducted with same condition that was used in the first reaction to impregnated $TiCl_4$ on formed $MgCl_2$.

5.2.1 Preparation's condition (temperature) effect on $Mg(OEt)_2/TiCl_4$ catalyst system

The catalysts were prepared without ID with different treatment temperature 30 and 90°C and same treatment time of 2 h, N302 and N902, respectively. Table 5.5 shows that N302 had a little higher Ti content than N902, 11.71 and 10.68 wt%., respectively. But N902 has higher catalytic activity than N302, 54.0 and 27.7 kgPE/gTiˑh for ethylene polymerization and 21.2 and 11.4 kgPP/gTiˑh for propylene polymerization, respectively. The reason may be because of washing step of these cat were conducted with different temperature, N302 was washed at 30°C but N902 was washed at 90°C, so at lower temperature, Ti compound by product as Ti-alkoxide species not easily removed from the catalyst [137]. Therefore, total Ti content of N302 higher than N902 but Ti active species of N902 much higher than N302, so higher activity was obtained.

Table 5.5: Catalyst preparation's condition Ti content and catalytic activity.

Catalyst	ID	Ti (wt%)	Catalytic activity (kg/gTi·h)		mmmm[a]
			C2	C3	(mol%)
N302	-	11.71	27.7	11.3	55.7
N902	-	10.68	54.0	21.2	56.5
E901	EB	8.15	14.4	64.4	71.6
E902	EB	4.52	18.9	256.4	77.7
E1102	EB	4.94	21.6	140.4	74.7
D902	IPIPDMP	3.84	8.1	47.0	83.2

Note: [a] Determined by ^{13}C NMR.

The original $Mg(OEt)_2$ precursor had lamellar structure on surface [138] with high porosity as shown in Figure 5.6(a-c). Figure 5.7 (a1-a2) show morphology of N302; it indicated that low activation temperature, spherical morphology of catalyst is obtained with small amount of fine particles. SEM technique revealed that fine particles were increased with temperature, as shown in Figure 5.7(b1). N902 had spherical morphology with fragmented particles as shown in Figure 5.7(b2). Catalyst surface shows significantly effect of activation temperature that lower temperature (30°C), the reconstruction process of new born $MgCl_2$ replicated secondary particles of original $Mg(OEt)_2$ precursor that had lamellar shape [138]. Therefore, N302 catalyst (secondary particle size of 0.55 µm) had similar surface structure to $Mg(OEt)_2$ precursor (secondary particle size of 0.83 µm). The $MgCl_2$ was formed by reaction of $TiCl_4$ and $Mg(OEt)_2$, the secondary particle size (crystallite plate) of $MgCl_2$ became smaller than $Mg(OEt)_2$ precursor , as shown in Figure 5.8 (a3).

Even though, low temperature condition could prevent catalyst particles from fragmentation and kept their surface structure as original precursor, however, preparation of catalyst at lower activation temperature, obtained catalyst could not polymerized ethylene with high activity compared with higher activation temperature condition. Conversely, N902 shows different architecture on surface as shown in Figure 5.8 (b3). It indicated that reconstruction process of $MgCl_2$ at high activation temperature in the absence of internal electron donor, the crystallite plate structure was melted and the surface became rough after treatment at $90^{\circ}C$. The reaction between $TiCl_4$ and ethoxy group of $Mg(OEt)_2$ is highly exothermic so the addition of $TiCl_4$ to the support while the reaction must be performed at low temperature to control heat in reaction system results to prevent the fragmentation of catalyst particles.

We propose that the chemical reaction of $Mg(OEt)_2$ and $TiCl_4$ that is produced the activated $MgCl_2$, the treatment temperature is an important parameter to control morphology of catalyst's particle. The reconstruction process of $MgCl_2$ was controlled by reaction temperature. The heat that applied to reaction system and the heat generation between reaction of $TiCl_4$ and $Mg(OEt)_2$ or $MgCl_2$ while catalyst preparation is the cause of uncontrollable morphology and fragmentation in catalyst's particle.

5.2.2 Internal electron donor effect on $Mg(OEt)_2$/$TiCl_4$/ID catalyst system

$Mg(OEt)_2$/$TiCl_4$ catalysts were prepared in the absence and presence of internal electron donor show remarkable influence of ID that control morphology of catalyst by decreasing fragmentation phenomena as shown in Figure 5.8.

Figure 5.7 (b1-b3) and Figure 5.7 (d1-d3) show SEM images of N902 and E902, it revealed that N902, recrystallization process of $MgCl_2$ was performed without recovering of lamellar structure of $Mg(OEt)_2$ precursor but E902 had different result that reconstruction of lamellar structure of catalyst surface was occurred with smaller plate size than original $Mg(OEt)_2$ precursor.

In the absence of internal electron donor, N902 catalyst could not recovered the plate crystallite structure of original $Mg(OEt)_2$ precursor so the catalyst surface could

not observed lamellar structure as shown in Figure 5.7 (b3). Catalyst preparation's condition effect on $Mg(OEt)_2/TiCl_4/ID$ catalyst system

Effect of treatment time (E901 and E902)

The conversion reactions of $Mg(OEt)_2$ to $MgCl_2$ according to Jeong [23].

$$Mg(OEt)_2 + ID + TiCl_4 \longrightarrow Mg(OEt)Cl + ID + Ti(OEt)Cl_3$$

$$Mg(OEt)Cl + ID + TiCl_4 \longrightarrow MgCl_2{\cdot}ID + Ti(OEt)Cl_3$$

$$Mg(OEt)_2 + ID + TiCl_4 \longrightarrow MgCl_2{\cdot}ID + Ti(OEt)_2Cl_2$$
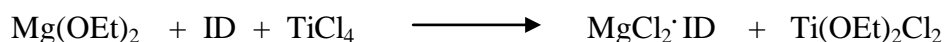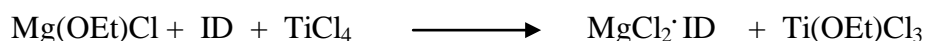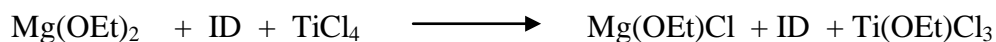
At the first step, $MgCl_2$ was formed by reaction of $Mg(OEt)_2$ with $TiCl_4$ in different preparation's conditions, various treatment temperature and treatment time, in the presence of ethyl benzoate as ID. Then, intermediately $MgCl_2$ product was activated with $TiCl_4$ and EB-containing catalysts; E901, E902 and E1102 were obtained.
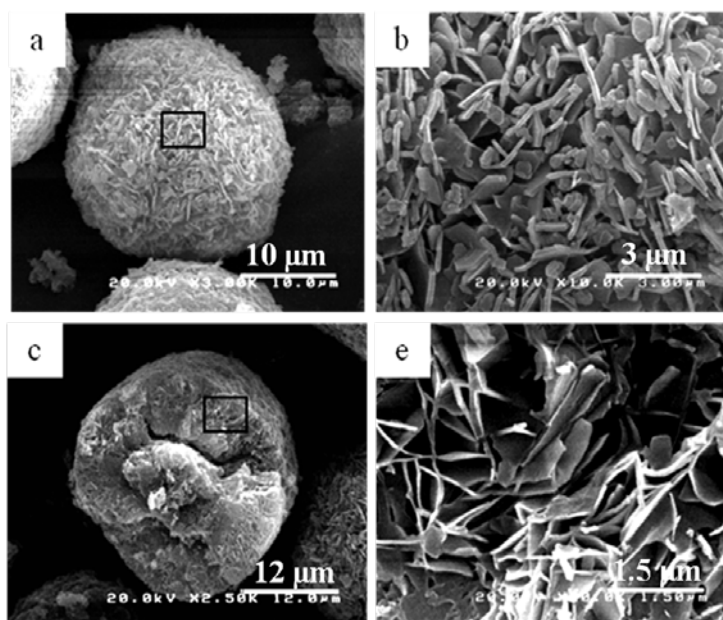
Figure 5.6: Morphology of the $Mg(OEt)_2$ precursor: (a) $Mg(OEt)_2$ particle (ca. 28.5 µm), (b) secondary particles (ca. 0.83 µm), magnification 10K and (c) Cross-section of $Mg(OEt)_2$ particle (secondary particles) ,magnification 20K.
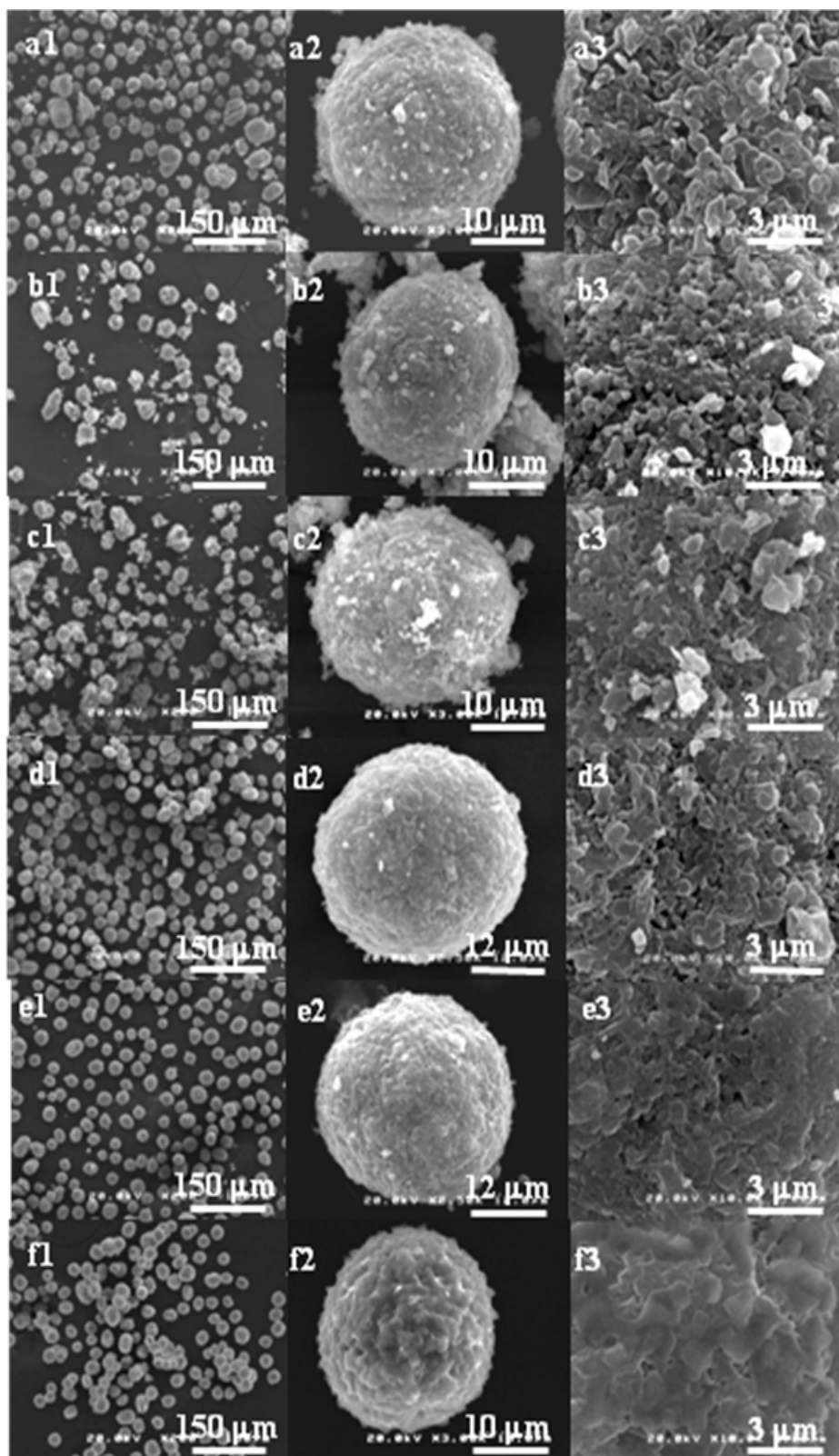
Figure 5.7: SEM image of catalysts at magnification 200x, 3,000x and 10,000x: a) N302, b) N902, c) E901, d) E902, e) E1102 and f) D902.

In this part, Mg(OEt)$_2$ was converted to MgCl$_2$ by chlorination reaction of TiCl$_4$ in the presence of EB as ID as the first step and impregnation of TiCl$_4$ on MgCl$_2$ support as the second step was studied. The effect of TiCl$_4$ treatment time on catalyst morphology was observed using SEM, it revealed that the reaction of Mg(OEt)$_2$ with TiCl$_4$ to form MgCl$_2$ in the presence of EB as ID in the first reaction, EB had significantly effect to control surface structure of final catalyst.

Figure 5.7 (c1) shows SEM image of E901, many fine particles was found with rough surface of catalyst's particle, as shown in Figure 5.8 (c2-c3), compared with E902 that shows significantly decreased amount of fine particle and smoother surface of catalyst. Therefore, the treatment time of Mg(OEt)$_2$ with TiCl$_4$ in the presence of EB, effect to morphology of secondary particle of catalyst and fragmentation phenomena.

The catalyst E901 and E902 were prepared using same TiCl$_4$ treatment temperature and different treatment time, 1 h and 2 h, for both the first reaction of Mg(OEt)$_2$ with TiCl$_4$ in the presence of EB and the second reaction to impregnate TiCl$_4$ on MgCl$_2$ support, respectively. The result shows different Ti content in catalyst, 8.15 and 4.52 wt%, for E901 and E902, respectively, as shown in Table 5.5.

It seems ID treatment time was the main key to control the amount of Ti loading on MgCl$_2$ [137]. Likewise, the effect of treatment time was confirmed in catalyst performance by ethylene and propylene polymerizations. E902 catalyst shows higher catalytic activity than E901, 18.9 and 14.4 kg PE/gTi·h for ethylene polymerization and 256.4 and 64.4 kg PP/gTi·h for propylene polymerization, respectively, as shown in Table 5.5.

Effect of treatment temperature. (E902 and E1102)

Both E902 and E1102 show significantly decreasing of the amount of fine particle but they show different surface structure, as shown in Figure 5.7 (d1-d3) and (e1-e3).

E902 had lamellar structure on catalyst's surface but E1102 the connection of plate was produced so the melting of lamellar structure was occurred because of high temperature treatment, as shown in Figure 5.7 d3 and e3, respectively.

Reconstruction process of lamellar structure of $MgCl_2$ (ethoxide type) supported catalyst at high temperature of 110^oC could not be recovered the original shape and size of plate crystallite structure of $Mg(OEt)_2$ precursor. Preparation of $Mg(OEt)_2$ containing internal electron donor catalyst with different treatment temperature, E902 and E1102 show some effect on catalyst performance. At 90°C, E902 has Ti content of 4.52 wt% but at over treatment temperature at 110°C, E1102 shows slightly higher Ti content of 4.94 wt% and it could produced higher yield for ethylene than E902; 21.6 and 18.9 kgPE/gTi·h, respectively. But propylene polymerization the opposite result was found that E1102 has significantly lower catalytic activity than E902; 140.4 and 256.4 kgPP/g Ti·h.

Effect of kind of ID (E902and D902)

The catalyst systems containing monoester (EB) or diether (IPIPDMP) as internal electron donor were synthesized with same catalyst preparation's condition to investigate the effect of different kind of internal electron donor compound on the catalyst morphology and their performance that was observed by polymerization of ethylene and propylene.

Figure 5.7 (d1-d3) and (e1-e3) show SEM images of E902 and D902, that had lamellar structure on the surface. It shows that both kind of ID, EB and IPIPDMP could reduce the fragmentation of catalyst's particles and good shape was obtained. Comparison of surface structure, it was found that E902 and D902, had lamellar structure on the surface but different both shape and size of their plate crystallite structure. E902 had clearly reconstructed lamellar structure look like original $Mg(OEt)_2$ precursor but D902 was observed the bigger plate crystallite size and connection of plate structure. Therefore, kind of internal electron donor is main parameter to control the surface structure of catalyst both shape and size, and the presence of internal electron donor significantly affected to control the replication of crystallite plate structure of catalyst.

Since, $MgCl_2$ support was produced by the reaction of $Mg(OEt)_2$ with excess $TiCl_4$ while the process , $Mg(OEt)_2$ structure was destroyed and changed to $MgCl_2$ structure by the reaction with $TiCl_4$. The size of plate crystallite was expected to greatly affect the smoothness and roundness of surface of intermediately $MgCl_2$ and

final catalyst. From such a viewpoint, the reason for the size of the plate crystallites changing remarkably with the reaction's condition [139].

Tanase [138] synthesized $Mg(OEt)_2$, they reported that the size of plate crystallites have a significantly affect the smoothness and roundness of $Mg(OEt)_2$ product, and catalyst performance. They suggested that, the size of the plate crystallites were changed in the process that used for preparing the product.

The catalyst performance with different kind of internal electron donor, EB and IPIPDMP, was investigated when the polymerization of ethylene and propylene were performed in the absence of external donor.

Table 5.5 shows that, at same catalyst preparation's condition, $90^{\circ}C$ and 2 h, E902; EB-containing catalyst has higher Ti content than D902, IPIPDMP-containing catalyst, 4.52 and 3.84 wt%, respectively. This result indicated that kind of internal electron donor caused a significantly different in Ti content of catalyst.

Internal electron donor such as monoester or diester compounds, predominantly adsorb on more acidic sites (110) faces of $MgCl_2$ and can be adsorb on (104) faces of $MgCl_2$ also [140-142] excluding diether donor that has strongly preference only one edge of the (110) face of $MgCl_2$ [143]. May be this difference Ti content because the preference of internal electron donor adsorption on $MgCl_2$ and different chemical structure of donor compound.

Additional, both polymerization of ethylene and propylene indicated that catalytic activity of catalyst E902, higher than D902, for ethylene polymerization; 18.9 and 8.1 kgPE/gTi·h and for propylene polymerization; 256.4 and 47.0 kgPP/gTi·h, respectively, as shown in Table 5.5.

From above results we can conclude that, the using of ID is an effective way to reduce heat while reaction proceed that has significantly affect to reduce the severe of fragmentation of catalyst particle results to control the reforming of secondary particles size and shape as well. Since, ID plays main function and a role like surfactant are the protect morphology of final catalyst from fragmentation [137,143].

We propose that $TiCl_4$ and ID treatment in preparation's conditions of catalyst are main important parameters to control shape and size of catalyst's structure.

Addition of EB as ID while chlorinating reaction between $Mg(OEt)_2$ and $TiCl_4$ to produce $MgCl_2$, in this step EB play an important role to control catalyst's particle similarly to using low temperature in $TiCl_4$ treatment step without ID, suggested that reconstruction process of $MgCl_2$ could be control by decreasing heat while activated reaction proceed. As the results, the adsorption of EB needs sufficient conditions such as treatment temperature and treatment time to adsorb ID on $MgCl_2$ surface and form the complex with $TiCl_4$.

In the case of free-ID catalyst, lower treatment temperature could produce the catalyst with much better morphology than high treatment temperature. But the disadvantage of decreasing of treatment temperature was found in N302 that had poor polymerizing performance.

In the case of ID-containing catalyst, the presence of ID is the main parameter to control catalyst morphology, but in the present work, we found that treatment temperature play a role to control the surface structure of particle. In case of $MgCl_2$-adduct support, the internal donor was believed to act as a cross-linking agent and it could enhance the morphology of catalyst and resultant polymer particles [144]. Additional, short treatment time for catalyst preparation in the presence of ID could not make enough amounts of adsorbed ID on $MgCl_2$ so Ti content in E901 higher than E902.

Therefore, we can concluded that the fragmentation phenomena in catalyst particle while reaction of $Mg(OEt)_2$ and $TiCl_4$, can control by using ID with optimized preparation's condition.

5.2.3 Crystallite structure
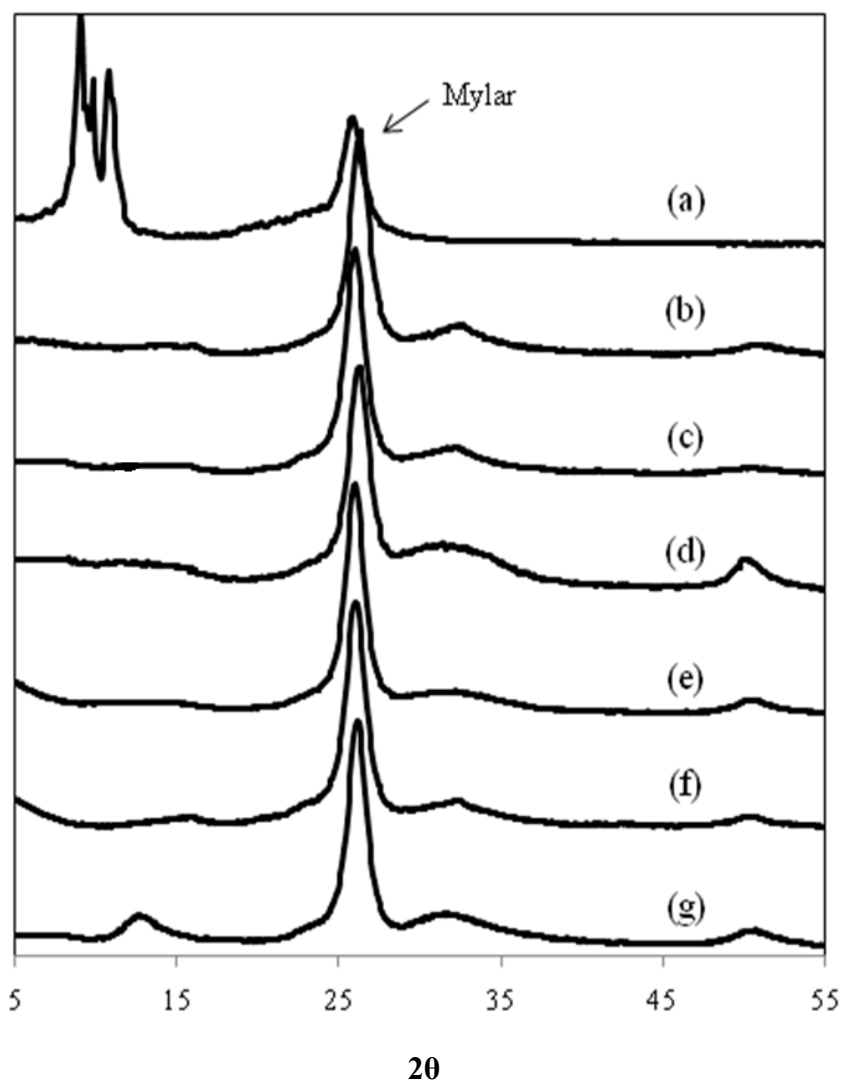
Figure 5.8: X-ray diffraction pattern of a) Mg(OEt)$_2$,b) N302, c) N902, d) E901 , e) E902, f) E1102 and g) D902.

Figure 5.8, shows x-ray diffraction (XRD) pattern of Mg(OEt)$_2$-based catalysts. The large peak at $2\theta = 26^\circ$ from mylar film which is used to protect the catalyst from exposure to the atmosphere. It revealed that, the characteristic peaks of Mg(OEt)$_2$ in the range of $2\theta = 9\text{-}11^\circ$ (Figure 5.8a) were disappeared in the XRD patterns of

$Mg(OEt)_2/TiCl_4$ and $Mg(OEt)_2/TiCl_4/ID$ catalyst systems, it indicated that the $Mg(OEt)_2$ were completely converted to $MgCl_2$ by chemical reaction with $TiCl_4$.

At the same catalyst preparation's condition treatment temperature of 90^oC and treatment time of 2 h, N902, E902 and D902 show broad peak in the range of $2\theta = 30\text{-}35^o$ and $2\theta = 50^o$, it indicated that disordering of crystallite structure of catalyst.

Some different of XRD pattern of three kinds of these catalyst were observed that at $2\theta = 50^o$, N902 show too broad halo compared with ID-containing catalyst, E902 and D902. Moreover, diether-containing catalyst, D902, shows sharp peak at $2\theta = 12^o$.

According to morphology results from above section, that show different feature of catalyst surface which were prepared without ID (N902) and with ID, EB (E902) and IPIPDMP (D902). Then, the catalyst performance was found that different catalytic activity of ethylene polymerization obtained using N902 > E902 > D902, respectively. It seems the crystallographic disordered structure of these catalysts with different ID that disorder related to activated degree [145].

Including of morphology, catalytic activity and XRD results, we could found some relationship between XRD pattern and morphology of these three catalyst systems that show individual feature on morphology, it could confirmed that the effect of catalyst preparation's condition and the presence of ID on catalyst properties. Even though, XRD pattern could not concluded the clear effect of preparation's condition and ID but we could say their crystallite structure were affected from preparation's condition parameter and ID that we should study more in the future.

The presence of ID in catalyst preparation effect on crystallite structure that occurred in formation of $MgCl_2$, that was confirmed in diffractograms of N902 and E902 that show similar pattern in the range of $2\theta = 11\text{-}18^o$ but E902 was slightly boarder, and N902 shows shifting of center of peak to right that similarly with E1102.

Among free internal electron donor ($Mg(OEt)_2/TiCl_4$) catalyst systems , N302 (Figure 5.8 b) shows slightly sharper peak at $2\theta = 29\text{-}38^o$ than N902 (Figure 5.8 c), it indicated that N902 more disorder in crystallite structure than N302, and related with more activation degree of N902 in ethylene polymerization, as shown in Table 5.5.

The diffraction peaks of $Mg(OEt)_2/TiCl_4/ID$ catalyst system were slightly boarder than those $Mg(OEt)_2/TiCl_4$ catalyst system. The different was found at $2\theta = 29\text{-}38^o$, the diffractogram of $Mg(OEt)_2/TiCl_4$ catalyst were sharper than $Mg(OEt)_2/TiCl_4/ID$ catalyst, it could be suggested that EB and IPIPDMP as internal electron donor in $Mg(OEt)_2$-based catalyst play some role in distortion of crystallite structure of formed $MgCl_2$ [146].

Among $Mg(OEt)_2/TiCl_4/EB$ catalyst systems, at treatment temperature of 90^oC, E902 (treatment time of 2 h) shows boarder peak than E901 (treatment time of 1 h), it indicated that higher disorder of crystallite structure of E902 (Figure 5.9 d) than E901 (Figure 5.8 e). Therefore, longer reaction time can produce more disordering of crystallite structure and higher temperature can make bigger crystallite size for $MgCl_2$(ethoxide type)/$TiCl_4$/EB catalysts. Moreover, E1102 was found sharper peak at $2\theta = 32^o$ than E902. It indicated that high treatment temperature trend to effect on crystallite size of catalyst.

$Mg(OEt)_2/TiCl_4/IPIPDMP$ catalyst (D902), shows recrystallization of $MgCl_2$ with dissolution of adduct form of $MgCl_2$/diether and macrostructure of catalyst surface have connection of plate to form the bigger lamellar structure on surface of IPIPDMP-containing catalyst.

Comparison of two kind of internal electron donor, E902 (EB) and D902 (IPIPDMP), it was found that D902 had shaper peak in the range of $2\theta = 15^o$ but in the range of $2\theta = 30\text{-}35^o$ and $50\text{-}55^o$, the XRD pattern look similarly with E902. The crystallite size (primary particle size) of D902 should be bigger than E902 as appeared in secondary particle size, according to SEM image that shown in Figure 5.8 e) and g), that secondary particle of D902 bigger than E902.

These results implied that monoester (EB) and diether (IPIPDMP) compounds affected to stack disordering of $MgCl_2$ (ethoxide type). EB could constructed crystallite structure to form activated $MgCl_2$ almost complete but diether compound, the crystallite structure of catalyst still have triple layer (ordered structure) of crystallite in plane (003). At $2\theta = 15^o$ indicated that plane (003) of $MgCl_2$ still remained. Therefore, kind of ID is an important parameter that affected to

crystallographic structure of $MgCl_2$ (ethoxide type) supported catalyst that EB-containing catalyst system, smaller crystallite size was obtained [147].

Moreover, donors affect the formation and crystallization process of $MgCl_2$ at a primary particle scale. However, SEM and XRD should not be directly correlated because of the scale difference. The lamellar or plate structure is generally composed by an agglomerate of primary crystallites rather than monolith. The fact that donors affected the crystallization process should not be directly related to that effects of donors on the reconstruction process of such that a higher-order structure. The morphology transformation from MGE to $MgCl_2$ might be based on dissolution of precursors into the liquid phase, for which donors played a non-negligible role.

5.3.4 Polymer properties

The mmmm pentad value of polypropylenes were shown in Table 5.5. Isotacticity of polypropylene was studied by 13C NMR spectroscopy and determined from the area of the resonance peaks of the methyl region [148].

As the results, mmmm pentad of the isotactic parts of polypropylene was varied ranging from 55.7 to 83.2 mol%.

The mmmm pentad of $Mg(OEt)_2/TiCl_4$ catalyst system without internal donor, N302 and N902, revealed that no significantly effect of temperature on isotacticity of polypropylene. N302 shows similarly isotacticity to N902, 55.7 and 56.5 mol%, respectively, which were prepared at 30 and 90 ^{o}C of reaction temperature, with same treatment time of 2 h.

Among $Mg(OEt)_2/TiCl_4/EB$ catalyst system, mmmm pentad value of E902>E1102>E901 : 77.7 , 74.7, and 71.6 mol%, respectively. The results indicated that high treatment temperature was required for isospecific sites production while too high treatment temperature reducing of isospecific site was occurred.

The influence of different kind of internal electron donor was found that IPIPDMP, diether compound shows an excellent performance to produce isotactic site of catalyst. D902 had highest mmmm pentad value of 83.2 mol%, compared with

E902, EB-containing catalyst and N902 free internal electron donor catalyst that show mmmm pentad value of 77.7 and 56.5 mol%, respectively.

The catalyst containing IPIPDMP (diether compound) gives a higher isotacticity than catalyst containing EB which typically need an external donor in addition to polymerization, monoester type internal donor was extracted to polymerization solution system while reaction proceed but the catalyst system containing a diether compound not need any external donor [149,150] so in this study, polymerizations were carried out without external donor, the using of IPIPDMP-containing catalyst show outstanding of isotacticity compared with EB-containing catalyst.

CHAPTER VI

CONCLUSIONS AND RECOMMENDATIONS

6.1 Conclusions

6.1.1 Mono-supported catalysts ($MgCl_2/TiCl_4$) and bi-supported catalysts ($SiO_2/MgCl_2/TiCl_4$)

6.1.1.1 The bi-supported catalysts had relatively constant activities with increasing of $[EtOH]/[MgCl_2]$ due to prevention of the Ti active species from further reaction with ethanol, while those of the mono-supported catalyst showed a remarkable reduction with increasing $[EtOH]/[MgCl_2]$ ratio.

6.1.1.2 The bi-supported catalysts retain the morphology of the SiO_2 precursor to the catalyst, with spherical shapes. The $[EtOH]/[MgCl_2]$ ratios affect the bi-supported catalyst morphology in terms of the impregnated film of $MgCl_2$ on SiO_2 surface.

6.1.1.3 The low $[EtOH]/[MgCl_2]$ ratio give better catalytic activity and particle morphology in $MgCl_2$-supported ZN catalyst, while the $MgCl_2/SiO_2$-supported ZN catalysts requires moderate $[EtOH]/[MgCl_2]$ ratios. The optimized $[EtOH]/[MgCl_2]$ value for preparing bi-supported catalysts with high activity and good morphology is 7.

6.1.1.4 The bi-supported catalyst has high specific surface area and porosity without any relationship between activity and surface area.

6.1.1.5 Thermal of the bi-supported catalysts are more stable than the mono-supported catalysts.

6.1.1.6 The ethanol remain in catalyst structure of bi-supported catalysts less than mono-supported catalysts.

6.1.1.7 Hydrogen addition in ethylene polymerization remarkably decreased the activity of the mono-supported ZN catalyst, while it had no effect on the bi-supported ZN catalyst system.

6.1.1.8 The bi-supported ZN catalyst had lower degradation rate than that of the mono-supported ZN catalyst.

6.1.2 Mg(OEt)$_2$-supported Ziegler-Natta catalysts.

6.1.2.1 The functional group of ID has significantly controlling the Ti content of catalyst.

6.1.2.2 The crystallite structure of catalyst was affected from preparation's condition and kind of ID considerably affected the crystallite structure of the catalyst.

6.1.2.3 The ID plays an important role to reduce the severity of reaction during catalyst preparation step.

6.1.2.4 For Mg(OEt)$_2$/ID/TiCl$_4$ catalyst, the internal donor treatment condition is the key parameter to control catalyst morphology, catalytic performance and isospecific site as well.

6.1.2.5 The mmmm pentad value of synthesized PP that using IPIPDMP-containing catalyst higher than EB-containing catalyst.

6.2 Recommendations

6.2.1 In this thesis have objectives to improve the catalyst performance and control particle morphology so the characterizations were conducted only on catalyst. The polyethylene was produced by MgCl$_2$-supported and SiO$_2$/MgCl$_2$-supported Ziegler-Natta catalyst in a part of hydrogen response study should be characterized the polymer properties such as molecular weight and molecular weight distribution by GPC and melting temperature by DSC. Because of the polyethylene were affected from the polymerization condition and catalyst system, which were the main parameters to control the polymer properties.

6.2.2 The Mg(OEt)$_2$-supported Ziegler-Natta catalyst was synthesized in the absence and presence of internal donor. From the results, internal donor play a role to control catalytic activity that implied to active species of catalyst so it should be characterized the amount of internal donor in catalyst by GC technique. Because of the competition between internal donor and TiCl$_4$ is the reason of titanium and internal donor contents in catalyst that effect on catalytic activity and isotacticity of polypropylene.

REFERENCES

[1] Carr, N. Ziegler-Natta catalyst. Encyclopedia Britannica (2010)

[2] Abboud, M., P. Denifl, et al. Study of the morphology and kinetics of novel Ziegler-Natta catalysts for propylene polymerization. Journal of Applied Polymer Science 98(5) (2005): 2191-2200

[3] Dashti, A., A. Ramazani Sa, et al. Kinetic and morphological study of a magnesium ethoxide-based Ziegler-Natta catalyst for propylene polymerization. Polymer International 58(1) (2009): 40-45.

[4] Forte, M. C. and F. M. B. Coutinho. Highly active magnesium chloride supported Ziegler-Natta catalysts with controlled morphology. European Polymer Journal 32(2) (1996): 223-231.

[5] Choi, J. H., J. S. Chung, et al. The effect of alcohol treatment in the preparation of $MgCl_2$ support by a recrystallization method on the catalytic activity and isotactic index for propylene polymerization. European Polymer Journal 32(4) (1996): 405-410.

[6] JalaliDil, E., S. Pourmahdian, et al. Effect of dealcoholation of support in $MgCl_2$-supported Ziegler-Natta catalysts on catalyst activity and polypropylene powder morphology. Polymer Bulletin 64(5) (2010): 445-457.

[7] Ye, Z.-Y., L. Wang, et al. Novel spherical Ziegler-Natta catalyst for polymerization and copolymerization. I. Spherical $MgCl_2$-support. Journal of Polymer Science Part A: Polymer Chemistry 40(18) (2002): 3112-3119.

[8] Ye, Z., L. Wang, et al. Study on preparation of spherical Ziegler-Natta catalyst. Journal of Polymer Materials 22(2) (2005): 115-120.

[9] Jamjah, R., G. H. Zohuri, et al. Morphological study of spherical $MgCl_2.nEtOH$ supported $TiCl_4$ Ziegler-Natta catalyst for polymerization of ethylene. Journal of Applied Polymer Science 101(6) (2006): 3829-3834.

[10] Wu, L., D. T. Lynch, et al. Kinetics of gas-phase ethylene polymerization with morphology-controlled $MgCl_2$-supported $TiCl_4$ catalyst. Macromolecules 32(24) (1999): 7990-7998.

[11] Zohuri, G., M. A. Bonakdar, et al. Preparation of ultra high molecularweight polyethylene using bi-supported $SiO_2/MgCl_2$ (spherical)/$TiCl_4$ catalyst: A morphological study. Iranian Polymer Journal (English Edition) 18(7) (2009): 593-600.

[12] Chung, J. S., H. S. Cho, et al. Preparation of the Ziegler-Natta/metallocene hybrid catalysts on $SiO_2/MgCl_2$ bisupport and ethylene polymerization. Journal of Molecular Catalysis A: Chemical 144(1) (1999): 61-69.

[13] Ko, Y., T. Han, et al. Temperature programmed decomposition of sillica-supported $MgCl_2$/THF/$TiCl_4$ catalyst and effect of thermal treatment on ethylene polymerization rate. Korean Journal of Chemical Engineering 14(5)

[14] Jiang, T., W. Chen, et al. Preparation of porous spherical $MgCl_2/SiO_2$ complex support as precursor for catalytic propylene polymerization. Journal of Applied Polymer Science 98(3) (2005): 1296-1299.

[15] Wang, J., L. Wang, et al. Ethylene polymerization using a novel $MgCl_2/SiO_2$-supported Ziegler-Natta catalyst. Polymer International 55(3) (2006): 299-304.

[16] Dong, Q., Z. Fu, et al. Strong influences of cocatalyst on ethylene/propylene copolymerization with a $MgCl_2/SiO_2/TiCl_4$/diester type Ziegler-Natta catalyst. European Polymer Journal 43(8) (2007): 3442-3451.

[17] Tanase, S., K. Katayama, et al. Particle growth of magnesium alkoxide as a carrier material for polypropylene polymerization catalyst. Applied Catalysis A 350(2) (2008): 197-206.

[18] Abboud, M., P. Denifl, et al. Advantages of an emulsion-produced Ziegler-Natta catalyst over a conventional Ziegler-Natta catalyst. Macromolecular Materials and Engineering 290(12) (2005): 1220-1226.

[19] Joseph, J., S. C. Singh, et al. Morphology controlled magnesium ethoxide: Influence of reaction parameters and magnesium characteristics. Particulate Science and Technology 27(6) (2009): 528-541.

[20] Carr, N. Ziegler-Natta catalyst. Encyclopedia Britannica (2010).

[21] Giannini, U. M., Cassata, A., Longi, P., and Mazzocchi, R. US 4,336,360 (1982).

[22] Sato, A., Tachibana, M. and Kikuta, K. British Pat. 2,028,843 (1980).

[23] U.S. Pat. 4,347,158 (Aug. 31, 1982), M. J. Kaus and N. D. Miro (to Dart Ind. Inc.).

[24] U.S. Pat. 4,288,579 (Sept. 8, 1981), M. Miyoshi, Y. Tajima, K. Matsuura, N. Kuroda, and M. Matsuno (to Nippon Oil Co., Ltd.).

[25] British Pat. 1,549,793 (Aug. 8, 1979), J. L. M. Van der Loos and J. W. M. Noben (to Stamicarbon).

[26] U.S. Pat. 4,415,713 (Nov. 15, 1983), S. Tokunaga, A. Kato, T. Kimoto, and K. Baba (to Toyo Stauffer Chemical Co.).

[27] U.S. Pat. 4,330,648 (May 18, 1982), M. B. Welch (to Phillips Petroleum Co.).

[28] U.S. Pat. 4,382,019 (May 3, 1983), C. C. Greco (to Stauffer Chemical Co.).

[29] U.S. Pat. 4,226,741 (Oct. 07, 1980), L. Luciani, N. Kashiwa, P. C. Barbe´, and A. Toyota (to Montedison and Mitsui Petrochemical Industries, Ltd.).

[30] U.S. Pat. 4,224,183 (Sept. 23, 1980), G. Staiger (to BASF AG).

[31] Eur. Pat. 17,895 (Oct. 29, 1980), G. Staiger (to BASF AG).

[32] Ger. Pat. 28 40 156 (Mar. 27, 1980), O. Mauz (to Hoechst AG).

[33] British Pat. 2,049,709 (Dec. 31, 1980), S. Yoshida, S. Masukaw, H. Nimura, and M. Kohno (to Mitsubishi Petrochemical Co.).

[34] Jpn. Pat. 54,116,079 (Sept. 10, 1979), T. Tanaka and co-workers (to Mitsui Toatsu Chem. Inc.).

[35] U.S. Pat. 4,325,836 (Apr. 20, 1982), R. A. Epstein and R. I. Mink (to Stauffer Chemical Co.).

[36] U.S. Pat. 4,329,253 (May 11, 1982), B. L. Goodall, A. A. Van Der Nat, and W. Sjardijn (to Shell Oil Co.).

[37] U.S. Pat. 4,332,697 (June 1, 1982), K. Kimura, H. Ohba, and A. Murai (to Toho Titanium Co., Ltd.).

[38] British Pat. 2,133,020 (July 18, 1984), N. Kuroda, K. Matsuura, M. Miyoshi, M.Okamoto, and T. Shiraishi (to Nippon Oil Co., Ltd.).

[39] British Pat. 2,159,523 (Dec. 4, 1985), Y. Tajima, W. Uchida, Y. Ganno, K. Kawabe, K. Matsuura, and M. Miyoshi (to Nippon Oil Co., Ltd.).

[40] U.S. Pat. 4,581,426 (Apr. 08, 1986), T. Asanuma and T. Shiomura (to Mitsui Toatsu Chemicals).

[41] U.S. Pat. 4,242,229 (Dec. 30, 1980), M. Fujii, S. Goto, and H. Sakurai (to Mitsubishi Petrochemical Co.).

[42] U.S. Pat. 4,343,721 (Aug. 10, 1982), B. L. Goodall and J. C. van der Sar (to Shell Oil Co.).

[43] U.S. Pat. 4,246,136 (Jan. 20, 1981), H. Ueno, M. Imai, N. Inaba, M. Yoda, and S. Wada (to Toa Nenryo Kogyo KK).

[44] Eur. Pat. 131,359 (Jan. 16, 1985), F. T. Kiff (to ICI PLC).

[45] U.S. Pat. 4,529,716 (July 16, 1985), V. Banzi, P. C. Barbe´ , and L. Noristi (to Montedison).

[46] U.S. Pat. 4,294,721 (Oct. 13, 1981), G. Cecchin and E. Albizzati (to Montedison).

[47] U.S. Pat. 4,469,648 (Sept. 04, 1984), M. Ferraris and F. Rosati (to Montedison).

[48] U.S. Pat. 4,399,054 (Aug. 16, 1983), M. Ferraris, F. Rosati, S. Parodi, E. Giannetti, G. Motroni, and E. Albizzati (to Montedison).

[49] U.S. Pat. 4,085,276 (Apr. 18, 1978), A. Toyota, K. Odawara, and N. Kashiwa (to Mitsui Petrochemical Industries, Ltd.).

[50] U.S. Pat. 4,742,139 (May 3, 1988), M. Kioka and N. Kashiwa (to Mitsui Petrochemical Industries, Ltd.).

[51] U.S. Pat. 4,410,451 (Oct. 18, 1983), R. E. Dietz andM. B.Welch (to Phillips Petroleum Co.).

[52] U.S. Pat. 4,948,770 (Aug. 14, 1990), R. C. Job (to Shell Oil Co.).

[53] U.S. Pat. 5,905,050 (May 18, 1999), J. Louhelainen and J. Koshinen (to Borealis Holding AS).

[54] U.S. Pat. 5,468,698 (Nov. 21, 1995), J. Koskinen and T. Garoff (to Borealis Holding AS).

[55] U.S. Pat. 4 414 132 (Nov. 7, 1983), B. L. Goodall, A. A. van der Nat, and W. Sjardijn(to Shell Oil Co.).

[56] U.S. Pat. 4,393,182 (July 12, 1983), B. L. Goodall, A. A. van der Nat, and W. Sjardijn(to Shell Oil Co.).

[57] B. L. Goodall, in R. P. Quirk, ed., Transition Metal Catalyzed Polymerizations, Alkenes and Dienes, Part A, Harwood Academic Publishers, New York, 1983, p. 355.

[58] U.S. Pat. 4,220,554 (Sept. 2, 1980), P. C. Barbe`, L. Luciani, and U. Scata` (to Montedison).

[59] U.S. Pat. 4,277,372 (July 7, 1981), A. S. Matlack (to Hercules Inc.).

[60] Eur. Pat. 49,467 (Apr. 14, 1982), S. Asahi and Y. Takeshita (to Idemitsu Kosan Co.).

[61] U.S. Pat. 4,472,521 (Sept. 18, 1984), E. I. Band (to Stauffer Chemical Co.).

[62] US. Pat. 4,652,541 (Mar. 3, 1987), M. Imai, T. Yamamoto, H. Furuhashi, H. Ueno, and N. Inaba (to Toa Nenryo Kogyo KK).

[63] Eur. Pat. 96,770 (Dec. 28, 1983), A. Shiga, T. Sasaki, Y. Naito, and J. Kojima (to Sumitomo Chemical Co.).

[64] Eur. Pat. 322,798 (July 5, 1989), M. Inoue, H. Soga, and M. Terano (to Toho Titanium Co., Ltd.).

[65] Eur. Pat. 459,009 (Dec. 4, 1991), M. Inoue, H. Soga, and M. Terano (to Toho Titanium Co., Ltd.).

[66] Eur. Pat. 426,139 (May 8, 1991), F. C. Twu, I. D. Burdett, and H. K. Ficker (to Union Carbide Chemicals and Plastic Co.).

[67] British Pat. 2,191,778 (Dec. 23, 1987), J. McMeeking (to ICI PLC).

[68] U.S. Pat. 4,186,107 (Jan. 29, 1980), K. P. Wagner (to Hercules Inc.).

[69] Jpn. Pat. 53,024,378 (Mar. 7, 1978), G. Kakogawa and co-workers (to Mitsubishi Chemical Ind., Ltd.).

[70] Jpn. Pat. 54,112,983 (Sept. 4, 1979), A. Shiga and co-workers (to Sumitomo Chemical Co., Ltd.).

[71] U.S. Pat. 4,297,463 (Oct. 27, 1981), H. Ueno, T. Yano, T. Inoue, S. Ikai, Y. Kai, and M. Shimizu (to Ube Industries).

[72] U.S. Pat. 4,857,613 (Aug. 15, 1989), R. Zolk, J. Kerth, and R. Hemmerich (to BASF AG).

[73] Eur. Pat. 437,264 (July 17, 1991), A. Monte and L. Noristi (to Himont Inc.).

[74] Eur. Pat. 506,074 (Sept. 30, 1992), A. Monte and L. Noristi (to Himont Inc.).

[75] U.S. Pat. 4,613,579 (Sept. 23, 1986), H. Furuhashi, T. Yamamoto, M. Imai, and H. Ueno (to Toa Nenryo Kogyo KK).

[76] Eur. Pat. 446,801 (Sept. 18, 1991), T. Ebara, K. Kawai, and T. Sasaki (to Sumitomo Chemical Co.).

[77] Eur. Pat. 371,664 (June 06, 1990), J. W. Kelland (to ICI PLC).

[78] Eur. Pat. 336,545 (Oct. 11, 1989), J. C. A. Bailly and S. Sandis (to BP Chemical Industry, Ltd.).

[79] U.S. Pat. 4,330,649 (May 18, 1982), M. Kioka, H. Kitani, and N. Kashiwa (to Mitsui Petrochemical Industries, Ltd.).

[80] Eur. Pat. 86,288 (Aug. 24, 1983), N. Kashiwa and Y. Ushida (to Mitsui Petrochemical Industries, Ltd.).

[81] U.S. Pat. 4,728,705 (Mar. 01, 1988), I. G. Burstain, S. M. Nestlerode, and R. C. Job (to Shell Oil Co.).

[82] Eur. Pat. 405,554 (Jan. 02, 1991), T. J. Pullukat and G. C. Meverden (to Quantum Chemical Corp.).

[83] U.S. Pat. 4,866,022 (Sept. 12, 1989), G. G. Arzoumanidis, N. M. Karayannis, H. M. Khelghatian, S. S. Lee, and B. V. Johnson (to Amoco Corp.).

[84] U.S. Pat. 4,866,022 (Sept. 12, 1989), G. G. Arzoumanidis, N. M. Karayannis, H. M. Khelghatian, S. S. Lee, and B. V. Johnson (to Amoco Corp.).

[85] U.S. Pat. 4,540,679 (Sept. 10, 1985), G. G. Arzoumanidis and S. S. Lee (to Amoco Corp.).

[86] Eur. Pat. 258,485 (Mar. 09, 1988), Z. Li, A. Yang, J. Yang, B. Mao, and Y. Zheng (to Beijing Research Institute of Chemistry).

[87] U.S. Pat. 4,703,026 (Oct. 27, 1987), M. Matsuura and T. Fujita (to Mitsubishi Petrochemical Co.).

[88] U.S. Pat. 4,551,439 (May 11, 1985), M. Harada, S. Miya, S. Yamada, and M. Iijima (to Chisso Corp.).

[89] Eur. Pat. 475,134 (Mar. 18, 1992), D. Hara, Y. Kondo, and M. Mori (to Tosoh Corp.).

[90] Eur. Pat. 461,775 (Dec. 18, 1991), J. C. Chadwick, D. P. Zilker, and C. R. Job (to Shell Oil Co.).

[91] Eur. Pat. 461,268 (Dec. 18, 1991), T. Ota, A. Sugahara, A. Tanaka, M. Toda, and H. Funabashi (to Idemitsu Petrochemical Co.).

[92] Eur. Pat. 436,801 (July 17, 1991), R. Matthes, H. Rauleder, T. Jostmann, K. D.Kassmann, and U. Horns (to Huels Chemische Werke AG).

[93] U.S. Pat. 5,145,821 (Sept. 08, 1992), C. K. Buehler and A. P. Masino (to Quantum Chem Corp.).

[94] Eur. Pat. 1,108,728 (June 20, 2001), No designation of inventors (to BP Chemicals, Ltd.).

[95] U.S. Pat. 6,191,239 (2001-02-20), R. R. Ford, W. A. Ames, K. A. Dooley, J. J. Vanderbilt, and A. G. Wonders (to Eastman Chemical Company).

[96] World Pat. 00/52,068 (Sept. 8, 2000), R. R. Ford, W. A. Ames, K. A. Dooley, J. J.Vanderbilt, and A. G. Wonders (to Eastman Chemical Company).

[97] Eur. Pat. 771,820 (May 7, 1997), E. D. Fowler, M. D. Awe, and R. J. Jorgensen (to Union Carbide Chemicals & Plastics Technology Corporation).

[98] World Pat. 95/35,164 (Dec. 28, 1995), Y. V. Kissin and R. I. Mink (to Mobil Oil Corp.).

[99] World Pat. 95/34,380 (Dec. 21, 1995), R. O. Hagerty, P. K. Husby, Y. V. Kissin, R. I. Mink, and T. E. Nowlin (to Mobil Oil Corp.).

[100] Galli, P., P. Barbe, et al. The activation of $MgCl_2$-supported Ziegler-Natta catalysts: A structural investigation. European Polymer Journal 19(1) (1983): 19-24.

[101] Fenza, S. : Unpublished results

[102] British Patent 2.000.514 to Montedison (1977).

[103] Bassi, I. W., F. Polato, et al. A new layer structure of $MgCl_2$ with hexagonal close packing of the chlorine atoms. Zeitschrift für Kristallographie 159(1-4) (1982): 297-302.

[104] Bassi, I. W., F. Polato, et al. A new layer structure of $MgCl_2$ with hexagonal close packing of the chlorine atoms. Zeitschrift für Kristallographie 159(1-4)

[105] Ferrari, A., A. Braibanti, et al. Refinement of the crystal structure of $NiCl_2$ and of unit-cell parameters of some anhydrous chlorides of divalent metals. Acta Crystallographica 16(8) (1963): 846-847.

[106] Bassi, I. W.: Unpublished results.

[107] Giannini, U. Polymerization of olefins with high activity catalysts. Die

[108] Bassi, I. W.: Unpublished results.

[109] Kashiwa, N. Super active catalyst for olefin polymerization. Polymer Journal 12(9) (1980): 603-608.

[110] Galli, P., P. Barbe, et al. The activation of $MgCl_2$-supported Ziegler-Natta catalysts: A structural investigation. European Polymer Journal 19(1) (1983): 19-24.

[111] Kashiwa, N. and A. Toyota. $MgCl_2$ supported titanium catalyst prepared by mechanical pulverization. Polymer Bulletin 11(5) (1984): 471-477.

[112] Bassi, I. W.: Unpublished results.

[113] Kashiwa, N. Super active catalyst for olefin polymerization. Polymer Journal 12(9) (1980): 603-608.

[114] Galli, P., P. Barbe, et al. The activation of $MgCl_2$-supported Ziegler-Natta catalysts: A structural investigation. European Polymer Journal 19(1) (1983): 19-24.

[115] Lu, H. and S. Xiao. Structure and behaviour of $SiO_2/MgCl_2$ bisupported Ziegler-Natta catalysts for olefin polymerization. Die Makromolekulare Chemie 194(2) (1993): 421-429.

[116] Ma, Z., L. Wang, et al. Study of propylene polymerization catalyzed by spherical $MgCl_2$-supported Ziegler-Natta catalyst system: Preparation of spherical support. Polymer - Plastics Technology and Engineering 44(8-9) (2005): 1475-1483.

[117] Noristi, L., E. Marchetti, et al. Investigation on the particle growth mechanism in propylene polymerization with $MgCl_2$-supported ziegler–natta catalysts. Journal of Polymer Science Part A: Polymer Chemistry 32(16) (1994): 3047-3059.

[118] Sozzani, P., S. Bracco, et al. Stoichiometric Compounds of Magnesium Dichloride with Ethanol for the Supported Ziegler-Natta Catalysis: First Recognition and Multidimensional MAS NMR Study. Journal of the American Chemical Society 125(42) (2003): 12881-12893.

[119] Chung, J. S., J. H. Choi, et al. Effect of ethanol treatment in the preparation of MgCl$_2$ support for the propylene polymerization catalyst. Macromolecules 28(5) (1995): 1717-1718.

[115] Ye, Z.-Y., L. Wang, et al. Novel spherical Ziegler-Natta catalyst for polymerization and copolymerization. I. Spherical MgCl$_2$-support. Journal of Polymer Science Part A: Polymer Chemistry 40(18) (2002): 3112-3119.

[121] Kim, I., J. H. Kim, et al. Kinetic study of ethylene polymerization by highly active silica supported TiCl$_4$/MgCl$_2$ catalysts. Journal of Applied Polymer Science 39(4) (1990): 837-854..

[122] Zohuri, G. H., F. Azimfar, et al. Polymerization of propylene using the high-activity Ziegler-Natta catalyst system SiO2/MgCl2 (ethoxide type)/TiCl4/di-m-butyl phthalate/triethylaluminum/dimethoxy methyl cyclohexyl silane. Journal of Applied Polymer Science 89(5) (2003): 1177-1181.

[123] Hakim, S., M. Nekoomanesh, et al. Investigating the behaviour of a Bi-supported SiO$_2$/TiCl$_4$/THF/MgCl$_2$ catalyst in slurry ethylene polymerization: Activity and molecular weight. Iranian Polymer Journal (English Edition) 17(3) (2008): 208-216.

[124] JalaliDil, E., S. Pourmahdian, et al. Effect of dealcoholation of support in MgCl$_2$-supported Ziegler-Natta catalysts on catalyst activity and polypropylene powder morphology. Polymer Bulletin 64(5) (2010): 445-457.

[125] Patthamasang, S., B. Jongsomjit, et al. Effect of EtOH/MgCl$_2$ molar ratios on the catalytic properties of MgCl$_2$-SiO$_2$/TiCl$_4$ Ziegler-Natta catalyst for ethylene polymerization. Molecules 16(10) (2011): 8332-8342.

[126] Yu.I. Yermakov, B. N. K. and V. A. Zakharov Chapter 5: Supported Halogenides of Transition Metals as Catalysts for Olefine Polymerization. Studies in Surface Science and Catalysis.199-250. Elsevier, 1981.

[127] Lu, H. and S. Xiao. Highly isospecific $SiO_2/MgCl_2$ bisupported catalyst for propene polymerization. <u>Die Makromolekulare Chemie</u> 194(7) (1993): 2095-2102.

[128] Kissin, Y., R. Mink, et al. Kinetics and mechanism of ethylene homopolymerization and copolymerization reactions with heterogeneous Ti-based Ziegler–Natta catalysts. <u>Topics in Catalysis</u> 7(1) (1999): 69-88.

[129] Kissin, Y. V., R. I. Mink, et al. Ethylene polymerization reactions with Ziegler–Natta catalysts. I. Ethylene polymerization kinetics and kinetic mechanism. <u>Journal of Polymer Science Part A: Polymer Chemistry</u> 37(23) (1999): 4255-4272.

[130] Kissin, Y. V. and A. J. Brandolini. Ethylene polymerization reactions with Ziegler-Natta catalysts. II. Ethylene polymerization reactions in the presence of deuterium. <u>Journal of Polymer Science, Part A: Polymer Chemistry</u> 37(23) (1999): 4273-4280.

[131] Kissin, Y. V. and L. A. Rishina. Hydrogen effects in propylene polymerization reactions with titanium-based Ziegler-Natta catalysts. I. Chemical mechanism of catalyst activation. <u>Journal of Polymer Science, Part A: Polymer Chemistry</u> 40(9) (2002): 1353-1365.

[132] Kissin, Y. V., L. A. Rishina, et al. Hydrogen effects in propylene polymerization reactions with titanium-based Ziegler-Natta catalysts. II. Mechanism of the chain-transfer reaction. <u>Journal of Polymer Science, Part A: Polymer Chemistry</u> 40(11) (2002): 1899-1911.

[133] Garoff, T., S. Johansson, et al. Decrease in activity caused by hydrogen in Ziegler-Natta ethene polymerisation. <u>European Polymer Journal</u> 38(1) (2002): 121-132.

[134] Zhao, Z., L. Wang, et al. Study on the microstructures of polypropylene synthesized by a novel $MgCl_2$-supported and low Ti-loading Ziegler-Natta catalyst. <u>Designed Monomers and Polymers</u> 10(6) (2007): 477-486.

[135] Kissin, Y. V. Main kinetic features of ethylene polymerization reactions with heterogeneous Ziegler-Natta catalysts in the light of a multicenter reaction mechanism. Journal of Polymer Science, Part A: Polymer Chemistry 39(10) (2001): 1681-1695.

[136] Garoff, T., S. Johansson, et al. Procatalyst for ethylene polymer production, method for its preparation and use. EP0688794, 1998.

[137] Forte, M. C. and F. M. B. Coutinho. Highly active magnesium chloride supported Ziegler-Natta catalysts with controlled morphology. European Polymer Journal 32(2) (1996): 223-231.

[138] Tanase, S., K. Katayama, et al. Particle growth of magnesium alkoxide as a carrier material for polypropylene polymerization catalyst. Applied Catalysis A 350(2) (2008): 197-206.

[139] Ye, Z.-Y., L. Wang, et al. Novel spherical Ziegler-Natta catalyst for polymerization and copolymerization. I. Spherical $MgCl_2$-support. Journal of Polymer Science Part A: Polymer Chemistry 40(18) (2002): 3112-3119.

[140] Yang, C. B., C. C. Hsu, et al. Infrared characterization of $MgCl_2$ supported Ziegler-Natta catalysts with monoester and diester as a modifier. European Polymer Journal 30(2) (1994): 205-214.

[141] Busico, V., P. Corradini, et al. Polymerization of propene in the presence of $MgCl_2$-supported Ziegler-Natta catalysts, 2. Effects of the co-catalyst composition. Makromol. Chem. 187(5) (1986): 1115-1124.

[142] Stukalov, D. V., V. A. Zakharov, et al. Adsorption species of ethyl benzoate in $MgCl_2$-supported Ziegler-Natta catalysts. A density functional theory study. J. Phys. Chem. C 114(1) (2010): 429-435.

[143] Zohuri, G. H., A. B. Kasaeian, et al. Polymerization of propylene using $MgCl_2$(ethoxide type)/$TiCl_4$/diether heterogeneous Ziegler-Natta catalyst. Polymer International 54(6) (2005): 882-885.

[144] Wang, L., H. J. Yu, et al. Preparation of novel $MgCl_2$-adduct supported spherical Ziegler-Natta catalyst for alpha-olefin polymerization. Journal of Applied Polymer Science 99(3) (2006): 945-948.

[145] Noto, V. D., A. Marigo, et al. MgCl$_2$-supported Ziegler-Natta catalysts: Synthesis and X-ray diffraction characterization of some MgCl$_2$-Lewis base adducts. Makromol. Chem. 193(1) (1992): 123-131.

[146] Lee, D.-H., Y.-T. Jeong, et al. Propylene polymerization with Mg(OEt)$_2$/benzoyl chloride/TiCl$_4$/triethyl aluminum/external donor catalyst systems. Journal of Applied Polymer Science 47(8) (1993): 1449-1461.

[147] Gerbasi, R., A. Marigo, et al. The activation of MgCl$_2$-supported Ziegler-Natta catalysts--II: Correlation between activity and structural disorder. European Polymer Journal 20(10) (1984): 967-970.

[148] Kakugo, M., T. Miyatake, et al. Microtacticity distribution of polypropylenes prepared with heterogeneous Ziegler-Natta catalysts. Macromolecules 21(2) (1988): 314-319.

[149] Chadwick, J. C., G. Morini, et al. Propene polymerization with MgCl$_2$-supported catalysts: effects of using a diether as external donor. Macromolecular Chemistry and Physics 198(4) (1997): 1181-1188.

[150] Morini, G., E. Albizzati, et al. Microstructure Distribution of Polypropylenes Obtained in the Presence of Traditional Phthalate/Silane and Novel Diether Donors: A Tool for Understanding the Role of Electron Donors in MgCl$_2$-Supported Ziegler-Natta Catalysts. Macromolecules 29(18) (1996): 5770-5776.

APPENDICES

APPENDIX A

CATALYST PREPARATION PROCEDURE

A.1: MgCl$_2$/TiCl$_4$ catalyst system.

MgCl$_2$ (3 g) + Ethanol + Heptane (60 ml)

dissolve at 80 °C

cool down to -20 °C

TiCl$_4$ (18 ml)

add drop wise

stir at T = 80 °C and hold for 1 h

TiCl$_4$ (18ml) + Heptane (18 ml)

stir at T = 95 °C and activate for 1 h

remove supernatant and wash with heptane

dry under vacuum at 60 °C

Final Catalyst
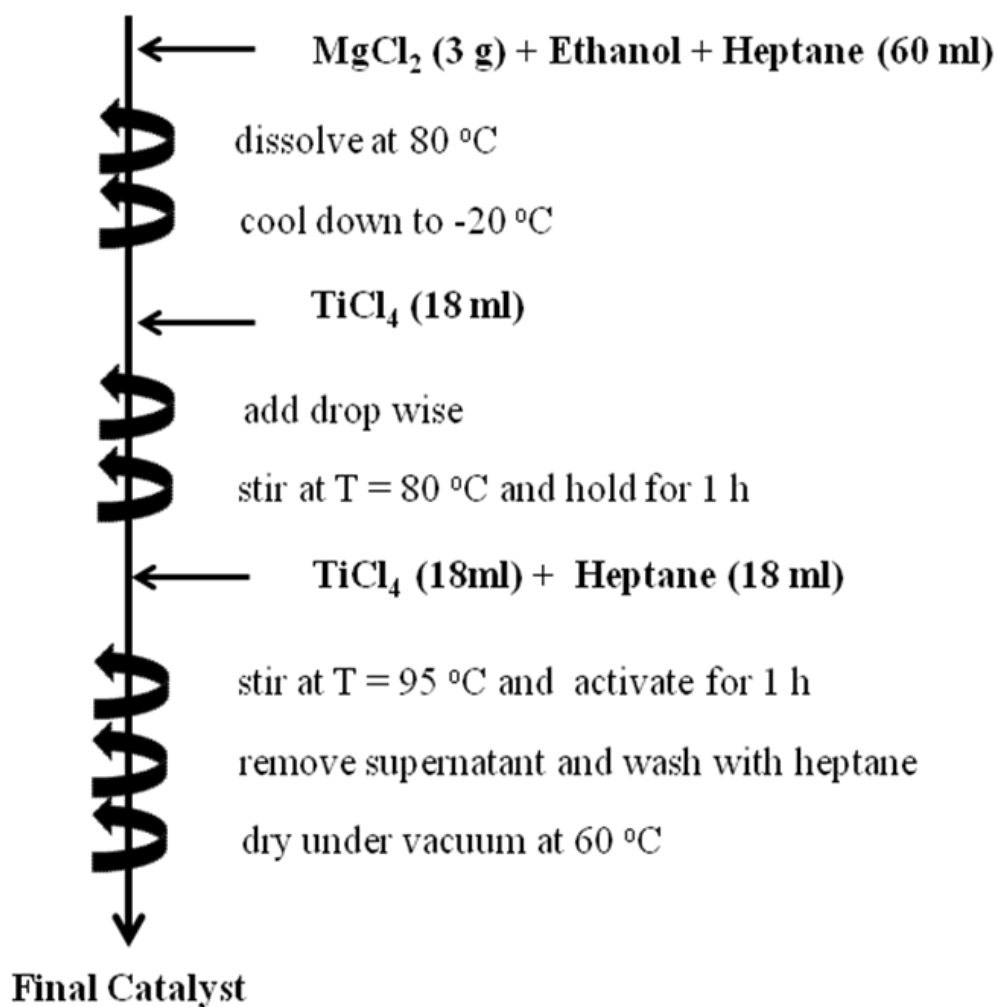
A.2: MgCl$_2$/SiO$_2$/TiCl$_4$ catalyst system.

MgCl$_2$ (3 g) + Ethanol + Heptane (60 ml)

dissolve

SiO$_2$ (6 g)

mix for 1 h

Heptane (60 ml)

wash with heptane

cool down to -20 °C

TiCl$_4$ (18 ml)

stir at T = 80 °C and hold for 1 h

TiCl$_4$ (18ml) + Heptane (18 ml)

stir at T = 95 °C and activate for 1 h

Final Catalyst

A.3: Mg(OEt)$_2$/TiCl$_4$ catalyst system.

Mg(OEt)$_2$ (10 g) + Toluene (60 ml)

suspend

TiCl$_4$ (20 ml)

add drop wise at T= -20 °C

rise to desire temperature

cook at **desired temperature** (°C)
for **2** h

Wash with Toluene

Toluene (50 ml) + TiCl$_4$ (20 ml)

cook at **desired temperature** (°C)
for **desired period** (h)

wash with heptane

N302 and N902

A.4: Mg(OEt)₂/TiCl₄/ID catalyst system.

Mg(OEt)$_2$ (10 g) + Toluene (60 ml)

suspend

TiCl$_4$ (20 ml)

add drop wise at T= -20 °C

rise to desire temperature

3 ml of InD (EB or IPIPDMP)

cook at **desired temperature** (°C)
for **desired period** (h)

Wash with Toluene

Toluene (50 ml) + TiCl$_4$ (20 ml)

cook at **desired temperature** (°C)
for **desired period** (h)

wash with heptane

E901 , E902 , E1102
or D902

APPENDIX B

^{13}C NMR SPECTRA OF POLYPROPYLENE

Table B.1 Assignments of the methyl and methylene resonances in ^{13}C NMR spectrum of polypropylene [1].

peak no.	δ (ppm)[a]	assignment
Methyl Resonances		
1	22.0–21.7	*mmmm*
2	21.7–21.4	*mmmr*
3	21.4–21.2	*rmmr*
4	21.2–21.0	*mmrr*
5	21.0–20.7	*mmrm + rmrr*
6	20.7–20.5	*rmrm*
7	20.5–20.0	*rrrm + rrrr*
8	20.0–19.7	*mrrm*
Methylene Resonances		
1	47.75–47.60	*mrmrm*
2	47.60–47.42	*mrmrr*
3	47.42–47.28	*rrmrr + mrrrm*
4	47.28–47.02	*mrrrr*
5	47.02–46.85	*rmmrm + rrrrr*
6	46.85–46.58	*rmmrr + mmmrm + mmmrr*
7	46.58–46.40	*rmrrm*

[a]Downfield of TMS.

APPENDIX C

IR AND RAMAN SPECTRA OF ZIEGLER-NATTA CATALYST

Table C.1 Characteristic IR and Raman vibrations of the Ziegler-Natta catalyst sample [2].

Vibration	Type of vibration	Region (cm^{-1})	
		IR	Raman
$C–H_{Ar}$	Stretching	3070	3080
CH_2/CH_3	Stretching	2800-3000	2800-3000
$C=O$	Stretching	1684	1685
$C=C_{Ar}$	Stretching	–	1592
CH_2/CH_3	Deformation vibration	1454	1449
CH_3	Symmetric deformation vibration	1392	1395
C–O–C	Asymmetric stretching	1308	1302
C–O–C	Symmetric stretching	1156	1156
$C–H_{Ar}$	In plane deformation vibration	–	1140
$O–C=O$	Asymmetric stretching	1082	–
$C–H_{Ar}$	In plane deformation vibration	–	1052
$O–C=O$	Symmetric stretching	934	–
C–H	Out of plane deformation vibration	736	647
M–O (Mg–O or Ti–O)	Stretching	460	–
Titanium compound	Stretching	–	419
M–O (Mg–O or Ti–O)	Stretching	350	350
M–O (Mg–O or Ti–O)	Stretching	314	303
Ti–Cl	Stretching	375	–
Ti–Cl	Stretching	365	–
Ti–Cl	Stretching	382	–
Mg–Cl	Stretching	233	238
Mg–Cl	Stretching	242	–

APPENDIX D

MAGNESIUM ETHOXIDE SUPPORTED ZIEGLER-NATTA CATALYST

D1: Cross-section of Mg(OEt)$_2$-supported Ziegler-Natta catalyst in the presence of EB and without EB.
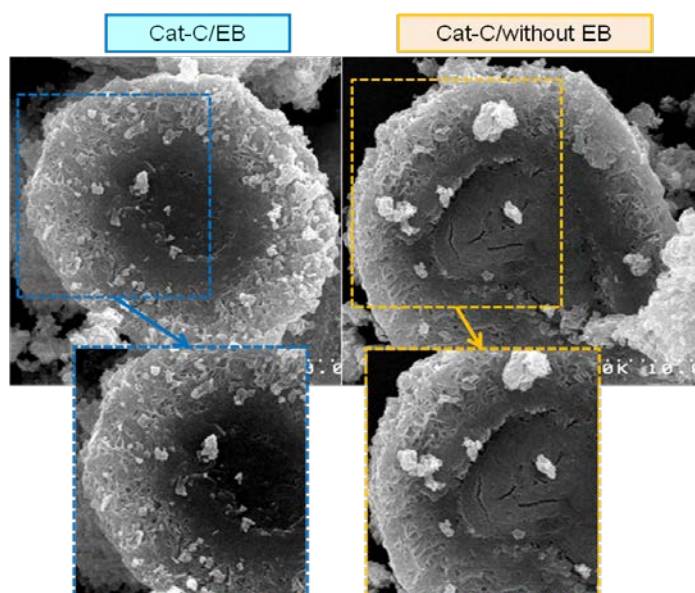
D2: SEM images of Mg(OEt)$_2$-supported Ziegler-Natta catalyst which were prepared with different temperature.
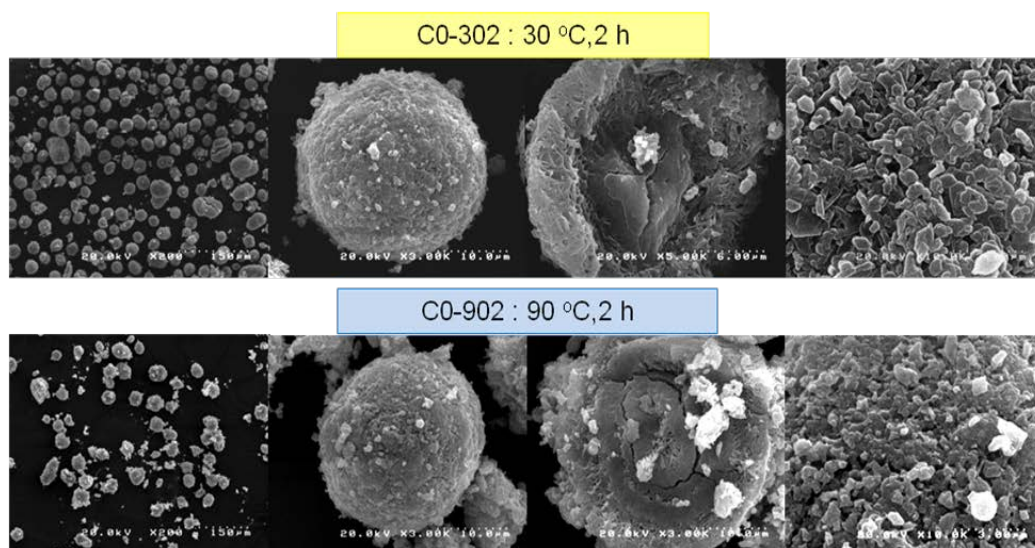
D3: SEM images of Mg(OEt)$_2$-supported Ziegler-Natta catalyst in the presence of EB which were prepared with different conditions.
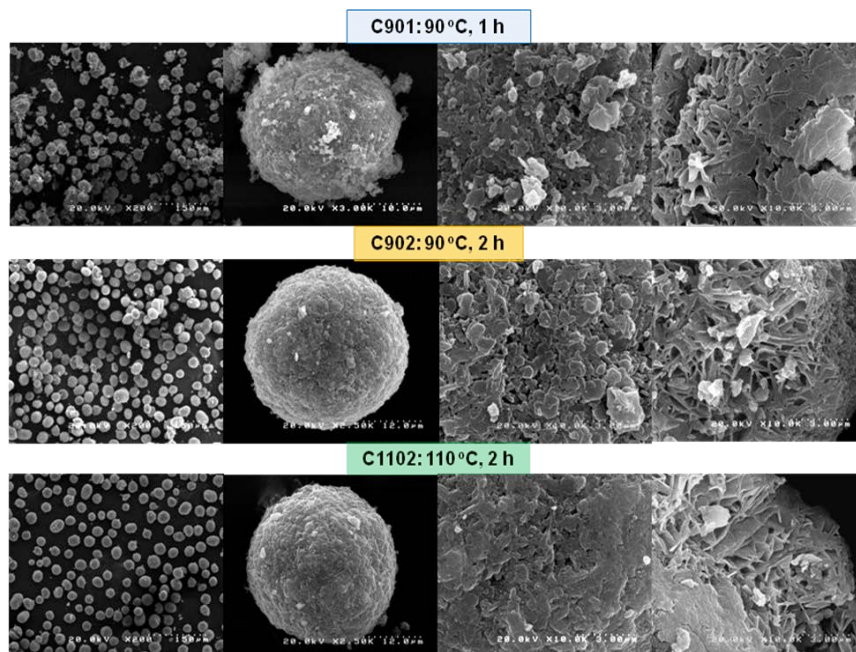
D4: SEM images of Mg(OEt)$_2$-supported Ziegler-Natta catalyst in the presence of EB and IPIPDMP as internal donors.
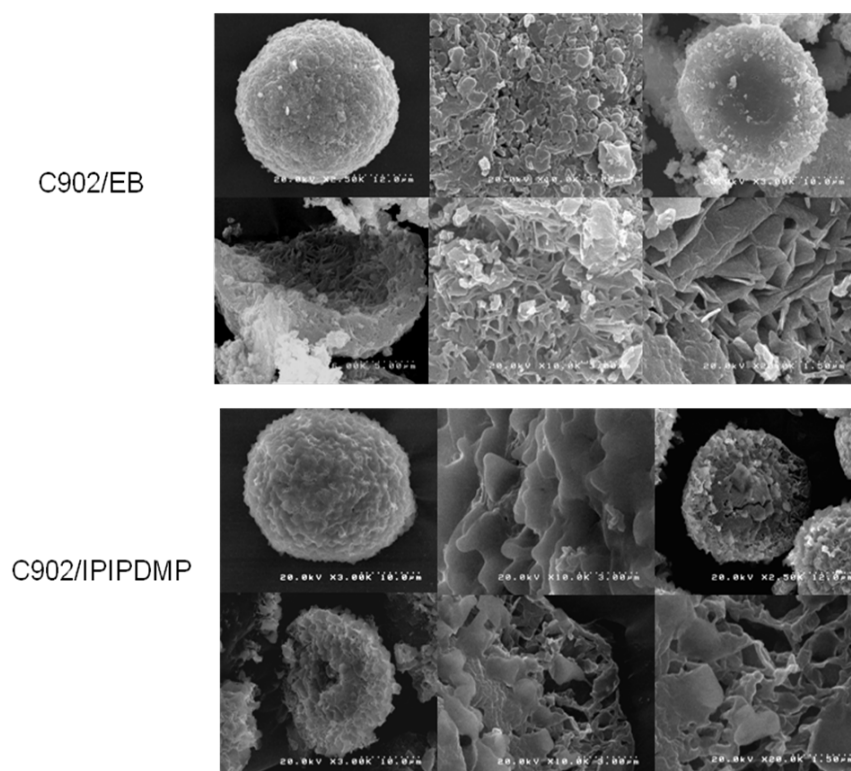
D5: TGA profiles of Mg(OEt)$_2$-supported Ziegler-Natta catalyst catalysts.
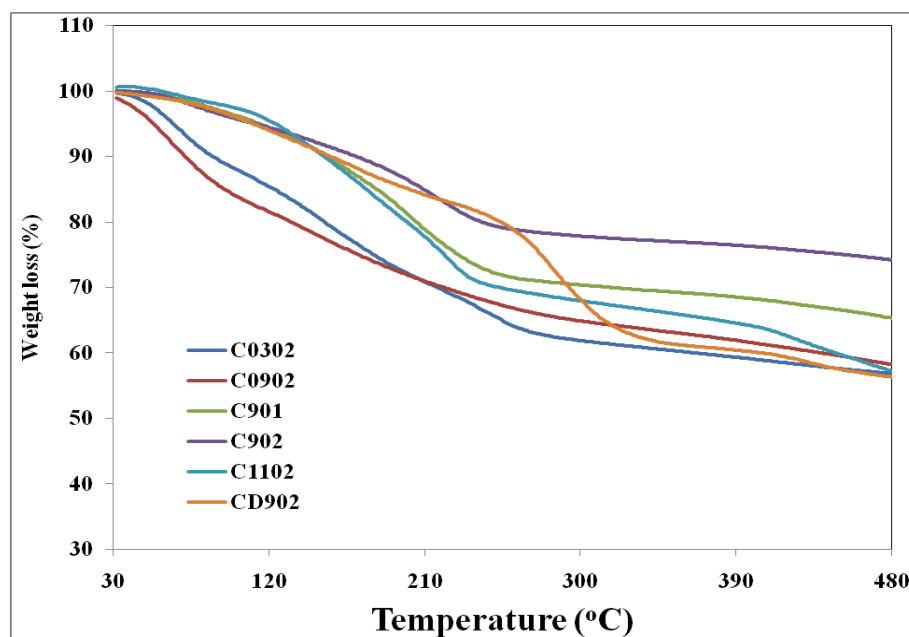
D6: Relative weight derivative profiles of Mg(OEt)$_2$-supported Ziegler-Natta catalyst catalysts.
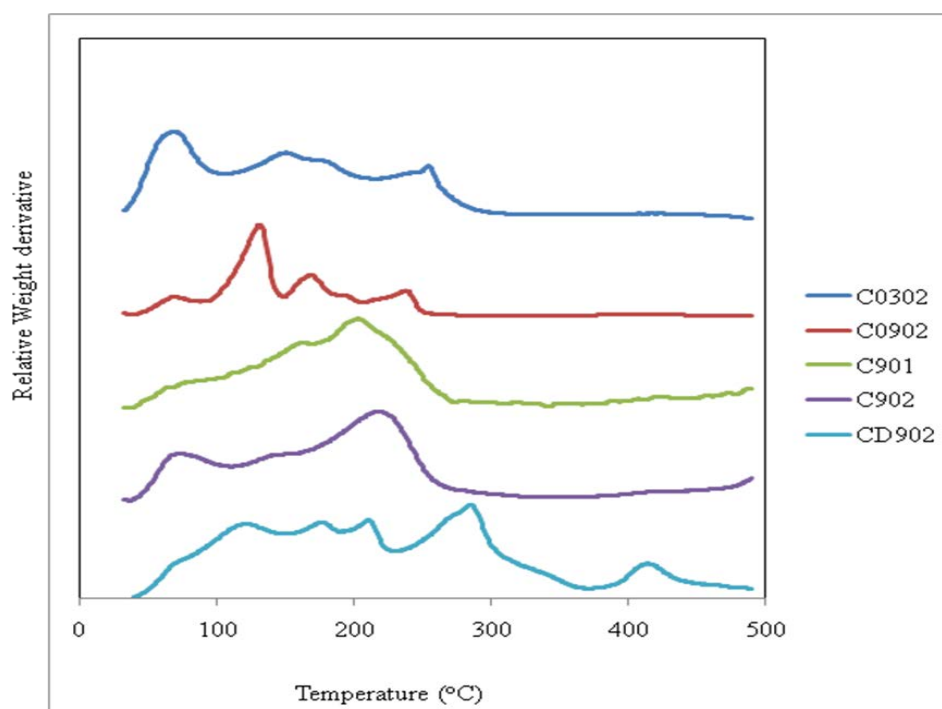
VITA

Supanan Patthamasang was born on June 25, 1982 in Nakhon Ratchasima, Thailand. After graduating from Pakchong School in 2000, she spent 5 years at Suranaree University of Technology for her Bachelor's degree in Chemical Engineering in 2005. Thereafter, she began her graduate studies at department of Chemical Engineering, Chulalongkorn University and joined catalysis and catalytic reaction engineering research group under financial support from PTT Public Co., Ltd. She had collaborated with Professor Minoru Terano and done the experiment parts of her research in Japan Advanced Institute of Science and Technology, from April, 2008 to September, 2008 and from November, 2010 to April, 2011. A part of her work was published in "Effect of EtOH/MgCl$_2$ Molar Ratios on the Catalytic Properties of MgCl$_2$-SiO$_2$/TiCl$_4$ Ziegler-Natta Catalyst for Ethylene Polymerization" Molecules, 16(10), 2011, 8332-8342.